Université Mohamed Khider Biskra

Faculté des Sciences et de la Technologie

Département : Génie électrique

جامعة محمد خيضر بسكرة

كلية العلوم والتكنولوجيا

قسم:الهندسة الكهربائية

Réf :…………..

المرجع :…………

Thèse présentée en vue de l'obtention du diplôme de

Doctorat en science en : Génie Electrique
Option : Automatique

Control and Optimization of an Autonomous Photovoltaic System using Metaheuristic Methods

Présentée par :
Houam Yehya

Soutenue publiquement le : 28/06/2021

Devant le jury composé de :

Pr. ZOUZOU Salah-Eddine	**Prof**	**Président**	**Université de Biskra**
Dr. TERKI Amel	**MCA**	**Directrice de thèse**	**Université de Biskra**
Pr. AZOUI Boubaker	**Prof**	**Examinateur**	**Université de Batna**
Pr. RAHMANI Lazhar	**Prof**	**Examinateur**	**Université de Sétif**
Pr. TOUMI Abida	**Prof**	**Examinatrice**	**Université de Biskra**
Pr. DRID Said	**Prof**	**Examinateur**	**Université de Batna**

Dedications

I dedicate this modest work to ..

The soul of my **dear mother,** Allah rest her and put her in paradise.

My **dear father Houam EL-Hafsi.**

The souls of **the heroes martyrs, my dear grandfather, Houam Mouhamed el-Tayeb,** and **my dear oncl Houam ismail,** "Allah have mercy on them and make their resting place in Paradise". They are martyrs of the Algerian national liberation war, in the commune of **Boukhadra, north of Tébessa,** which affiliated to the fifth zone, the first historical region "Aouras-Nmamcha". They joined to el-jihad with the National Liberation Army (ALN) after the national work strike of eight-day January 28-February 4, 1957. The first as a moujahid and electrician, and the second as a moujahid and nurse.

The soul of the great woman, my **dear grand-mother,** Allah rest her and put her in paradise.

My **dear wife**

My **dear daughters, Roueya and Rahaf.**

My **dear brothers Mouhamed el-Taher and Ismail** and my **dear sisters.**

My dear friends.

Everyone that I esteem and hold dear.

Acknowledgments

Firstly, I thank **Allah** for all the generosity he has given us, and he taught us from his vast knowledge.

Then, I would like to express my heartfelt gratitude to the thesis director, **Dr. TERKI Amel**, for her guidance, support, and encouragement. In addition to hers sage advice, constructive criticism, and useful suggestions to complete my doctoral thesis.

I would like to express my heartfelt gratitude to the president of the jury **Pr. ZOUZOU Salah-Eddine** from Biskra University and the members of the jury: **Pr. AZOUI Boubaker** from Batna University, **Pr. RAHMANI Lazhar** from Sétif University, **Pr. DRID Said** from Batna University and **Pr. TOUMI Abida** from Biskra University. For give us the honor of agreeing to participate in this jury. I appreciate yours pertinent comments and valuable questions, which shows yours interest in the subject, yours useful comments helps me to have a greater perspective on my work.

I am very indebted to **my parents** to support me to complete this research work successfully, and in particular to **my mother,** Allah rest her and put her in paradise, whose prayers and precious advice have greatly helped me to realize all the achievements of my life, especially to complete my doctoral thesis.

I want to thank **my dear wife** for her support and assistance to make this work successful. Finally, I would like to dedicate this work to **my two dear daughters Roueya and Rahaf**.

HOUAM Yehya

Abstract of the thesis

The sun is an almost inexhaustible source of energy that returns to the surface of the earth a radiation that represents each year about 15000 times the energy consumption of humanity. It appears as an important source such that the amount of solar energy that reaches the surface of the earth during a day is greater ten times than that consumed.Through the photovoltaic effect, the energy contained in the sunlight can be converted largely at electrical energy. The geographical location of Algeria favors the development of the use of solar energy but always its yield has been considered insufficient for produce an important energy. Among several parameters influencing this yield are the irradiation flux and the temperature. Several studies have been presented to improve the power yield and thus profit the maximum of the power conversion obtained. we propose in this study, application of the different techniques: classic, artificial intelligence and metaheuristic, in order to ameliorate the performances of the maximum power point tracking (MPPT) controller and maximize the output power of the photovoltaic generator intended to an autonomous photovoltaic system under varying environmental conditions.

Keywords: Global maximum power point tracking (GMPPT), Meta-heuristic Methods, Partial Shading Case (PSC), Photovoltaic (PV), Standalone system.

Resumé de la thése

Le soleil est une source d'énergie quasi inépuisable qui renvoie à la surface de la terre un rayonnement qui représente chaque année environ 15 000 fois la consommation énergétique de l'humanité. Il apparaît comme une source importante telle que la quantité d'énergie solaire qui atteint la surface de la terre pendant une journée est dix fois supérieure à celle consommée. Grâce à l'effet photovoltaïque, l'énergie contenue dans la lumière du soleil peut être convertie en grande partie en énergie électrique. La situation géographique de l'Algérie favorise le développement de l'utilisation de l'énergie solaire mais toujours son rendement a été jugé insuffisant pour produire une énergie importante. Parmi plusieurs paramètres influençant ce rendement figurent le flux d'irradiation et la température. Plusieurs études ont été présentées pour améliorer le rendement énergétique et ainsi profiter au maximum de la conversion de puissance obtenue. nous proposons dans cette étude, l'application des différentes techniques: classique, intelligence artificielle et métaheuristique, afin d'améliorer les performances de la commande Maximum Power Point Tracking (MPPT) et maximiser la puissance de sortie du générateur photovoltaïque destiné à un système photovoltaïque autonome dans des conditions environnementales variables.

Mots clés: Suivi le point global de puissance maximale, Méthodes Méta-heuristique, Cas d'ombrage partiel, Photovoltaïque. système autonome

ملخص الاطروحة

تعد الشمس مصدرًا لا ينضب للطاقة ويستقبل سطح الأرض إشعاعًا يمثل كل عام حوالي 15000 ضعف استهلاك الطاقة للبشرية تقريبًا. ولهذا تعد الطاقة الشمسية من اهم واكبر مصادر الطاقة النظيفة حيث أن كمية الطاقة الشمسية التي تصل إلى سطح الأرض خلال يوم واحد أكبر بعشر مرات من تلك المستهلكة ، ومن خلال التأثير الكهروضوئي ، يمكن تحويل الطاقة الموجودة في ضوء الشمس إلى طاقة كهربائية. يشجع الموقع الجغرافي للجزائر على تطوير استخدام الطاقة الشمسية ولكن دائمًا ما يعتبر انتاجها من الطاقة الشمسية غير كافٍ. من بين العديد من العوامل التي تؤثر على الاستغلال الامثل للطاقة الشمسية نجد تدفق الإشعاع ودرجة الحرارة. تم تقديم العديد من الدراسات لتحسين إنتاجية الطاقة وبالتالي ربح الحد الأقصى من تحويل الطاقة. نقترح في هذه الدراسة ، تطبيق التقنيات المختلفة: الحوسبة الناعمة وبالتحديد التقنيات الميتاهيريستيكية الحديثة و طرق الذكاء الاصطناعي، من أجل تحسين أداء تتبع نقطة الطاقة العظمى الناتجة من المولد الكهروضوئي وبالتالي استخراج اكبر طاقة ممكنة داخل نظام كهروضوئي مستقل و تحت ظروف بيئية متغيرة.

الكلمات المفتاحية: تتبع النقطة العظمى للاستطاعة الكبرى، الطرق الميتاهيريستيكية، حالة التظليل الجزئي، الكهروضوئية، النظام المستقل.

Abstract of the thesis

The sun is an almost inexhaustible source of energy that returns to the surface of the earth a radiation that represents each year about 15000 times the energy consumption of humanity. It appears as an important source such that the amount of solar energy that reaches the surface of the earth during a day is greater ten times than that consumed. Through the photovoltaic effect, the energy contained in the sunlight can be converted largely at electrical energy. The geographical location of Algeria favors the development of the use of solar energy but always its yield has been considered insufficient for produce an important energy. Among several parameters influencing this yield are the irradiation flux and the temperature. Several studies have been presented to improve the power yield and thus profit the maximum of the power conversion obtained. we propose in this study, application of the different techniques: classic, artificial intelligence and metaheuristic, in order to ameliorate the performances of the maximum power point tracking (MPPT) controller and maximize the output power of the photovoltaic generator intended to an autonomous photovoltaic system under varying environmental conditions.

Keywords: Global maximum power point tracking (GMPPT), Meta-heuristic Methods, Partial Shading Case (PSC), Photovoltaic (PV), Standalone system.

Resumé de la thése

Le soleil est une source d'énergie quasi inépuisable qui renvoie à la surface de la terre un rayonnement qui représente chaque année environ 15 000 fois la consommation énergétique de l'humanité. Il apparaît comme une source importante telle que la quantité d'énergie solaire qui atteint la surface de la terre pendant une journée est dix fois supérieure à celle consommée. Grâce à l'effet photovoltaïque, l'énergie contenue dans la lumière du soleil peut être convertie en grande partie en énergie électrique. La situation géographique de l'Algérie favorise le développement de l'utilisation de l'énergie solaire mais toujours son rendement a été jugé insuffisant pour produire une énergie importante. Parmi plusieurs paramètres influençant ce rendement figurent le flux d'irradiation et la température. Plusieurs études ont été présentées pour améliorer le rendement énergétique et ainsi profiter au maximum de la conversion de puissance obtenue. nous proposons dans cette étude, l'application des différentes techniques: classique, intelligence artificielle et métaheuristique, afin d'améliorer les performances de la commande Maximum Power Point Tracking (MPPT) et maximiser la puissance de sortie du générateur photovoltaïque destiné à un système photovoltaïque autonome dans des conditions environnementales variables.

Mots clés: Suivi le point global de puissance maximale, Méthodes Méta-heuristique, Cas d'ombrage partiel, Photovoltaïque. système autonome

ملخص الاطروحة

تعد الشمس مصدرًا لا ينضب للطاقة ويستقبل سطح الأرض إشعاعًا يمثل كل عام حوالي 15000 ضعف استهلاك الطاقة للبشرية تقريبًا. ولهذا تعد الطاقة الشمسية من اهم واكبر مصادر الطاقة النظيفة حيث أن كمية الطاقة الشمسية التي تصل إلى سطح الأرض خلال يوم واحد أكبر بعشر مرات من تلك المستهلكة ، ومن خلال التأثير الكهروضوئي ، يمكن تحويل الطاقة الموجودة في ضوء الشمس إلى طاقة كهربائية. يشجع الموقع الجغرافي للجزائر على تطوير استخدام الطاقة الشمسية ولكن دائمًا ما يعتبر انتاجها من الطاقة الشمسية غير كافٍ. من بين العديد من العوامل التي تؤثر على الاستغلال الامثل للطاقة الشمسية نجد تدفق الإشعاع ودرجة الحرارة. تم تقديم العديد من الدراسات لتحسين إنتاجية الطاقة وبالتالي ربح الحد الأقصى من تحويل الطاقة. نقترح في هذه الدراسة ، تطبيق التقنيات المختلفة: الحوسبة الناعمة وبالتحديد التقنيات الميتاهيريستيكية الحديثة و طرق الذكاء الاصطناعي، من أجل تحسين أداء تتبع نقطة الطاقة العظمى الناتجة من المولد الكهروضوئي وبالتالي استخراج اكبر طاقة ممكنة داخل نظام كهروضوئي مستقل و تحت ظروف بيئية متغيرة.

الكلمات المفتاحية: تتبع النقطة العظمى للاستطاعة الكبرى، الطرق الميتاهيريستيكية، حالة التظليل الجزئي، الكهروضوئية، النظام المستقل.

Scientific Production

I. Publications International

1. **Journal:** Journal of Electrical Engineering & Technology". Published by Springer, Journal indexed in ISI Thomson base, Scopus
   Title of paper: An Efficient Metaheuristic Technique to Control the Maximum Power Point of a Partially Shaded Photovoltaic System Using Crow Search Algorithm (CSA). J. Electr. Eng. Technol. (2021)16:381-402,
   DOI 10.1007/s42835-020-00590-8
   Authors: Yehya Houam, Amel Terki, Noureddine Bouarroudj.

2. Proceeding of Publisher IEEE Xplore, published in 01 Sept 2020.
   Title of paper: Soft Computing Methods for Tracking the Global Maximum Power Point of Photovoltaic System Subjected to Partial Shaded Conditions.
   Authors: Y. Houam, A. Terki, K .Touafek, A. Si Tayeb.
   L'article est publié à travers la conference: The first International Conference on Sustainable Renewable Energy Systems and Applications (ICSRESA'19). Tébessa Algeria.

3. Proceeding of Publisher IEEE Xplore, date of publication 02 May 2019.
   Title of paper: A New Design of Lead-Acid Battery Charger Based on Non-Inverting Buck-Boost Converter for the Photovoltaic Application.
   Authors: D. Rezzak, A. Sitayeb, **Y. Houam**, K. Touafek, N. Boudjer.
   Via the 6th International Renewable and Sustainable Energy Conference
   (IRSEC 2018) Morocco.

II. International Communications

1. ICSRESA'2019. The International Conference on Sustainable, Renewable Energy Systems and Applications, TEBESSA Algeria, 04-05 Dec 2019.
   Title of paper: Soft Computing Methods for Tracking the Global Maximum Power Point of Photovoltaic System Subjected to Partial Shaded Conditions.
   Authors: Y. Houam, A. Terki, K. Touafek and A.Si Tayeb.

2. IRSEC'2018 International Renewable and Sustainable Energy Conference, Rabat, Morocco, 5-8 Dec 2018
   Title of paper: Design and realization of an electrical module of control and energy management for hybrid energy systems photovoltaic - Networks electrical –
   generator. **Authors:** A. Si tayeb, D. Rezzak, **Y. Houam.**

3. IRSEC'2018, International Renewable and Sustainable Energy Conference, Rabat, Morocco, 5-8 Dec 2018
   Title of paper: new design of lead acid battery charger based on non- inverting buck boost converter for PV application.
   Authors: D. Rezzak, A. Si Tayeb, **Y. Houam,** K. Touafek , N. Boudjerda.

4. SIENR'2018, Séminaire International sur les Energies Nouvelles et Renouvelables, URAER Ghardaïa Algeria 2018.
Title of paper: Gestion du transfert d'énergie dans un système hybride autonome à base des modules photovoltaïque.
Authors: D. Rezzak, A. Si Tayeb, **Y. Houam**, K. Touafek, N. Boudjerda.

5. ICENT'2017 International Conference on Electronics and New Technologies, M'sila Algeria 14-15 Nov 2017
Title of paper: A comparative study of the maximum power point tracking methods for PV systems
Authors: Y. Houam, L. Saidi, K. Touafek, M. Adouane, D.Rezzak, A. Si Tayeb.

Table of Contents

Chapter I: State of the art and basic principles of MPPT Methods

Chapter II: Partial shading effects on both PV module and different PV array configurations

Chapter III: Simulation of metaheuristic MPPT methods under changing conditions

Chapter IV: Simple and Efficient metaheuristic technique to control the Maximum power of autonomous PV system

List of Figures

Chapter I

Chapter II

Chapter III

Chapter IV

List of Tables

Chapter I

Chapter II

Chapter III

Chapter IV

List of Abbreviations

PV: Photovoltaic

MPPT: Maximum Power Point Tracking

3S3P 3-Series-3-Parallel

CSA: Crow Search Algorithm

P&O Perturb and Observe

HC hill climb

LMPPT local maximum power point tracking

FFA Flashing Firefly Algorithm

ABC artificial bee colony

ACO Ant Colony Optimization

MFA: Modified Firefly Algorithm

MPP: Maximum power point

GMPP: Global maximum power point

CS cuckoo search MPPT

PSC Partial Shading Conditions

IC Incremental Conductance

PSO Particle Swarm Optimization

GWO grey wolf optimization

FPA: Flower Pollination Algorithm

ELPSO-P&O: Enhanced Leader PSO-P&O

FLC Fuzzy Logic Control

ANN Artificial Neural Network

PSO-ANFIS: hybrid method Adaptive Neuro Fuzzy Inference System based PSO.

P&O-PSO: hybrid method Particle Swarm Optimization combined with Perturb and Observe.

EL-PSO: hybrid method Enhanced Leader based Particle Swarm Optimization.

DLCI: Dynamic Leader Based Collective Intelligence.

List of Symbols

D: Duty cycle

ΔD: Step size of the duty cycle

D_{ibest}^{k} : best current duty cycle at iteration k

r: Random number

w: Inertial weight

x_{i}^{k} : Position of crow i at iteration k

m_{j}^{k} : Memory of crow j at iteration k

N: number of crows in the flock

T: Absolute temperature (°K)

v: Particle velocity (speed)

D_{gbest} : best global duty cycle

P_{i}^{k} : PV power at iteration k for the crow i

c_1, c_2: Acceleration coefficients

fl : is the flight length

AP: Awareness probability

k: iteration

P_{max}^{k} : Maximum PV power at iteration k

q: The charge of the electron (C)

k: Boltzmann constant (J/K)

V: Lyapunov function

General Introduction

The huge increase in worldwide energy consumption, is inexorably leading to the exhaustion of traditional energy sources (fossil fuels). the increasing of consumption energy as a results of the rapid growth in population, the unabated usage of technology, frequent human movement and the ever-increasing level of lifestyle, This phenomenon has resulted in two major concerns, namely energy sustainability and environmental concerns. The latter, which manifests itself in the form of climate change, is seriously jeopardizing the earth civilization. The limited reserves of the latter and the pollution they cause compel us to search for sustainable clean energy sources. The challenge today is to tackle the climate change and greenhouse warming by utilizing clean and affordable renewable energy (RE) sources [1-2]. Energy generated from renewable natural resources, such as solar, wind, rainfall, tidal, geothermal heat, etc have been applied for electric power generation. Compared to conventional fossil energy sources (coal, oil and natural gas), RE sources have the following major advantages (1) they are refilled from natural resources; therefore they are sustainable and will never run out, (2) when generating, they emit little or no carbon dioxide. It can be concluded that RE appears to be the ideal and effective solution to deal with the environmental problems. Today, solar energy is gaining ground as a preferred alternative due to its many merits such as the fact of being free, available, non-polluting, noise-free and easy to install [3]. For the past several decades, solar photovoltaic (PV) energy has emerged as one of the preferable RE sources. The sun radiates an enormous amount of energy onto the earth's surface every day, which, if properly harvested, would be more than sufficient to provide the demand of the whole world. The main advantages of PV power system can be attributed to its low operational cost, almost maintenance-free and environmentally friendly. Regardless of the high cost of solar panels, PV power generation systems, in particular the grid-connected type, have been commercialized in many countries due to its potential medium and long-term economic prospects. Furthermore, generous financial schemes, for example, the feed-in tariff and subsidized policies, have been introduced by various countries, resulting in rapid growth of the industry[3].

However, despite these tangible benefits, the main hindrance for public acceptance of PV system is still apparent, i.e. the high capital investment. This is primarily due to the high panel price. Although the price per watt has declined rapidly over the past decade, PV power remains considerably above the cost of conventional electricity. Grid-parity, i.e. the point at which the price of PV power per unit is less than or equal to the price of the electricity provided by the

power utility companies, is still a long way to go. With regards to this concern, it is imperative that whatever available energy captured by the panels to be the optimally processed. An enormous amount of work has been carried out to enhance the solar cell design and its fabrication technologies. Whilst these efforts are crucial, it is equally important to continually improve the overall performance at the system level.

Despite the advantages of solar source energy, the extracted power from photovoltaic generator is always influenced by changing weather conditions making it difficult to control power generation [4] especially if subjected to partial shading, which causes power inefficiency and prevents a PV system from operating optimally. Hence the need for an effective MPPT controller capable of extracting the maximum power under changing external conditions.

One area of immense interest is the maximum power point tracker (MPPT).

Due to the non-linear I-V characteristics of the PV source, the tracking of the maximum power point (MPP) at various environmental conditions can sometimes be a challenging task.

The effectiveness of an MPPT controller, and hence that of a PV system, is primarily dependent on the adopted MPPT method. Therefore, a lot of research effort has been directed to that field over the last decades. Researchers have proposed different MPPT algorithms to maximize PV power. The field of research in maximum power point tracking (MPPT) methods is experiencing great progress with a wide range of techniques being suggested, ranging from simple but ineffective methods to more effective but complex ones. Therefore, it is very important to propose a strategy that is both simple and effective in controlling the global maximum power point (GMPP) for a photovoltaic (PV) system under changing weather conditions, especially in partial shading cases (PSCs). Therefore, this thesis proposes a new simple an efficient design of an MPPT controller based on a metaheuristic optimization technique to attenuate the undesirable effects of partial shading on the tracking performances of standalone PV systems. A review paper in Ref [5] has shown that MPPT methods can be classified into conventional, soft computing, and hybrid methods.

In an attempt to attenuate the demerits of existing MPPT techniques, this thesis proposes a new control strategy of global maximum power for isolated PV systems using metaheuristic Crow Search Algorithm, the proposed MPPT technique can mitigate the adverse effects of partial shading on the tracking performances of a GMPPT controller.

1.1 Background and thesis motivation

With the increasing of consumption energy in worldwide, which inexorably leading to the exhaustion of traditional energy sources. The limited reserves of the latter and the pollution they cause compel us to search for sustainable clean energy sources. Today, solar energy is gaining ground as a preferred alternative due to its many merits such as the fact of being free, available, non-polluting, noise-free and easy to install [1][2]. Despite these advantages, the extracted power from photovoltaic generator is always influenced by changing weather conditions making it difficult to control power generation [4] especially if subjected to partial shading, which causes power inefficiency and prevents a PV system from operating optimally. Hence the need for an effective MPPT controller capable of extracting the maximum power under changing external conditions. The effectiveness of an MPPT controller, and hence that of a PV system, is primarily dependent on the adopted MPPT method. In this thesis, the maximum power point tacking unit was developed to maximize the extracted PV power for standalone PV system subjected to all changing weather conditions.

1.2 Problem statement

PV systems are installed near urban areas, where buildings, trees and lot of objects naturally form shadows, which can also be produced by clouds. Fig.1 shows exemples of partially shaded PV system, which includes series-connected PV modules modules, DC-DC converter (boost in our work).

The shadow form a grand problem for PV system because it degrade the performance of the entire PV system, and decrease its generated output power. The shading problem produces hot spotting in PV cells that is a reliability problem in PV panels, where a mismatched cell heats up significantly and degrades PV panel output power. High PV cell temperature due to hot spotting can damage the cell encapsulate and lead to secondary breakdown, where both cause permanent damage to the PV panel, thus the shading problem is considerably malfunction maximum power extraction from PV modules.

This thesis will outline novel strategy of control to track the maximum power point of partially shaded PV system using an efficient metaheuristic optimization technique, which could be used to enhance the output power of shaded PV solar cells and ensure an optimal operating under all changing weather conditions.
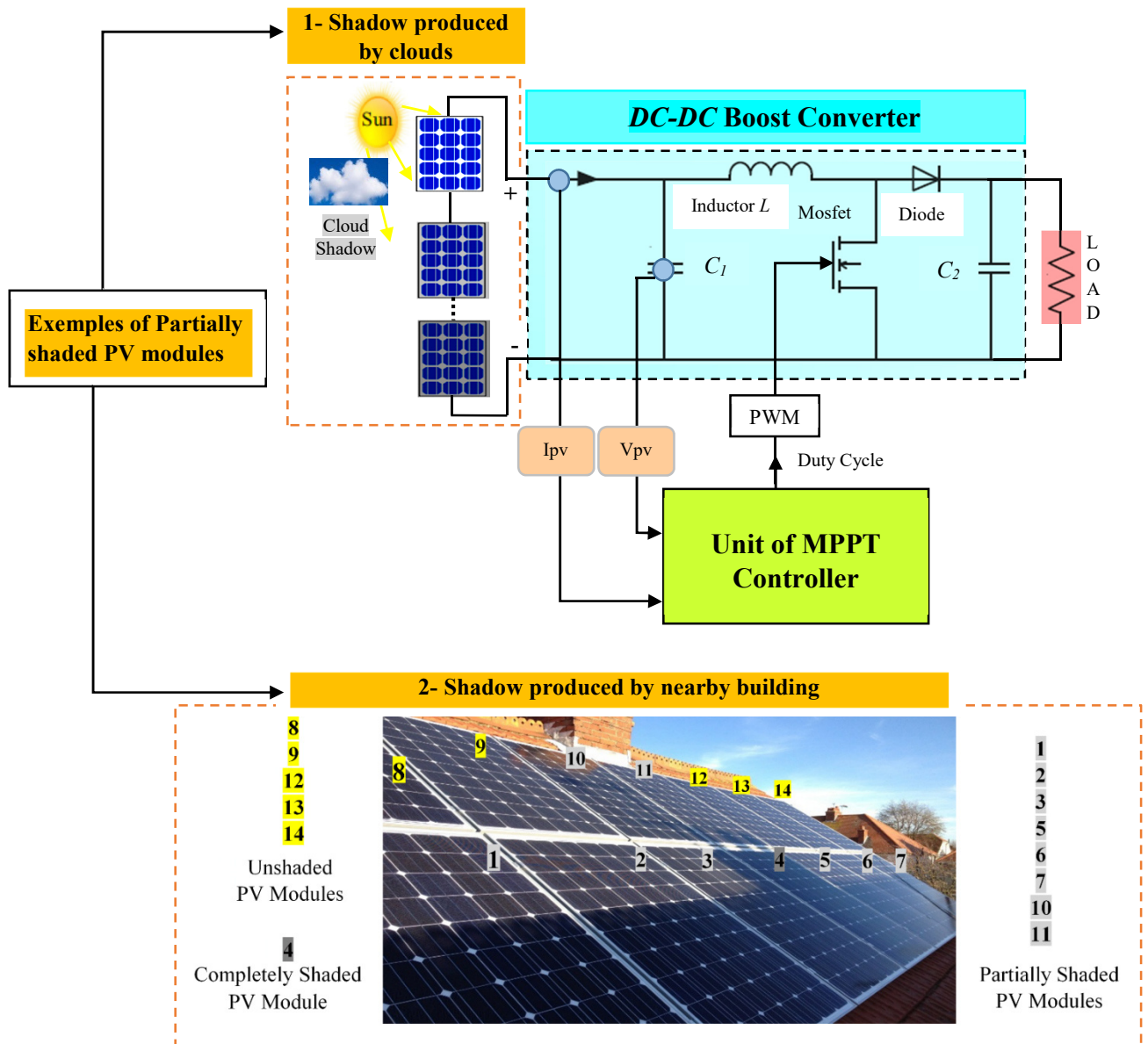
Fig. 1. General diagram of an autonomous PV system with a MPPT controller and examples of partial shade

1.3 Aim and objectives

The main aim of this research work is to develop and implement a robust and efficient MPPT controller can be ensure optimal operating of PV system under all changing weather conditions.

1.4 Thesis contributions

This thesis demonstrates research contribution and technical advancement over the existing solutions. This contribution can be described as follows:

The main contribution of this thesis is attempt to develop a new fast and efficient control strategy of the global maximum power point (GMPP) for partially shaded standalone PV system

using metaheuristic optimization technique named Crow Search Algorithm (CSA) to mitigate the adverse effects of partial shading on the tracking performances of the GMPPT controller. The idea of this contribution is combines good performances of CSA based GMPPT controller on the one hand and the simplicity of algorithm processes with few tuning parameters (only two) on the other hand. Additionally, it decreases the difficulties and the cost of implementation, and reduces the calculation time. A large number of tuning parameters (four to seven parameters) in many MPPT methods increase the computational load and require a high-end microcontroller. In comparison with existing MPPT techniques. The proposed CSA technique requires setting only a few parameters (two parameters) to obtain a good performance, where it ensure the following good tracking performances: fast convergence towards GMPP, high efficiency in extracting of maximum power from a PV panel and robustness under all changing atmospheric conditions. Our study focused on PV isolated systems, given its great importance, the latter is used in many clean energy extraction systems such as PV water pumping systems in agricultural rural areas, electricity domestic rural, street lights, electric cars, space system, etc.

This contribution presented in **chapter 4**, it is published in:

"Journal of Electrical Engineering & Technology". Publisher Springer.

Title of paper "An Efficient Metaheuristic Technique to Control the Maximum Power Point of a Partially Shaded Photovoltaic System Using Crow Search Algorithm (CSA)". J. Electr. Eng. Technol. (2021) 16:381-402.

Authors: Yehya Houam, Amel Terki, Noureddine Bouarroudj.

1.5 Thesis outline

This thesis is organized into four chapters as follows:

Chapter 1:

This chapter gives a state of art of the existing MPPT methods, in addition to an overview on the factors influencing the efficiency of the photovoltaic system. in this part we have explained the basic principles of the most used classical and modern MPPT techniques.

Chapter 2:

This chapter explain the partial shading problem and its influences in the extracted PV power performance from PV generators. In this part we simulates the models of PV cells and some PV array configurations under uniform irradiation case and various partial shading cases, Four PV array configurations have been tested including S, P, SP, TCT. To show the effects of partial

shading (PS) on the electrical characteristics Power-Voltage (P-V) and Current-Voltage (I-V) of each proposed model, where all tests have been carried out using MATLAB/Simulink software.

Chapter 3:

In this chapter, we checks the tracking performances of the three MPPT methods that include two metaheuristic methods are Particle Swarm Optimization (PSO) and Cuckoo Search (CS) and one traditional method is Perturb and Observe (P&O) for a standalone PV system equipped by DC-DC boost converter. We perform this simulation under four different cases contain fixed and variable weather conditions depending of the irradiation levels and temperature. In addition, this chapter presents a quantitative comparison between the proposed MPPT methods P&O, PSO and CS.

Chapter 4:

This chapter presents a new contribution in MPPT methodologies literatures that is new design of a fast and efficient MPPT controller based on metaheuristic optimization technique called Crow Search Algorithm (CSA). This new control strategy is designed for mitigating the unwanted effects of partial shading on the tracking performances of global maximum power point GMPP for a standalone PV system. Based on simulation results using MATLAB/Simulink software, an accurate quantitative and qualitative comparison have been carried out in this chapter between CSA based MPPT technique and others classic and metahueristic MPPT methods are P&O and PSO.

Chapter I

State of the art and basic principles of MPPT methodologies

| Chapter I | State of the art and basic principles of MPPT Methodologies |

I.1. Introduction

The evolution of smart isolated PV systems concept has accelerated the widespread use of PV systems and solar energy that plays a vital role in off-grid generation systems. However, there are several challenges for PV power generation such as low power conversion efficiency and increased installation cost. Further, the maximum output power from a PV system largely varies under changing atmospheric conditions. The recent literature reveals that more researches have been carried out to increase the performance of the PV system. The efficiency can be increased by implementing highly efficient material for manufacturing solar cells, finding appropriate MPPT techniques to identify maximum power point and to avoid load mismatch problems and on DC-DC converters [6]. Maximum power point tracking is a major challenge in the use of PV systems since the current -voltage (I-V) and power-voltage (P-V) curves are nonlinear in nature. To complicate further, this characteristic curves depend on solar insolation and ambient temperature. As these parameters vary continuously, tracking MPP is a major problem. However, when the PV arrays in a PV power generation system receive uniform solar insolation, there exists a single MPP in the P-V curve. MPPT is then performed using several traditional methods and few of the prominent schemes are perturb and observe (P&O), incremental conductance (INC) and hill climbing (HC) method. These methods vary in complexity, sensors required, convergence speed, and cost of the system. It is worth mentioning that the traditional MPPT schemes are effective and time tested under uniform solar insolation alone. but some of PV arrays can be expose to partial shadow due to neighboring buildings, trees, poles, and moving clouds. Under partially shaded conditions (PSC), the P-V curve becomes more complex as it is characterized by multiple power peaks. The maximum power point among the multiple peaks is termed as global maximum power point (GMPP) and all other peaks are called as local maximum power points (LMPPs). The traditional MPPT schemes referred in the previous paragraph which are useful for uniform insolation cannot be effectively used for MPPT under partially shaded conditions since these methods cannot distinguish between LMPPs and GMPP [7]. for this reason, several researches have been undertaken to solve this problem, as recent research has provided several effective methods under all changing natural conditions, which are called soft computing (SC) techniques that includes the

inteligence artifficiel (AI) methods and methaheuristics methods, which we will focuses our study. This section gives the state of the art of MPPT methodologies and basic principles of MPPTs techniques that existing in literatures moreover, we present in this chapter an overview of the most important factors that influence the efficiency of photovoltaic systems.

I.2. State of the art of MPPT methodologies:

A review paper in ref [8] has shown that MPPT methods can be classified into conventional, soft computing, and hybrid methods. The conventional MPPT methods has been reviewed by Ahmed and Salam in ref [9], the authors mentioned many conventional MPPT methods as Perturb and Observe (P&O), Incremental Conductance (IC), Hill Climbing (HC), Extremum Seeking Control (ESC), Fibonacci Searching Ripple Correlation Control (RCC), Fractional Short Circuit (FSC), Fractional Open Circuit (FOC) and more. Conventional methods operate well in uniform conditions of irradiation and temperature but are inefficient in tracking GMPP and exhibit poor performance under partial shading conditions [10], while Soft Computing (SC) techniques include artificial intelligence (AI), metaheuristic and evolutionary algorithms (EA).

For artificial intelligence based MPPT, Salah and Ouali in ref [11] used fuzzy logic control (FLC) for the MPPT problem; they confirmed the superior tracking performance of FLC based MPPT technique compared to Artificial Neural Network (ANN). Despite FLC merits, it is largely dependent on the characteristics of the PV system and requires a prior knowledge of the design specifications. Karatepe and Hiyama in ref [12] indicated that FLC and ANN are incapable of tracking GMPP under PSCs. Adaptive neuro-fuzzy inference system (ANFIS) technique combines fuzzy logic with neural network. Ismail and Bendary [13] demonstrated the efficiency of the ANFIS based MPPT controller for 60 MW grid-connected hybrid PV systems. They used two ANFIS controllers: one for controlling the battery charging process and the other for on/off battery switching as another power source is connected to the grid depending on load change. Shaik and Kannappan [14] designed an efficient control system with an Adaptive Neuro-Fuzzy Interface for a rule-based controller to protect the energy storage system in hybrid electric vehicles from nonlinearities and uncertainties. We can find improved AI based MPPT. Adly and Besheer [15] designed an optimized adaptive fuzzy based MPPT controller using Ant Colony Optimization (ACO) for a standalone PV system.

Recent researches proposed several metaheuristic optimization methods that are widely used to solve difficult optimization problems in engineering and many other important areas. These recent metaheuristic methods guarantee high efficiency and reasonable computational cost in the resolution process [16]. Some of the most used metaheuristic optimization methods in literature are Particle Swarm Optimization (PSO), Cuckoo Search (CS), Bat Algorithm (BA), Artificial Bee Colony (ABC), Grey Wolf Optimization (GWO), Firefly Algorithm (FA), Flower Pollination Algorithm (FPA), Mine Blast Optimization (MBO), Salp Swarm Algorithm (SSA) and Dragonfly Optimization Algorithm (DFO). We can use metaheuristic methods to mitigate the drawbacks of conventional and AI based MPPT methods. Miyatake et *al*. [17] implemented PSO for experimental MPPT tests under PSCs using a DSP (TMS320C32) platform and the results proved that the method is able to find the GMPP even under complex PSCs, outperforming fixed voltage, hill climbing, and Fibonacci techniques. Many improvements in the standard PSO have been introduced for MPPT application such as Deterministic PSO (DPSO) in ref. [18], Adaptive Perceptive PSO (APPSO) in ref [19], Leader PSO (LPSO) in ref [1]. However, the modified PSO methods have become hugely complex with increasing number of parameters [20]. Ahmed and Salam [21] used Cuckoo Search algorithm (CS) to track GMPP for gradual, steep and rapid changes of irradiance and temperature. The best tracking performance of CS method has been verified by simulation and experimental results. Sundareswaran et *al*. [22] developed the Artificial Bee Colony (ABC)-based MPPT technique for two different PV array configurations under PSC; the experimental results showed that the developed technique rapidly reached the GMPP and reduced power oscillations. Mohanty et *al*. [23] verified experimentally the successful implementation of GWO via dSPACE1104 for resistive and inductive loads in PSCs.

Gravitational Search Algorithm (GSA) is a metaheuristic optimization technique inspired by the Newtonian laws of gravity and motion [24], Li et *al* [25] introduced an improved GSA based MPPT, they enhanced the search precision of GMPP and reduced the oscillations by adding dynamic weight, related factors of memory and population information exchange in the standard GSA. Kaced et *al*. [20] utilized Bat algorithm (BA) for MPPT to handle the shading problem and demonstrated that this method can reach rapidly the global peak GMPP under PSCs through simulation and experimental validation using FPGA card. Wu and Yu [26] proposed the improved Bat Algorithm (IBAT)-based MPPT by introducing an adaptive weight parameter to improve the global searching ability of the algorithm. They ensured a fast and accurate tracking of GMPP, and confirmed that the proposed method outperforms

many MPPT methods such as P&O, IP&O, PSO, FA, FPA, ABC and BA under various PSCs. Ram and Rajasekar [10] succeeded experimentally in confirming the ability of FPA to converge to GMPP in less time under all shading cases using Arduino card. The authors Abdalla et *al*. [27] revealed the capability of Wind Driven Optimization (WDO) technique to track GMPP by simulation under PSCs in comparison to PSO, Differential Evolution (DE), Harmony Search Algorithm (HSA), Bat Algorithm (Bat), Sine-Cosine Algorithm (SCA), Cuckoo Search (CS), and Genetic Algorithm (GA). The novel meta-heuristics methods proposed by Mirza et *al*. [2] are Adaptive Cuckoo (ACOA), Dragonfly Optimization Algorithm (DFO) and combined General Regression Neural Network technique with Fruit Fly Optimization Algorithm (GRNN-FFOA), and their results revealed that the proposed techniques outperform P&O, PSO, ABC, CS and PSO-Gravitational Search Algorithm (PSO-GSA) in term of tracking performances under PSCs.

In spite of the excellent performances of the mentioned meta-heuristic methods under PSCs, most of them suffer from some drawbacks such as structure complexity, high number of tuning parameters, weak compromise in the exploration-exploitation process search [20] in addition to the problem of randomness. To solve these shortcomings, researchers suggested combining two methods in a hybrid one to keep the benefits of each method [1] as is the case of P&O-PSO, GWO-FLC, ANFIS-GA, DE-PSO and PSO-GSA. For the hybrid methods, Lian et *al*. [28] introduced P&O-PSO to reduce the convergence time for a large search space of particles and the excellent performances of the proposed method were verified using an experimental setup. In another contribution, DE-PSO method was developed by Seyedmahmoudian et *al*. [29] to decrease the negative impact of arbitrary coefficients on the search process. Simulation and experimental results confirmed the superior performance of Differential Evolution-PSO (DE-PSO) method with respect to reliability, speed and accuracy in GMPP tracking under PSC. Yet it has a problem of oscillation within the tracking period. With the rapid progressing of Genetic Algorithm (GA) in the area of optimization, the controllers designing field with GA has gradually become a significant direction [30]. Sundareswaran et *al*. [31] proposed a GA-P&O technique combining GA with P&O under PSCs; first, they selected six uniformly distributed chromosomes for three iterations in GA and then initialized the duty cycle of P&O to ensure efficient and rapid tracking of GMPP. Mohamed et *al*. [32] demonstrated through simulation results the successful implementation of PSO-GSA technique for tracking the GMPP compared to GWO, Moth-Flame Optimization (MFO) and Salp Swarm Algorithm (SSA) methods. While combining the benefits of each

method, the hybrid technique remains complex in structure with many parameters, resulting thereby in long computation time and difficult hardware implementation [1].

Table I.1 summarizes the different most important existing MPPT methods in literature.

Table I.1 Summary of the most important existing MPPT methods in literature

Authors	Year	MPPT technique	Converter	Simulation or Experimental	Contribution
Elgendy et al.[33]	2014	Perturb and observe P&O	Buck	Matlab + DSP TMS320F2812	Verified the performance of P&O for resistive and motor-pump loads under uniform and rapidly changing irradiance with high perturbation rates.
Chen et al.[34]	2016	Fuzzy logic control FLC		PSIM + DSP TMS320LF 2407	Confirmed the best performance of FLC based auto-scaling variable step-size compared to fixed step of INC.
Kaced et al.[20]	2017	Bat Algorithm BA	Buck-Boost	Matlab + FPGA (Xilinx Virtex -5)	Assessed the performance of BA algorithm compared with P&O and PSO under PSC.
Ram and Rajasekar [10]	2016	Flower Pollination Algorithm FPA	Boost	Matlab + Arduino	Evaluated the performance of FPA compared with P&O and PSO under PSC.
Eltamaly et al. [35]	2019	Hybrid GWO-FLC	Boost	Matlab/Simulink	Proved the superior performance of GWO-FLC in terms of dynamic GMPP catching and MPPT power efficiency in PSCs
Ram et al.[36]	2019	Hybrid Enhanced Leader PSO-P&O ELPSO-P&O	Boost	Matlab + Arduino	Used ELPSO initially to find the global best leader then introduce P&O after the detection of the global solution space.
Shi et al.[37]	2017	Hybrid Incremental Conductance and Firefly Algorithm INC-FA	Boost	Matlab +DSP	Adapted INC for repaid search for a single peak, then use FA, which has more powerful global search ability
Fathy and Rezk.[38]	2016	Mine Blast Optimization MBO	Boost	Matlab/Simulink	Evaluated the performance of MBO compared with TLBO under PSC
Ahmed and Salam.[39]	2018	Enhanced Adaptive P&O	Buck-Boost	Matlab+DSpace (DS1104)	Used a smart oscillation detection scheme with dynamic boundary condition based on an intelligent prediction feature.
Seyedmahmoudian et al. [40]	2016	Radial Movement Optimization RMO	CUK	Matlab	Evaluated the performance of RMO algorithm compared with PSO under PSC.
Sundareswaran et al.[41]	2014	Firefly Algorithm FA	Boost	Matlab + PIC16F876	Confirmed the best performance of FA compared with P&O and PSO under PSC.
Yang et al.[42]	2019	Memetic Salp Swarm Algorithm MSSA	Boost	Matlab+DSpace (DS1104)	Introduced a multiple independent salp chains in SSA to develop new Memetic SSA (MSSA) for MPPT in PSC, and proved that they outperform INC, GA, ABC, CS, GWO, TLBO and SSA
Yang et al. [43]	2019	Dynamic Leader Based Collective Intelligence Algorithm DLBCI	Buck-Boost	Matlab + dSpace	Introduced multiple sub-optimizers feature in DLBCI to ensure deeper exploitation by various searching mechanisms.

I.3. Factors influencing in efficiency the photovoltaic systems

I.3.1. Materials of solar cells

After recognizing the importance of solar cells materials to increase the efficiency of PV systems researches were carried out to improve the efficiency by employing the proper material for manufacturing the solar cell. According to scientific literature, the cost effective and more efficient solar cell materials have been evolved through three generations by crossing the stages of continuous improvement from one generation to another. Among them, the solar cells of the first generation are mainly made of single silicon crystal with moderate efficiency but at high cost. Continuous research on cost reduction and efficiency improvement paved way for the development of thin film second generation solar cells which are cost effective and has enhanced cell efficiency. Thin film solar cells are more flexible, easy to handle and low current losses due to presence of more number of layers. The solar cells of third-generation are based on dye sensitized, polymer, Nano-crystals materials and Nano-porous materials, which produces the highest efficiency [6].
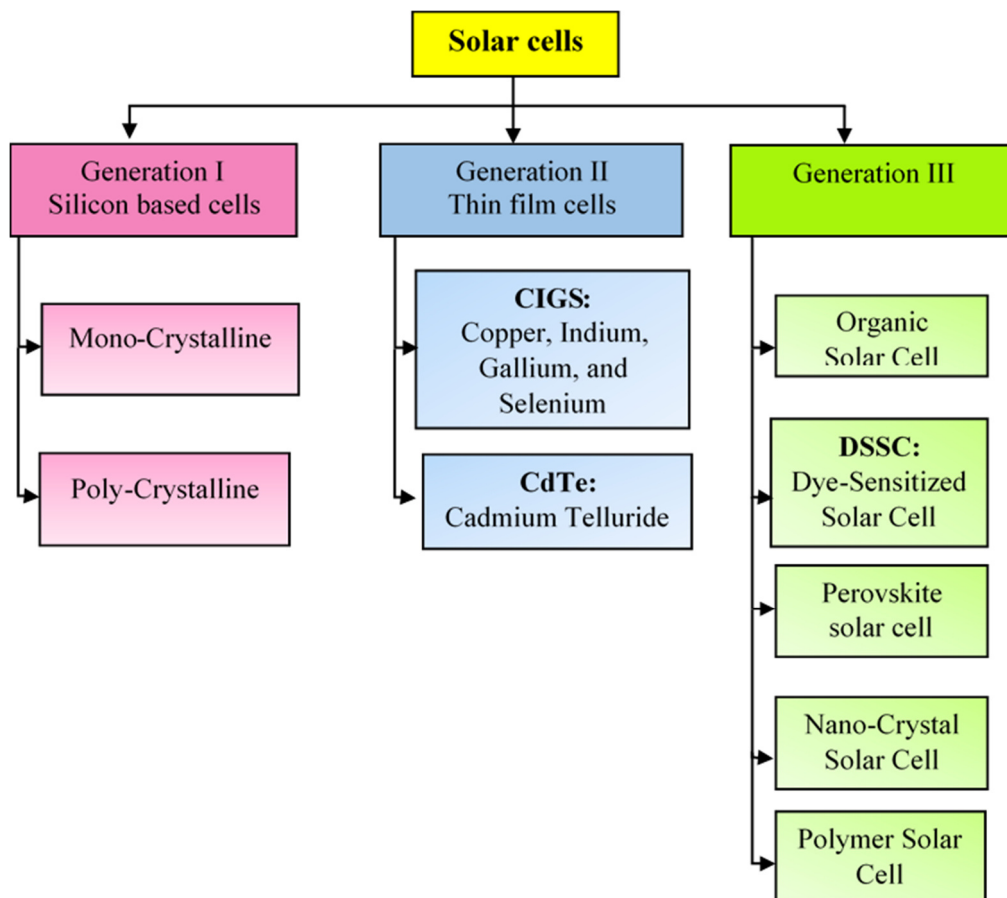
Fig.I.1 Classification of Solar Cells [6].

This section studies the role of solar cell materials on the efficiency of the PV System. Fig.I.1 shows the summarization of solar cells classification based on generations.

The efficiency of the solar cell materials is shown in the Fig. I.2 [6].
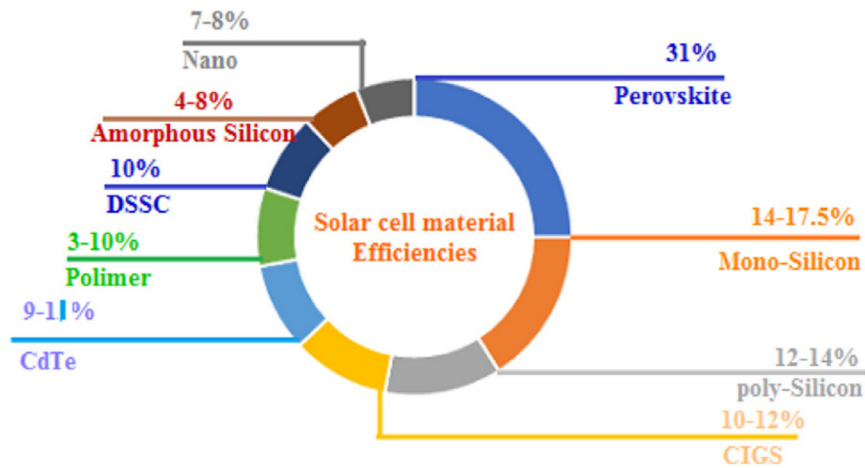
Fig.I.2. Efficiency of various PV materials [6].

I.3.2. DC-DC converter

A DC-DC converter is an electronic circuit used to transfer the power from source to load. For tracking solar power, which are stochastic in nature. a DC-DC converter along is inserted in between the load and PV module, that it controlled with MPPT algorithm to achieve load matching and ensure that the PV system is operating near MPP, and extracting maximum power from PV panel [44]. The efficiency of the solar PV systems depends on DC-DC converter, to analyze the performance of the PV systems that can employ many DC-DC converter topologies, there are large number of DC/DC converters and it is more than 500 prototypes approximately the available DC-DC converters are classified into six generations and presented in this section as:

- First generation (classical converters: Buck, Boost, Buck-Boost, SEPIC, Push-Pull, and Half Bridge).
- Second generation (multi-quadrant) converters.
- Third generation (switched-component SI/SC) converters.
- Fourth generation (soft-switching: ZCS/ZVS/ZT) converters.
- Fifth generation (synchronous rectifier SR) converters.
- Sixth generation (multiple energy-storage elements resonant MER) converters [6].

The classification of converters is shown in Fig. I.3.
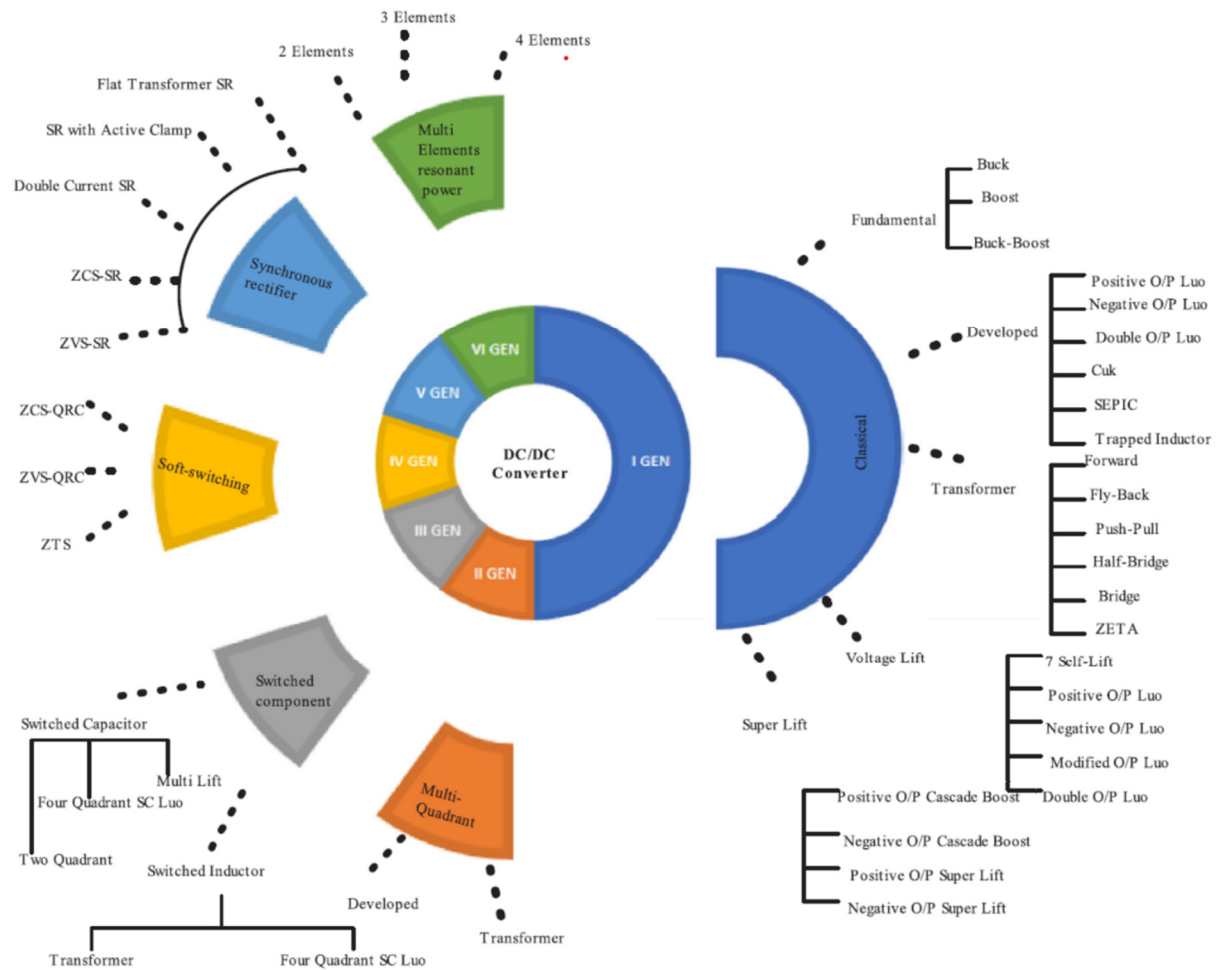
Fig. I.3. Classification of DC/DC converters [6].

I.3.3. Maximum power point tracking techniques

Photovoltaic system has several advantages like sustainability, less maintenance cost, free operation, and absence of complex parts, environment friendliness, and so forth. A main drawback is the high initial cost, so it has become necessary to operate the system at its maximum power point (MPP) at given solar irradiation. This has necessitated the incorporation of maximum power point tracking (MPPT) techniques with photovoltaic systems. MPPT technique is generally used in combination with a power converter to optimize the performance of large-scale photovoltaic modules. The MPPT technique makes the photovoltaic system to generate maximum power regardless of variation in environmental parameters like ambient temperature, and solar irradiation. Since the MPP location varies in a nonlinear manner with respect to these environmental parameters, tracking the maximum power point is a difficult task and has been successfully performed using various techniques [45].

The MPPT techniques can be classified into three main categories:

- **Classic techniques:** such as Perturb and Observe (P&O), Incremental Conductance (IC) Hill Climbing (HC), Fractional Open Circuit Voltage (FOCV) and Fractional Short Circuit Current (FSCC).

- **Soft Computing techniques:** this category include the modern techniques such as Fuzzy Logic Control (FLC)-based techniques, Artificial Neural Network (ANN)-based techniques and metaheuristic-based techniques.

- **Hybrid MPPT techniques** Hybrid MPPT technique is a combination of conventional/soft computing or soft computing/conventional or soft computing/soft computing [8].

I.3.3.1. Classic MPPT techniques

The popular classic techniques like P&O, HC & IC are capable of tracking maximum power only under uniform irradiation and these methods utterly fails when partial shading occurs i.e., panels in an array receive unequal irradiation. Whilst the main shortcoming of Fractional Short Circuit (FSC) and Fractional Open Circuit (FOC) method is that it is less accurate and these techniques are only favored in low power applications. Further, classic methods show poor convergence, slow tracking speed and high steady state oscillations. Therefore to track MPP under partial shading conditions conventional methods need to fused with other methods for better performance. Meanwhile a new adaptive P&O technique having modifications from fixed step size to variable step size have been proposed in [46] [47]. Even-though the above alterations have enhanced its performance but not sufficient enough under all operating conditions [48].

I.3.3.2. Soft Computing MPPT techniques:

Conventional methods MPPT techniques fail to track MPP effectively under rapidly changing atmospheric conditions and under partial shading conditions PSC's. As an alternative to timeworn conventional methods, Soft Computing Algorithms have been put forth in the field of solar PV research based MPPT, they are introduced to track MPP under PSC's and all changing atmospheric conditions more effectively and quickly. Most attractive features of SC techniques are:

- Approximation to achieve tractability.
- Ability to handle non-linearity.
- Adaptability to atmospheric conditions such as PSC's and rapid changes in irradiance.

- Low cost.
- Uncertainty.
- Tolerance for imprecision.
- Robustness.
- Wide exploration in search pace.
- Coherent skill to reach global optimal regions these methods is considered a prime choice for non-linear optimization [10] [48].

The methods that fall under soft computing techniques for MPPT application are Fuzzy Logic Control (FLC), Artificial Neural Network (ANN), Genetic Algorithm (GA), and metaheuristic techniques that include Particle Swarm Optimization (PSO), Chaotic approach, Differential Evaluation (DE), Cuckoo Search (CS), Bee Colony Search algorithm (ABC), Ant Colony Optimization (ACO), Fireflies Algorithms (FA) and Random Search methods (RS). The soft computing techniques, which used in MPPT, are classified in Fig. I.4. [49].

Among the soft computing methods, ANN and FLC are knowledge-based system where it requires a detailed knowledge while implementing the algorithm. ANN and Fuzzy Logic are effective in tracking MPP but require large memory for training and rules implementation [8].
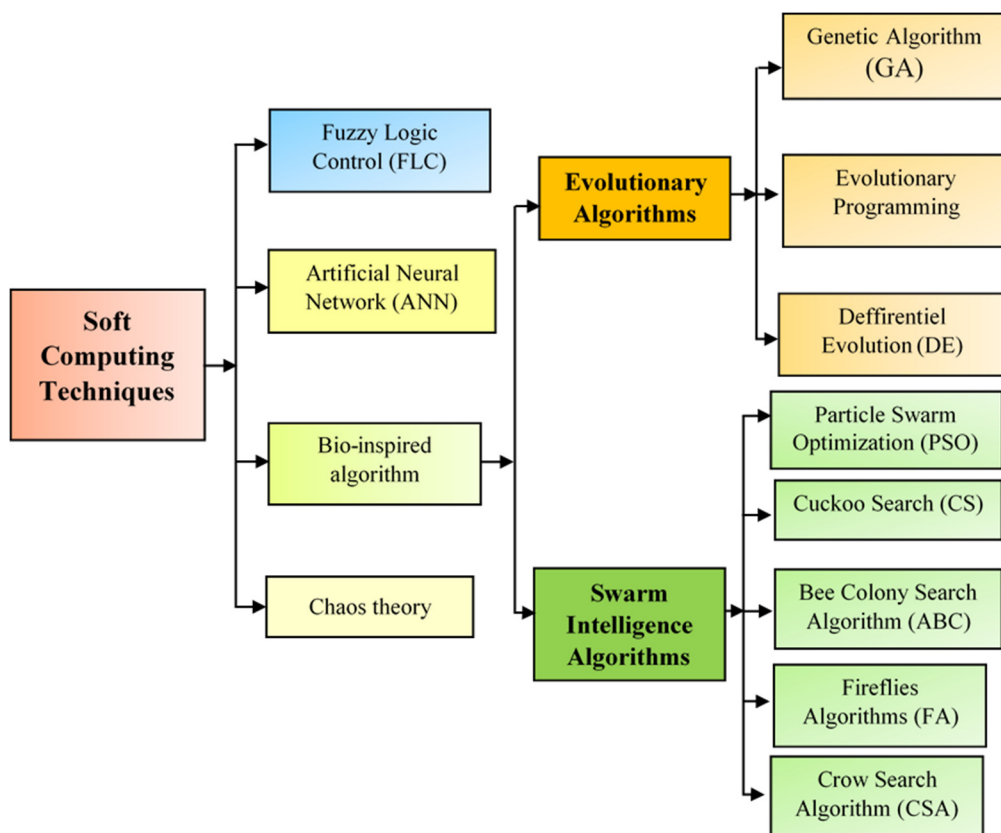
Fig. I.4. Soft computing techniques used for MPPT application [49].

In particular, the fuzzy logic method suffers from a severe drawback that the rules cannot be changed, once it is defined. Further, these algorithms are heavily pounded in reaching global maximum under partial shaded conditions. Since the amount of training involved is quite high, it makes its implementation even more complex. In a similar way, Fibonacci and DIRECT MPPT based approaches faces similar drawback and made these algorithms unfeasible in reaching global optimum [48].

I.4. Basic principles of MPPT methods

I.4.1. Perturb and observe P&O

The Perturb-and-Observe P&O is the most frequently used technique to track the maximum power because of its simple structure, P&O technique works by perturbing the PV system by incrementing the array operating voltage and observing its impact on the array output power. Because of constant step width, the system faces high oscillation especially under unstable environmental conditions. Some techniques used waiting time to avoid high oscillation; however, it also makes the MPPT slower to respond to weather changes. Also, this technique suffers from wrong operation, especially in case of multiple local maxima when working in partial shading conditions [50]. The flowchart of P&O based MPPT is shown in Fig. I.5.
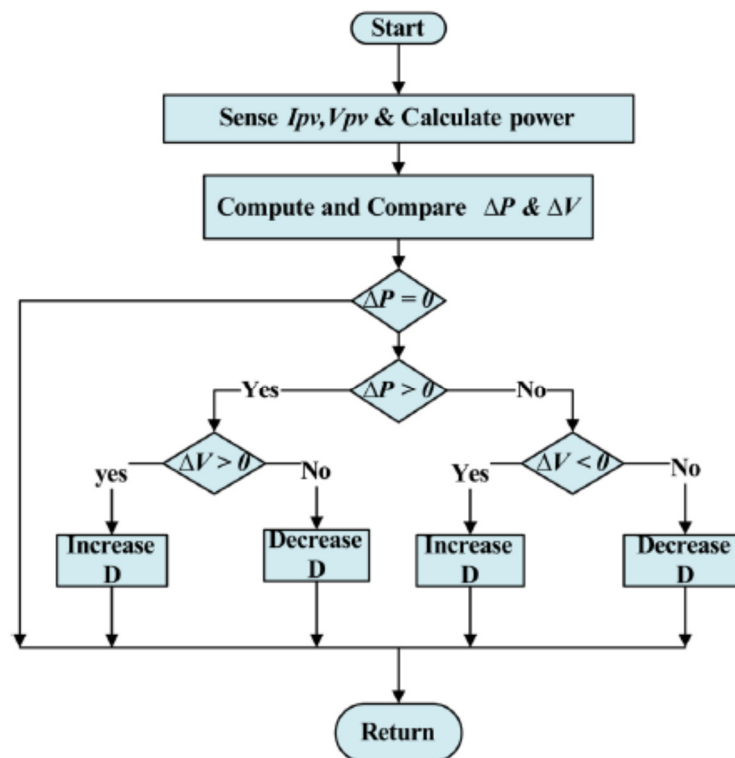
Fig. I.5. Flowchart of P&O based MPPT algorithm [50].

Many modifications for this technique have been presented in literature. A common problem in this technique is that the PV module terminal voltage is perturbed every MPPT cycle. Therefore, when the MPP is reached, the output power oscillates around its MPP, resulting in power loss in the PV system. A modified P&O technique has been introduced in [51] to remedy this problem by multiplying the change in the duty ratio by dynamic constant depending on the previous change in the extracted power. Another technique [52] used artificial neural network to predict this multiplying constant. These techniques increase the complexity of the system and may cause more oscillations in stable weather conditions [50].

I.4.2. Incremental conductance (IC) method

To track MPP, Incremental Conductance (IC) method utilizes the ratio of incremental conductance to instantaneous conductance value of the PV module. The flowchart for simple INC based MPPT method is shown in Fig. I.6 As an alternative to the P&O method, through the IC method, based on differentiating the PV power with respect to voltage and setting the result to zero which formulate as:

$$\frac{dP_{pv}}{dV_{pv}} = I_{pv} + V_{pv}\frac{dI_{pv}}{dV_{pv}} = 0 \tag{I-1}$$
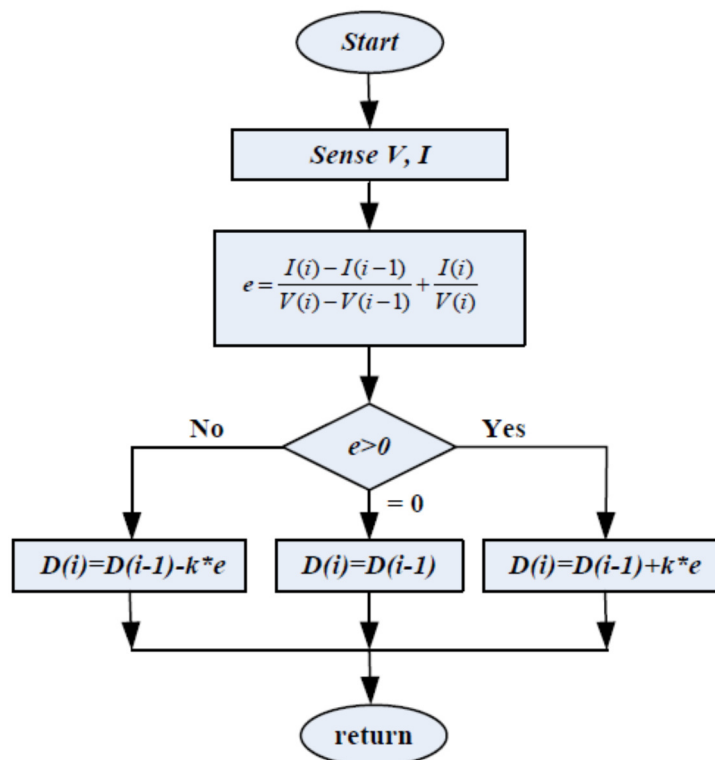
Fig. I.6. Flowchart for Incremental conductance algorithm based MPPT [48].

For MPP tracking applying IC algorithm follows three common steps:

1. When (dP/dV= 0), the error is zero and Vmp can be achieved.

2. When (dP /dV > 0), (i.e.,) (dP/dV > − I/V), the MPP is dragged to- wards the left of the curve (error is positive).

3. When (dP/dV< 0) (i.e.,) (dP/ dV< − I/V), the MPP is dragged to- wards the right of the curve (error is negative).

INC method tracks the MPP accurately by comparing the INC dI/dV and chord conductance I/V. This algorithm presents the advantage that no oscillation occurs around the MPP in steady state. However, the drawback of the method is the complexity to design its controller. INC method showed excellent performance for steady change in irradiated conditions. However, it fails to reach equilibrium state quickly and the converter duty cycle continues to oscillate around the MPP [48].

I.4.3. Fuzzy logic controller (FLC) method

Fuzzy logic is a superset of conventional (Boolean) logic that has been extended to handle the concept of partial truth: the truth values between ''completely true" and ''completely false". Value between truth and false can be recognized by Fuzzy logic. With fuzzy logic, propositions can be represented with degrees of truthfulness and falsehood. For example, the statement today is sunny, might be 100% true if there are no clouds, 80% true if there are a few clouds and 0% true if it rains all day. Mathematical model of system is not required in FLC, hence non linear systems can easily dealt with FLC. Process structure for a critical FLC is shown in Fig. I.7.
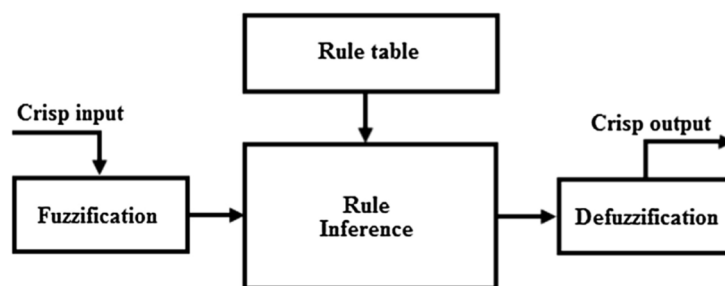
Fig. I.7. Basic fuzzy logic structure [53].

FLC is implemented in three stages:

➢ Fuzzification, crisp inputs are fuzzified into linguistic variables based on the membership functions.

➢ Fuzzified inputs are then compared with the fuzzy rule base for making decision. Rule base provides certain possible combinations to satisfy various conditions.

➢ Defuzzification, linguistic variable are converted back to analog signal by defuzzification process which control the power converter. Error and change in error is given as input to FLC. Error is calculated from irradiance, temperature, PV voltage, PV current or out power [53].

Fuzzy systems are generally classified based on the type of IF-THEN rules. The two most prevalent fuzzy systems are the MAMDANI and the Takagi-Sugeno-Kang (TSK) models. These two systems differ in the way their rules are formulated.

➢ Takagi-Sugeno-Kang TSK Model: IF x is A_i AND y is B_i THEN z is (ax+ by+ c).

➢ Mamdani model: IF x is A_i AND y is B_i THEN z is C_i, where, a, b, c, A_i, B_i and C_i are the constants, and x and y are the inputs and z is the output.

The rules usually depend on the selected linguistic variables. Many of the proposed schemes generally take ΔP, ΔV and/or ΔI or their ratios as inputs, and the change in duty cycle, ΔD as the output. Fuzzy logic controllers generally mimic either the P&O or the Incremental Conductance algorithms. [53] [54]. The proposed fuzzy logic controller based MPPT has two inputs and one output. The two FLC input variables are the error E and change of error CE at sampled times k defined by:

$$E(k) = \frac{P(k) - P(k-1)}{V(k) - V(k-1)} \tag{I-2}$$

$$CE(k) = E(k) - E(k-1) \tag{I-3}$$

Where $P(k)$ and $V(k)$ is the instant power and voltage of the photovoltaic generator. The input $E(k)$ shows if the load operation point at the instant k is located on the left or on the right of the maximum power point on the PV characteristic, while the input (CE) expresses the moving direction of this point. The output of the Fuzzy controller (dD) is given by equation (I-4):

$$D(k) = D(k-1) - dD \tag{I-4}$$

Several FLC based MPPT techniques has been proposed in many recent researches, they results revealed that the FLC based MPPT perform better when compared to conventional methods like P&O, INC and ANN-based MPPT [53].

I.4.4. Evolutionary algorithms (EAs)

Evolutionary computation is an iterative process, to increase the development of the population. This population is then picked out in a directed random search using multiprocessing to accomplish the trusted end. Such procedures are frequently moved by biological methods of evolution Different kinds of evolutionary algorithms, their combined forms, and implementation strategies for harvesting maximum power in PV systems are explained in this section [49].

I.4.4.1. Genetic algorithm (GA) based MPPT

Genetic algorithm (GA) is a well-known metaheuristic optimization algorithm, which is inspired from natural evolution, mutation, crossover and selection. In GA, a population of search agents (chromosomes) try to find global optimum. At each generation, new chromosomes are generated by reproductive operators such as crossover and mutation, then, based on objective values, selection operator selects the chromosomes of next generation. These stages continue until termination criterion is met. The best chromosome of the last generation is given out as global optimum of the problem in hand [55].Now the GA is applied to MPPT problems where the chromosomes are taken either the values of voltage, current or frequency. The PV panel equation can be treated as the fitness equation. Then it is processed through different stages of GA finally the highest possible fitness value is chosen to generate the maximum power from the PV Array [49]. In ref [56] GA has been used for MPPT application. Simulations for different cases are PSC, changes in irradiation, temperature, and loads, confirm that GA outperforms P&O and IC.

I.4.4.2. Evolutionary programming (EP)

Evolutionary programming (EP) has five different stages namely, recombination, mutation reproduction, natural selection and survival of the fittest. Objective function will play a major role in the optimization problem by finding the solution of individuals in the population. Evolution of the population finally takes place later the recurring function of the above operators [49]. Evolutionary programming search for optimum value by evolving a population of solutions over iterations. During each iteration process, a new generation of population is produced from the previous generation of population. Mutation operator is used for this production by perturbing with a random value. After this, candidates are evaluated for their

fitness. The winners of the competition process are the most optimum solutions and they move forward as subsequent generation after survival. In this way, the global optimum solution among all candidates will result at the end. This searching technique is iterative and the search process stops after a termination criterion is achieved. The termination rule may be a given number of iterations or outcome of a same best solution for certain generations [45]. EP based MPPT harvest maximum power from PV systems that initiates with several randomly generated candidates and finally a suitable solution is found over several iterations. It was basically proposed as an alternate technique of classic artificial intelligence in computing. Further, it was modified to apply for solutions of optimization problems. Particularly, it is used in partial shading situations. Hashim et al [57] confirmed that the evolutionary programming shows better performance as an accurate and robust approach than GA algorithm. Generally, evolutionary programming appears to be an outstanding algorithm for MPP tracking in PV array systems during partial shading situations [45].

I.4.4.3. Differential evolution (DE)

DE is a stochastic, optimizer based evolutionary algorithm. It optimizes a problem by maintaining and creating a population of candidate solutions according to its simple formulae, and then keeping whichever candidate solution that exhibits the best fitness. As with other evolutionary techniques, DE relies on initial random population generation, which is then, improved using selection, mutation, and crossover [58]. The searching procedures of DE-MPPT algorithm are illustrated in Fig. I.8 [59].

DE has three main advantages:

- Able to locate the true and accurate global optimum regardless of the initial parameter values
- Fast convergence.
- Utilizing few control parameters so that it will be easy to use.

In terms of optimization procedure, DE is similar to GA. However, unlike GA, which relies on crossover, DE primarily utilizes the mutation operation (i.e. difference vector) as a search and selection mechanism to direct the search toward the prospective regions in the search space During the mutation phase, the donor vector dv_i, is created using the following equation:

$$dv_i = D_{best} + F*(d_{r1} - d_{r2})$$ (I-5)

Where r_1 and r_2 denote random integers, F denotes scaling operator. d_{r1} and d_{r1} represent the selected vectors by random way.
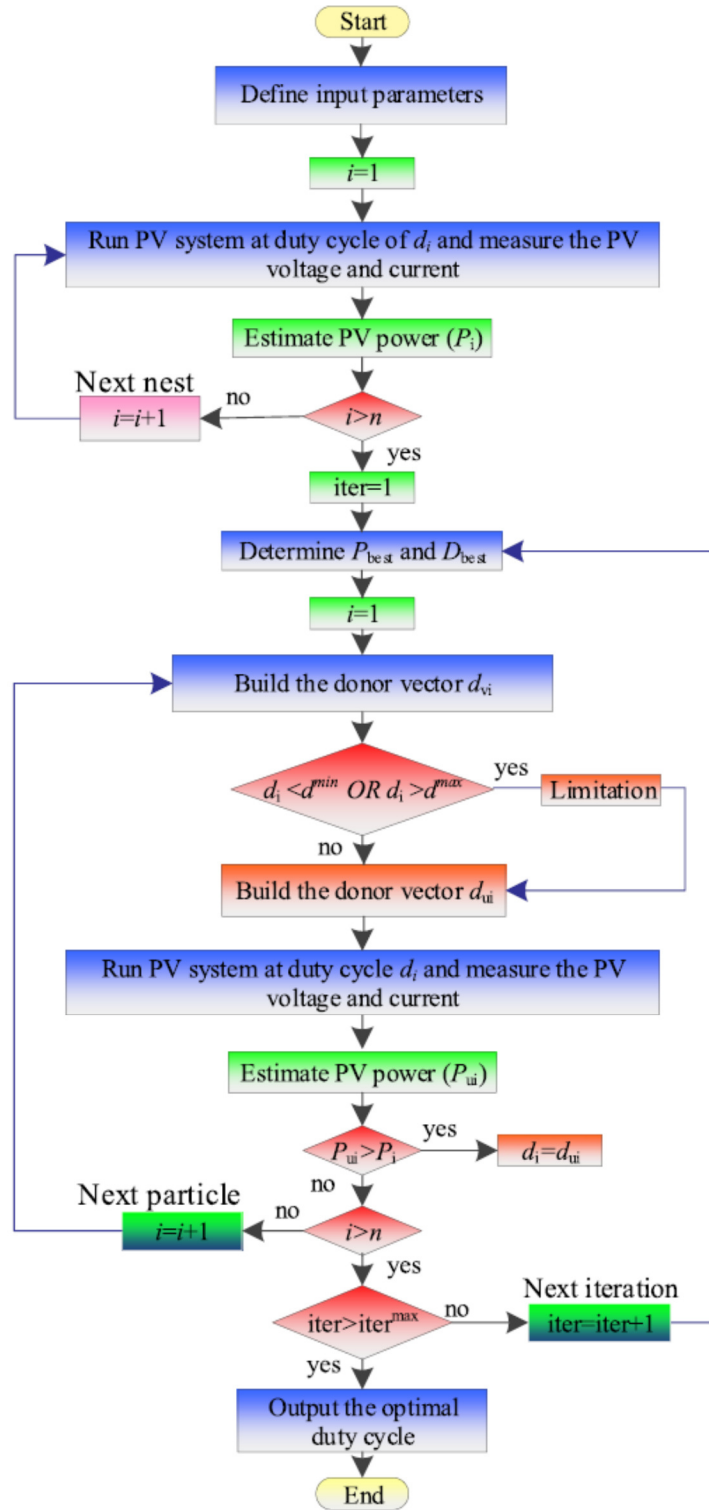
Fig. I.8 The searching procedure of DE based MPPT algorithm [59].

Then the resultant vector is limited according to the maximum and minimum boundaries as follows:

$$dv_i = \begin{cases} dv_i = d_{\max} \rightarrow if \quad dv_i > d_{\max} \\ dv_i = d_{\min} \rightarrow if \quad dv_i < d_{\min} \end{cases} \tag{I-6}$$

Next, the crossover phase is started. During this phase, the trail vector is created based on the following equation:

$$du_i = \begin{cases} dv_i & if \quad rand \leq C_r \\ d_i & otherwise \end{cases}$$ (I-7)

where C_r is the control parameter of crossover.

Final phase is the selection phase. The cost functions corresponding to trial and target vectors are compared. Based on the best cost function, the best vector is selected to continue in the next iteration based on the following relation. The duty cycle of higher amount of power is utilized as the next target vector as follows [59]:

$$d_{i+1} = \begin{cases} du_i & if \quad f(du_i) \geq f(d_i) \\ d_i & otherwise \end{cases}$$ (I-8)

In the MPPT problem, the fitness function is the PV equation, while the duty cycle, $X_i(j)$ is defined as the population. The latter is randomly initialized within the initial parameter bounds, i.e. fitness function. If the trial vector obtains a better fitness value than the target vector, then the trial vector replaces the target vector in the next generation. The process is repeated through generations until the stopping condition is reached, usually a good fitness value [58]. Authors in ref [60] proposed a novel method where DE can track MPP faster than P&O under both constant and sudden variations in partial shading conditions. The algorithm is less complex than other SC-based MPPT, such as ANN and FLC

I.4.4.4. Particle swarm optimization (PSO)

Swarm intelligence is the collective behavior of decentralized, self-organized systems, inspired by the natural or biological behavior. Particle swarm optimization (PSO) is an optimization method that iteratively trying to improve a candidate solution (known as particle) with regard to a given measure of quality. These particles move around in the search-space according to simple mathematical formulae, exploiting their position and velocity. Each particle's is influenced by its own best position and the best known positions in the search space, guided by the neighborhoods best position. The general idea of particles movement in PSO is illustrated by Fig. I.9. [58]. The particles position and velocity are updated based on Eqs. (I-9) and (I-10). In this work, the particle swarm position and the fitness are taken as the duty cycle and PV system output power respectively. The particle position D_i is updated by the following relations:

$$D_i^{k+1} = D_i^k + v_i^{k+1} \tag{I-9}$$

Where i is the number of particles $1 \leq i \leq N$, N is the number of population. v_i^{k+1} denotes step size at iteration $k+1$.

$$v_i^{k+1} = wv_i^k + c_1 r_1 (P_{best} - D_i^k) + c_2 r_2 (G_{best} - D_i^k) \tag{I-10}$$

Where w denotes inertial weight. c_1 and c_2 denote the acceleration coefficients. r_1 and r_2 are random values from [0, 1].

P_{best} denotes local best position of i particle. G_{best} denotes global best position in swarm [59].
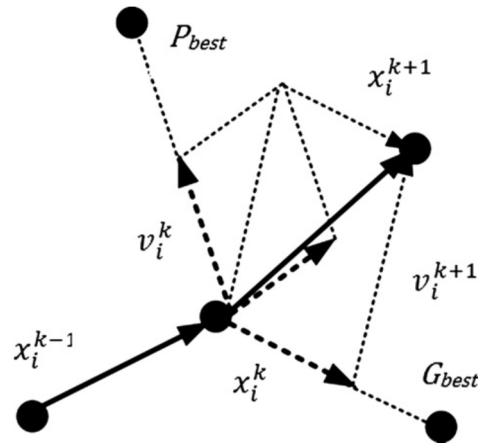
Fig. I.9. Particles movement in PSO

Searching mechanism of PSO based tracker begin with randomly number of duty cycles. Then, each one is applied to PVPS. The system current and voltage are measured in order to estimate PVPS power. Such power represents the fitness function of particle i. Next, the comparison between new fitness value and power corresponding to P_{best} stored in the history is done. In case of the new estimated power is more than the old one, it is selected as the best fitness value. After evaluating all particles, old velocity and position for each can be updated based on Eqs. (I-9) and (I-10). When the stopping criterion is achieved, PSO based tracker stopped and gives optimal duty cycle which corresponds to global power [61].

I.4.4.5. Cuckoo Search (CS) method

CS is an optimization algorithm, inspired by the parasitic reproduction strategy of cuckoo birds. It is observed that several species of cuckoos perform brood parasitism, i.e. by laying their eggs in other birds' (host birds) nests. Usually three types of brood parasitism are seen (1) intraspecific, (2) cooperative and (3) nest takeover. Some cuckoo species such as Tapera are

intelligent enough to mimic the shape and color of the host bird to increases its reproduction probability. The cuckoos lay their eggs at some specific time so that their eggs hatch earlier than the host bird's own. After the early hatching, cuckoos destroy some of the host bird's eggs to increase the chance of their chicks getting more food. It is also a common phenomenon that the host birds discover the cuckoo's eggs and destroy these. Sometimes they abandon their nest completely and go elsewhere to build a new nest. CS used three idealized rules based on cuckoo's brood parasitic behavior:

➢ Each cuckoo lays one egg at a time and places it in a randomly chosen nest.

➢ The best nest with the highest quality of eggs will carry over to the next generation.

➢ The number of available nests is fixed and the number of eggs (laid by a cuckoo) discovered by the host bird maintains a probability P_a, where $0 < P_a < 1$.

When generating a new solution $x(k + 1)$ for a cuckoo, a Lévy flight is performed as dictated by the following expression:

$$x_i^{k+1} = x_i^k + \alpha \oplus l\acute{e}vy(\lambda) \qquad (I\text{-}11)$$

Where x_i^k is samples/eggs, $\underline{i}$ is the sample number, k is the number of iteration and $\alpha > 0$ is the step size. Based on the constraints imposed by the optimization problem, it is important to tune the value of α to get desired step size. In most cases α used as in Eq. (I-11), i.e.

$$\alpha = \alpha_0 \left(x_j^k + x_i^k \right) \qquad (I\text{-}12)$$

where α_0 is the initial step change. In Eq. (I-12), the difference between two samples is used to determine the subsequent step size. The product $\oplus$ in Eq. (I-11) indicates entry-wise multiplication i.e. a is multiplied with all samples individually. The value of *Lévy* (*k*) is found from Lévy distribution given in Eq. (I-13) [21].

$$L\acute{e}vy(\lambda) \approx u = l^{-\lambda}, \quad \left(1 < \lambda < 3 \right) \qquad (I\text{-}13)$$

The main target is reaching the optimum *DC-DC* converter duty cycle related to global MPP. Accordingly, *DC-DC* converter duty cycle has been used as a variable to be optimized. PV power has been used as the fitness function. Based on Lévy flight, the duty cycle can be updated by the following equation:

$$D_i^{k+1} = D_i^k + \alpha \oplus l\acute{e}vy(\beta) \approx D_i^k + k_{l\acute{e}vy} \times \left(\frac{u}{|v|^{\beta^{-1}}} \right)(D_{best}^k - D_i^k) \qquad (I\text{-}14)$$

Where $\beta = 1.5$, $k_{Lévy}$ denotes the Lévy multiplying coefficient, u and v can be estimated based on normal distribution curves.

$$u \approx N\left(0, \ \sigma_u^2\right) \quad and \quad v \approx N\left(0, \ \sigma_v^2\right) \tag{I-15}$$

Where the variables σ_u and σ_v are defined as follows:

$$\sigma_u = \left(\frac{\Gamma(1+\beta) \times \sin(\pi \times \beta/2)}{\Gamma(\frac{1+\beta}{2}) \times \beta \times 2^{\frac{(\beta-1)}{2}})} \right)^{1/\beta} \quad and \quad \sigma_v = 1 \tag{I-16}$$

The flowchart of CS based MPPT is shown in Fig. I.10.
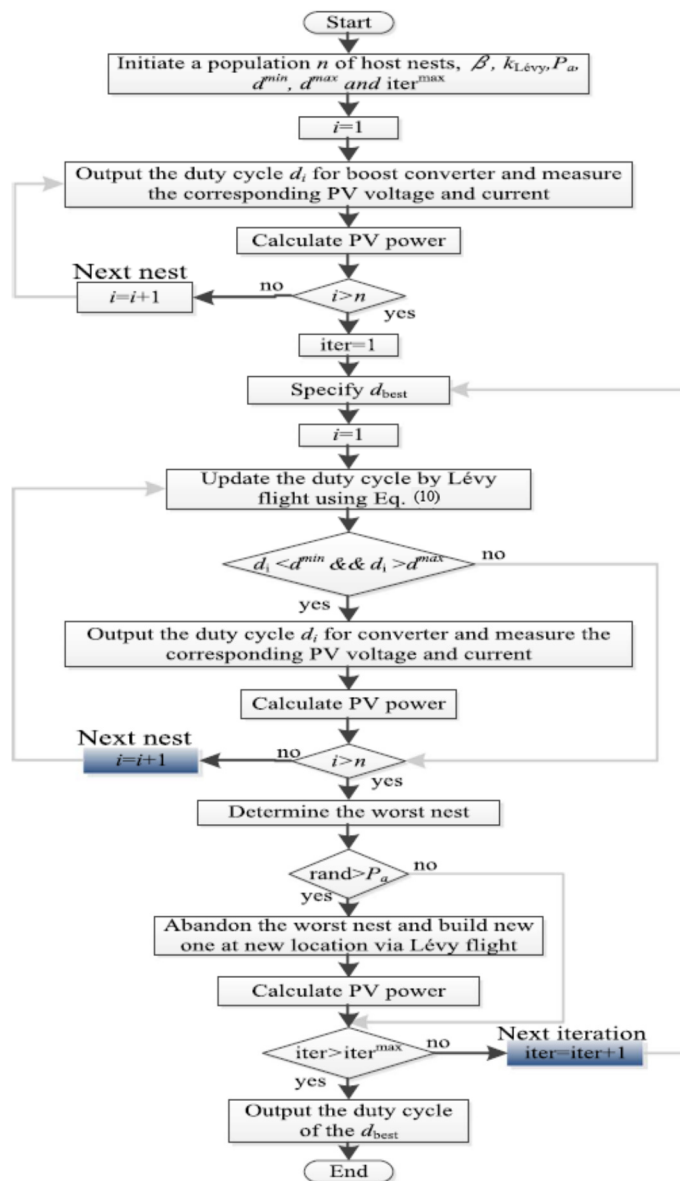
Fig. I.10. Flowchart of Cuckoo Search (CS) based MPPT method [61].

The searching mechanism of CS based MPPT begins by randomly duty cycles. Then, each one is applied to PV system. The system current and voltage are measured in order to estimate PVPS power. Such power represents the fitness value. The duty cycle related to best fitness function has been selected as current best nest (D_{best}). Next, Lévy flight is applied based on Eq. (I-13) in order generate new nests. New finesses' values are tested through the PVPS. Afterwards, the worst nest is randomly destroyed with a probability Pa, this process simulates the behavior of the host bird discovering the cuckoo's eggs and destroying them. The new nest is replaced by the destroyed one via Lévy flight, then the PV power is measured and the current best nest is selected. When the stopping criterion is achieved, CS based tracker stopped and gives optimal duty cycle, which corresponds to global power [61].

I.4.4.6. Flower Pollination Algorithm (FPA)

FPA is introduced in 2012, by Xin Yang in ref [62] this approach is motivated from the action of flower pollination. The term of pollination can be defined as the physiological process of plants mating. In general, there are two kinds of pollination namely self and cross pollinent. Self pollination is happened when pollen of one flower fructifies the same flower or another flower in the same kind of plant. Whereas, crosspollination occurs when grains of pollen moved from various plant. The two common methods to prevalence the pollen between flowers are abiotic and biotic pollination. The abiotic pollination is occurred by the help of wind and rain. Moreover, this kind account 10% off pollination and it is not required for any pollinators.

The biotic pollination occurs by the help of birds and animals and accounts 90% of pollination. Four rules must be taken under consideration for designing and implementing the FPA algorithm.

- Firstly, Biotic and crosspollination are considered as global pollination process and may occur over a large distance where levy flights are utilized for transfer pollens.
- Secondly, abiotic- and self-pollination are considered as local pollination.
- Thirdly, flower constancy is deemed as production possibility proportional to the matching among two flowers involved.
- Finally, the occurrence of both local and global pollination have controlled and monitored using switch probability.

According to the previous four steps, the mathematical model can be represented as follows:

Firstly, the approach initializes its controlling parameters with upper and lower bounds of duty cycle with tracking the value of PV output power. The maximum power is selected as the best one, and then the donor vector of duty cycle is generated, the later is fed to the converter

with measuring the corresponding power, the updating process is taken place in case of power increase [59]. The flowchart for implementation of FPA based MPPT is shown in Fig. I.11.
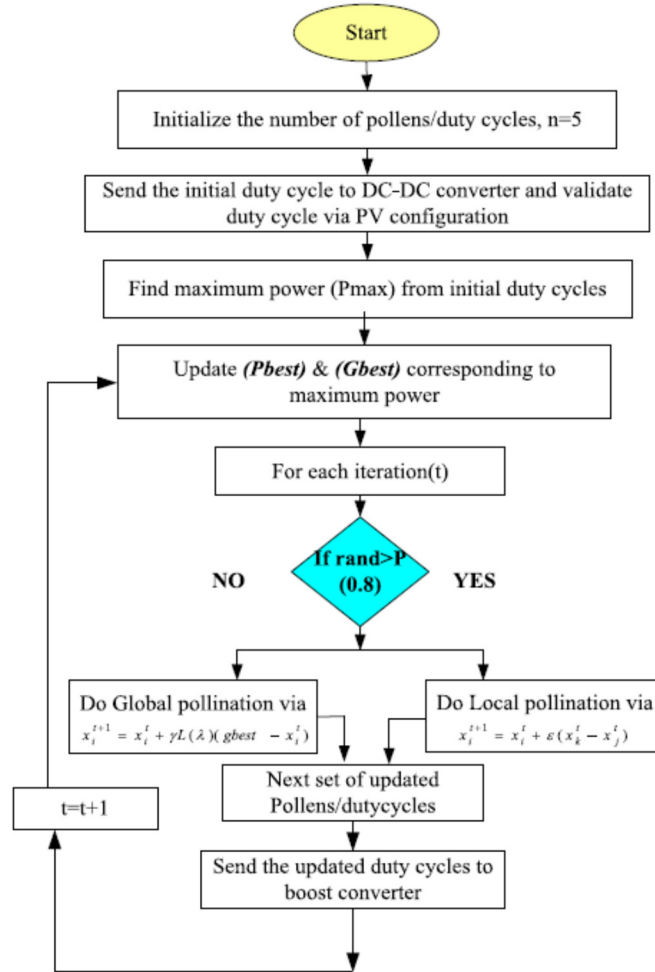
Fig. I.11. Flowchart for FPA implemented MPPT [63]

The characteristic equation of global pollination and flower constancy from the first rule and third rule is given as follow:

$$x_i^{k+1} = x_i^k + \gamma L(\lambda)(g_{best} - x_i^k) \qquad (I-17)$$

where x_i^{k+1} is the pollen for the same kind of flower at iteration k, g_{best} is the best value of duty cycle, is scaling factor that utilized for making control on step size and $L(\lambda)$ is Levy flights which is accountable to move a pollens to various kinds of flowers and assist to enhance the pollination strength and determined by the following equation [63]:

$$L(\lambda) \approx \frac{\lambda \Gamma(\lambda) \times \sin(\pi \lambda / 2)}{\pi} \times \frac{1}{S^{1+\lambda}} \qquad where \ (s \gg s_0 > 0) \qquad (I-18)$$

The characteristic equation of local pollination from the second and third rule is given as follows:

$$x_i^{k+1} = x_i^k + \varepsilon(x_j^k - x_f^k) \qquad \text{(I-19)}$$

where x_j^k and x_f^k are pollen from various flowers of the same kind of plant. $\varepsilon \in [0 \ 1]$ [63].

Generally, to implement FPA in MPPT, firstly the Flower pollination approach initializes its controlling parameters with upper and lower bounds of duty cycle with tracking the value of PV output power. The maximum power is selected as the best one, and then the donor vector of duty cycle is generated, the later is fed to the converter with measuring the corresponding power, the updating process is taken place in case of power increase [59].

I.4.4.7. Firefly algorithm (FA) based MPPT

It is a swarm intelligence based problem optimization technique, which is based on the collective actions of tropical fireflies. The fireflies interact with each other through flashing pattern. They attract each other for mating purpose through flashing behavior. The rate, rhythm, and intensity of flashing by a firefly attracts other fireflies (both sexes). The flashing phenomenon also catch the attention of prey.

Fig. I.12. Behavior of fireflies [45].

The basis features of FA technique are given by following three rules.

- All fireflies are supposed to be unisex. Their interaction (attraction between each other and movement) is independent of sex.
- The attraction phenomenon depends only upon the brightness. The relative brightness makes one of them to move towards other. Firefly with less brightness moves towards the

one having high brightness. The attraction among fireflies decreases with the increase in distance, as it reduces the brightness. If all the fireflies in whole colony seems to have same flashing intensity, then they start to move randomly.

- ▪ The fitness value of the objective function determines the flashing intensity (brightness) of a firefly

The behaviour attractiveness of firefly can be modelled mathematically using a decreasing function as given in following equation:

$$\beta(r) = \beta_0 e^{-\gamma(r_{ij})^m}, \ m \geq 1 \tag{I-20}$$

Where, r_{ij} is the distance between two adjacent flies, γ is the absorption coefficient, and β_0 is the initial attractiveness at r = 0 (two fireflies at same position or nearby in search space). The distance r can be computed as a Euclidean or Cartesian distance as given in Eq. (I-21)

$$r_{ij} = \left\| x_i - x_j \right\| = \sqrt{\sum_{l=1}^{d} (x_{i,l} - x_{j,l})^2} \tag{I-21}$$

The movement of fireflies modelled mathematically using the following equation:

$$x_i^{k+1} = x_i^k + \beta_0 \times e^{-\gamma(r_{ij})^m} \times (x_j - x_i) + \alpha \times (rand - 0.5) \tag{I-22}$$

The α is a parameter which controls the size of step, while rand is a random number vector. Using the FOA-based MPPT method, the converter duty cycle represents the position of the firefly and the output generated power of PV system is the brightness of each butterfly. The steps involved in firefly algorithm based MPPT approach are given in following algorithm.

1- Set parameters: constants, population, stop criterion.
2- Initialize fireflies and the range of allowable solution space.
3- While not meeting stop criterion do.
4- Evaluate brightness (PV output power) for position of all fireflies.
5- Update the position of fireflies with less brightness to converge towards the brightest fireflies based on Eq. (I-20).
6- End while
7- Reinitiate the FA process, if a change is detected in power output [45].

I.4.4.8. Grey Wolf Algorithm based MPPT

Grey wolf optimization (GWO) is a population-based optimization technique, based on the hierarchical leadership and the hunting behavior of the grey wolf. When seeking prey,

greywolves can be classified into four types based on the fitness evaluation of each type where the first type possesses the highest fitness and the fourth is the worst. Circling behavior by the wolves is a key step in the hunting procedure, for the purpose of designing the main steps of GWO algorithm as shown in Fig. I.13 [64] [65].
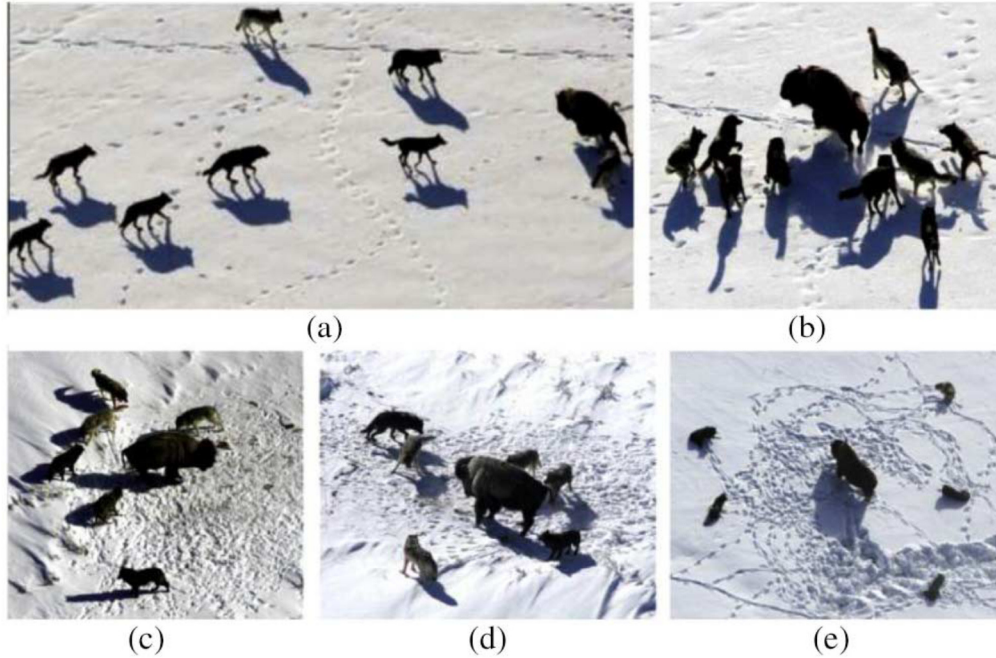
Fig. I.13. Hunting behavior of grey wolves: (a)-(c) chasing and tracking prey
(d) encircling prey and (e) attacking prey [65]

Grey wolves have three main steps in their hunting behavior [64]:

(1) searching, tracking, and approaching prey.

(2) pursuing and encircling prey.

(3) attacking prey

The GWO method applied for MPPT problem, where the number of participating grey wolves represents the converter's duty cycles and the MPP is prey being hunted.

The Circling behavior of the wolves is mathematically represented by Eq. (I-24).

$$\vec{D} = \left| \vec{C} \vec{X}_p(k) - \vec{X}_p(k) \right| \tag{I-23}$$

$$\vec{X}_p(k+1) = \vec{X}_p(k) - \left| \vec{A}.\vec{D} \right| \tag{I-24}$$

Where t is the number of the iteration, X_p and X are the positions vectors of the prey and the grey wolf, respectively; and A, C and D are the coefficient vectors calculated by:

$$\vec{A} = 2\vec{a}.\vec{r}_1 - \vec{a} \tag{I-25}$$

$$\vec{c} = 2.\vec{r}_2 \qquad\qquad\qquad (\text{I-26})$$

Where components of 'a' are linearly decreased from 2 to 0 across iterations and r_1, r_2 are random vectors in [0, 1]. GWO optimization method is applied to MPPT where the number of participating grey wolves represents the converter's duty cycles and the MPP is prey being hunted. For number of grey wolves, i.e., duty ratios, the controller measures V_{pv} and I_{pv} through sensors and computes the output power [64].

To implement the GWO-based MPPT, duty cycle D is defined as a grey wolf. Therefore, Eq. (I-23). can be modified as follows:

$$D_i^{k+1} = D_i^k - A.D \qquad\qquad\qquad (\text{I-27})$$

Thus, the fitness function of the GWO algorithm is formulated as:

$$P(D_i^k) > P(D_i^{k-1}) \qquad\qquad\qquad (\text{I-28})$$

Where P represents power, D is duty cycle, i is the number of current grey wolves, and k is the number of iterations [65]. The parameters affecting performance of GWO-based MPPT algorithm are exploration and exploitation factor, population size, and maximum number of iterations. Advantages of GWO are easy to implement, few parameters to set, and good tracking accuracy. Disadvantages of GWO are low tracking speed [64].

I.4.4.9. Artificial bee colony (ABC) based MPPT

The Artificial bee colony (ABC) MPPT is derived from the foraging behavior of bees. In general, the bees search for its food from different colonies from which collective intelligence emerges for maximizing the nectar amount in the hive [48]. The ABC algorithm is based on the behaviour of three types of artificial bees: employed bees, onlooker bees, and scouts bees. In such a way, a bee searching for food is called an employed bee. Also, a bee that makes decisions to choose a food source at the hive is considered as an onlooker. Finally, scout bees are bees whose food sources cannot be improved through a predefined number of trials, thus, their food sources are abandoned [66]. For MPPT the output power of the PV system is regarded as the nectar amount, and the duty ratio D of the dc–dc converter is the decision variable that is termed as food source position in ABC algorithm [22]. In such a way, the optimization problem has only one parameter to be optimized duty cycle [66]. The formula used in ABC MPPT for initial selection of duty cycle generation and updating is given in Eqs. (I-29) and (I-30).

$$D_i = D_{min} + r.(D_{max} - D_{min}) \tag{I-29}$$

$$D_i^{new} = D_i + \phi_i.(D_j - D_f) \tag{I-30}$$

Where D is the duty cycle, i is the iteration number, ϕ_i is the random number between [-1, 1] and 'D_j, D_f'are randomly chosen duty cycles, r is a random vector in [0, 1]. This algorithm ensures proper tracking under dynamic weather conditions where proper convergence is ensured [48].

I.4.4.10. Bat Algorithm (BA) based MPPT

Bat algorithm is a population based optimization algorithm inspiredby the echolocation features of microbats in locating their foods [20]. It is developed by Yang in 2010 in ref [67] It has widely been adopted to deal with problems associated with global and local maximum points. This algorithm considers the singular microbats features to hunt and navigate during the search for prey, even on complete darkness. According to the echolocation behavior of the microbats, in this section the following considerations are carried out:

1) All bats use their echolocation to detect the distance from the prey. Furthermore, they are capable to know the difference between foods and physical barriers.
2) The bats fly randomly with velocity v_i at position x_i, considering a fixed frequency fvmin varying wavelength λ and loudness A_0 during the search for prey. According to the distance from the target, the bats can automatically adjust either wavelength or frequency of their pulse emission rate (r $\in$ [0,1]), where 0 means none pulse, while 1 represents the maximum pulse emission rate;
3) Although the loudness may vary in different schemes, it is considered that intensity changes occur from a high positive value A_0 to a minimum value A_{min}.

Besides the aforementioned considerations, the frequency f_v is fixed at $[f_{v\,min}, f_{v\,max}]$ interval for the wavelength $[\lambda_{min}, \lambda_{max}]$ interval, where f_v is given in Hz and λ in mm. the frequency is defined as $f_v \in [0, f_{v\,max}]$. It is well-known that large frequencies present short wavelength, i.e., the bats need to navigate between short distances. Usually, the microbats navigate between short intervals of a few meters [68].Fig. I.14. shows the flowchart of the bio-inspired Bat-based MPPT algorithm [68]. During the optimization task, every bat is randomly assigned a frequency which is drawn uniformly from $[f_{min}, f_{max}]$. Then, the velocity v_i and the position x_i of each bat at time step k are defined and updated with following equations:

$$f_i = f_{min} + \beta.(f_{max} - f_{min}) \qquad (I\text{-}31)$$

$$v_i^{k+1} = v_i^k + f_i.(x_i^k - x^*) \qquad (I\text{-}32)$$

$$x_i^{k+1} = x_i^k + v_i^{k+1} \qquad (I\text{-}33)$$

Where $\beta \in [0\ 1]$ is a vector randomly drawn from a uniform distribution. $* x$ is the current global best location (solution) which is achieved after comparing all the solutions among all the N bats at each iteration t. If a random number is greater than the pulse emission r_i^t, then the exploitation stage is selected and the position x_i^{k+1} is replaced by the solution generated by the local search.
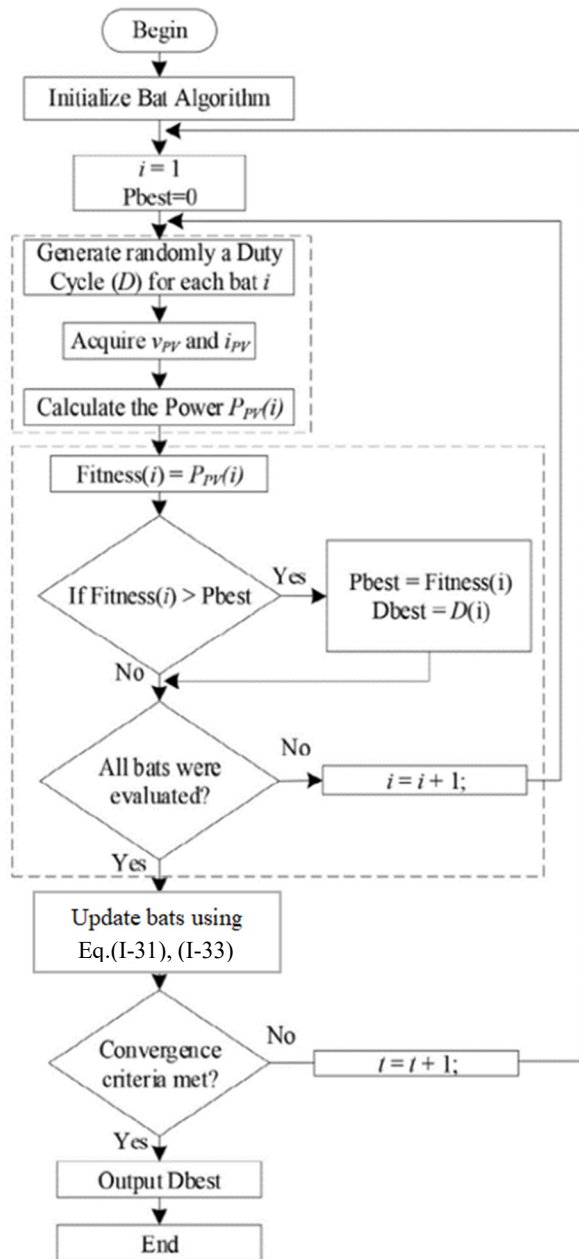
Fig. I.14. Bat Algorithm (BA) based MPPT [20]

As a result, a new solution is drawn locally by using a random walk around the current best solution

$$x_i^{new} = x^* + \in A^k \tag{I-34}$$

If a random number is smaller than the loudness A_i^k and the new solution improve the fitness value, this means that the bat is moving towards the prey (the optimal solution). Then, the new solution is accepted and its loudness and emission rates are updated to control the exploration and exploitation. It is suggested that loudness decreases from positive value A_i^k to $A_{min} = 0$ whereas the pulse rate of pulse emission increases from 0 to R_i

$$A_i^{k+1} = \alpha.A_i^k \tag{I-35}$$

$$r_i^{k+1} = R_i.(1 - e^{-\gamma.k}) \tag{I-36}$$

where α is a constant in the range of [0 1] and γ is a positive constant, A_i^0 and R_i are set to 1 [20].

I.4.4.11. Teaching Learning Based Optimization Algorithm (TLBO)

TLBO which developed by Patel and Reo emulates the classical process of teaching-learning occurs in schools. A number of students are taken into account in the population and some subjects presented to them. These subjects represent the different design variable of the optimization problem. The fitness function is represented by the results of students. During process of optimization, the teacher is represented by the optimum solution in each phase. TLBO process contains two stages, called student stage and teacher stage. During these two stages, teacher attempts to enhance student's level by changing the knowledge. In the first stage, the teacher directly conveys knowledge between students and he attempts increasing the mean result inside the group into his level in terms of knowledge. The knowledge is transferred to students by the interaction among themselves during the second stage.

In this section, one design variable (subject) offered to a group of learners (n students).

The DC/DC converter duty cycle (D_i) represents the student and the output power of a PV system taken as the fitness function. During the teacher stage, the DC/DC converter is updated using (6) which represents the difference between the value of the teacher and the mean value of the students

$$D_{i+1} = D_i + r.(D_{i\ best} - T_F.D_{i\ mean}) \tag{I-37}$$

Where D_{i+1} is the duty cycle for the next iteration; $D_{i\ best}$ is the teacher value; $D_{i\ mean}$ is the student's mean value; T_f is the teaching factor; r is the random number between [0 1]. After finishing the first stage, one learner (D_x) tries to enhance his knowledge by the interaction with another randomly one (D_y) through the student stage. Equations (I-38) and (I-39) control the updating process in the second stage.

$$D_{new} = D_x + r.(D_y - D_x) \quad if \quad P_{pv}(D_y) > P_{pv}(D_x) \tag{I-38}$$

$$D_{new} = D_x + r.(D_x - D_y) \quad if \quad P_{pv}(D_x) > P_{pv}(D_y) \tag{I-39}$$

The mechanism of searching process by TLBO technique operate as follow: Firstly, appropriate variables have to be selected for the search. The total number of students is defined as n, in this work; the learner's represents DC/DC converter duty cycles. The initial duty cycles (learners) are applied to PVPS. Then, the corresponding PV voltage and current are measured. These values have been used to estimate the PV power which represents the fitness value of each learner i. After that, student which has best fitness value is selected to be a teacher for the group. After evaluation of all learners, the duty cycle must be modified based on Eq. (I-37) Afterwards, select randomly any two learners and update the duty cycle according Eqs. (I-38) and (I-39). These steps are executed for a certain number of iterations until the all students reach at the optimum solution, which represents the optimum duty cycle corresponding to global MPP [69].

I.4.4.12. Gras Shopper Optimization (GHO) Based MPPT

Among the vast group of swarm-based intelligent algorithms, Gras Shopper Optimization (GHO) is an outstanding member. It was first, introduced by Mirjalili in [70]. GHO mimics the natural behavior of grasshoppers and its life cycle consists of 2 sub cycles. Namely nymph and adult cycle. In the nymph cycle, the motion is constrained. It provides better local exploration. In the adult cycle, abrupt fast jumps at random intervals help to avoid predators and explore more areas. The balance between exploration and exploitation and excellent social interaction are key features. The optimization is done for minimizing or maximizing a cost function Fig. I.15. shows the corrective pattern between individual particles in a GHO swarm. The distance between two consecutive particles is balanced by a comfort zone, which affects social interaction, attraction, and repulsion.
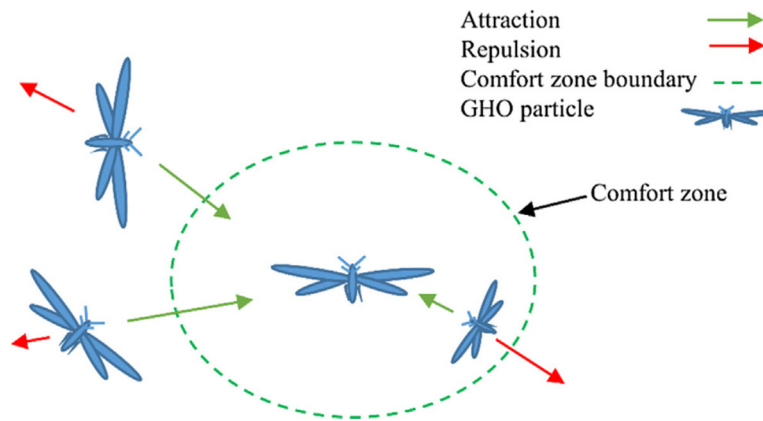
Fig. I.15. The corrective pattern between individuals in a GHO swarm [71]

GHO is applied to track GMPP due to its fast convergence and its least oscillations in the steady-state. At the beginning, the population is randomly initiated in the range of 0–1. Here the search space represents the duty cycle of the DC-DC converter [71]. Mansoor et al in the ref [71]. confirmed the effectiveness of the proposed GHO over existing bio-inspired MPPT techniques are P&O, ABC, PSO, DFO, PSO-GS, and CS. Results show that the proposed GHO is highly robust with the tracking efficiency of up to 99.5%. The oscillation reduction of up to 85% is achieved along with 14–60% faster tracking. Experimental validation on low-cost setup further solidifies the practicality of the proposed technique in real-world applications.

I.4.4.13. Butterfly Optimization Algorithm (BOA)

Aygül et al, in the ref [72]. proposed butterfly optimization algorithm (BOA) for global optimization. The algorithm mimics mating and food search behavior of butterflies. The two main parameters of the algorithm are the location of food and the location of the partner.

There are three main characteristics of butterflies in this algorithm:
1. One butterfly should be able to attract all other butterflies thanks to its fragrance.
2. Butterflies change its location randomly or toward the butterfly that has the most intense smell.
3. The landscape of the objective function determines the stimulus intensity of butterflies.

BOA consists of three stages are Initialization, Iteration and Final Phase. Each run of the algorithm starts with the initialization. After that, the search phase is performed with iterations. At last, the final phase is performed when the best solution is found. In the initialization stage, the objective function and the solution space is defined. Also, values assigned to the parameters in the algorithm. After that, an initial population that will preserve its number during the

simulation is created. Next, the butterflies are randomly distributed in the search space and the fitness and fragrance values of them are calculated. In the iteration phase, the butterflies change their position and the fitness values are calculated for new positions. After that, the fragrance of butterflies are generated according to Eq. (I-40).

$$f = c.I^a \qquad\qquad (I\text{-}40)$$

Where I is stimulus intensity, f is the fragrance, a is value depend on fragrance and c is the sensory modality. The algorithm consists of two main stages; Global and local search phases. Global search phase is shown in Eq. (I-41).

$$x_i^{k+1} = x_i^k + f_i.(r^2.g^* - x_i^k) \qquad\qquad (I\text{-}41)$$

Where x_i^k stands for the solution vector, g^* stands for the best solution in the current iteration, f_i is the fragrance of the ith butterfly and r is a random number. Local search phase is shown in Eq. (I-42).

$$x_i^{k+1} = x_i^k + f_i.(r^2.x_j^k - x_i^k) \qquad\qquad (I\text{-}42)$$

Where x_i^k and x_j^k stands for i^{th} and j^{th} butterflies in the solution space respectively.

Until the stop criteria are satisfied the iteration process continues [72]. In BOA based MPPT approach, the vector x_i^{k+1} represents the duty cycle of DC/DC converter at iteration $(k+1)$, while the considered fitness function is the total PV extracted power P_{pv} [73].

I.4.5. Hybrid MPPT techniques

Hybrid MPPT techniques are composed by a combination of conventional and soft computing or soft computing/conventional or soft computing/soft computing, in order to handle the negative effect of shade and track the GP accurately and efficiently [8]. We presents, in this part an overview of the most used hybrid MPPT methods.

I.4.5.1.Hybrid method PSO-P&O

The hybridization of P&O with PSO for MPPT application proposed in refs [28] and [74]. At the beginning of the algorithm PSO is used for global search and then P&O is used at the final stage. PSO method is employed for searching the GMPP. The hybrid method finds the GMPP in a shorter time than normal PSO method. In literature different shading cases are tested

to verify the efficacy of the proposed method. The boost converter with interleaved topology is used to reduce ripple current, improve reliability and increase the efficiency. The proposed PSO- P&O method tracks the GMP easily and has faster convergence time and also better dynamic response than normal PSO method.

I.4.5.2. Hybrid method Artificial Bee Colony-P&O (ABC-P&O)

The authors in [75]. Designs a new hybrid algorithm for MPPT of PV systems under PSC, which employs ABC algorithm in the first stage and P&O algorithm in the second stage. In ABC-P&O, ABC algorithm is initially adopted for GMPP tracking and then P&O algorithm is adopted to track LMPP, which can effectively combine the excellent local searching ability of P&O algorithm and global searching ability of ABC algorithm to generate optimal duty cycle For booster converter. Simulation results clearly indicate ABC-P&O algorithm can achieve accurate tracking performance with high efficiency, high tracking speed, and minimum payback time. The overall flowchart of ABC-P&O algorithm is depicted in Fig. I.16. [76].
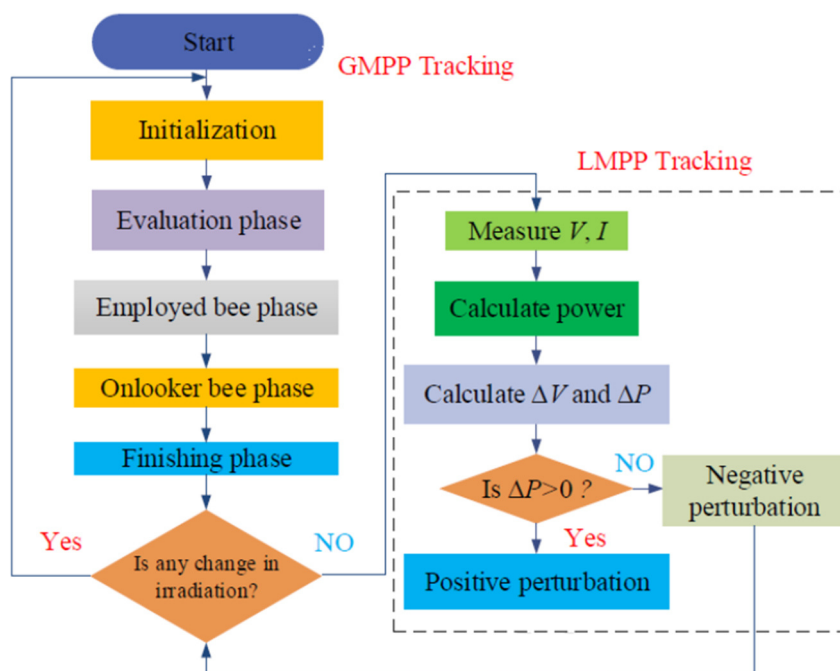
Fig. I.16. Flowchart of hybrid algorithm ABC-P&O based MPPT [76]

I.4.5.3. Hybrid method Grey wolf optimization with P&O (GWO-P&O)

Mohanty et al. [65] introduced hybrid GWO and P&O optimization techniques to track the MPP at Dynamic PSC. The idea behind this study is to use GWO for fast catching the GMPP and move to P&O to reduce the calculation manipulation in the MPPT and to reduce the ripple

contents in the output power. The hybrid GWO-P&O based MPPT proved the better performance of technique compared to GWO. The results of this study showed a fast response for catching the GMPP and lower oscillations compared to the other MPPT techniques.

I.4.5.4. Hybrid method GWO with Fuzzy logic (GWO-FLC)

The MPPT technique metaheuristic based GWO suffer from oscillations around the GMPP in addition it cannot catch the variant GMPP under variant PSC. For solve this problem Eltamaly et *al* in ref [35] hybridized GWO with FLC controller to reduce the oscillations in power around the GMPP. In addition, two efficient initialization techniques are proposed to re-initialize the GWO in order to catch the dynamic or variant GMPP. The first initialization technique is based on predefined time T_{PD} that depends on the frequency of PSC of the site. The second initialization technique based on the PSC change.

```
Pold=0,
Do while (t <=Maximum Number of iterations)
Initialize the grey wolf populations Di (i=1,2,…….,Nw) where, 0.9>Di>0.1
Initialize a, A, and C
Calculate the fitness of each search wolf Pi (i=1,2,…….,Nw)
Dα: is the duty ratio (wolf) associated with the best search grey wolf.
Dβ: is the duty ratio (wolf) associated with the second best search grey wolf.
Dδ: is the duty ratio (wolf) associated with the third best search grey wolf.
Pnew=P(Dα)
        Do while (Pnew-Pold)<ε1)
        Update the position of the current wolf
        Update a, A, and C
        Calculate the fitness of each search wolf Pi (i=1,2,…….,Nw)
        Update Dα, Dβ, and Dδ
        Update D1, D2, D3, and D
        Pold=Pnew ; Pnew=P(D)
        t=t+Δt
        end Do
        tt=0
        Do while ((Pnew-Pold)<ε2)
        Use the FLC to get D and its corresponding power
        tt=tt+Δtt
        End Do
End Do
```

Fig. I.17. Pseudo code of GWO-FLC based MPPT [35]

The condition for terminating the GWO and giving the role to the FLC to complete the control of the MPPT on the GMPP that has been already caught using the following conditions:

$$\left|P_{new}-P_{old}\right|\leq\varepsilon_1 \qquad\qquad\qquad (I\text{-}43)$$

Where P_{new} is the current power generated from PV system, P_{old} is the value of pervious iteration of the simulation, and ε_1 is the allowable limit before transferring the control from GWO to FLC, which equals to 2% of the generated power. The condition for terminating the FLC and go back to the GWO to re-initialize the agents to search for the new GMPP under the

New PSC using the following conditions:

$$\left| P_{new} - P_{old} \right| \leq \varepsilon_2 \qquad \text{(I-44)}$$

Where ε_2 is the allowable limit before transferring the control from FLC to GWO, which equals to 5% of the generated power. The pseudo code that summarize the steps of the hybrid GWO-FLC with PSC change reinitialized are shown in Fig. I.17. [35]

I.4.5.5. Hybrid method Bat-Beta (Bat-B) based MPPT

The authors in the paper [68] proposed a new hybrid based MPPT algorithm based the combination of the Bat method with Beta algorithm intends to overcome the drawback of Beta algorithm, which is the dependence on the PV module characteristics. In addition, to improve the tracking efficiency after the convergence to the GMPP. Thus, the adopted methodology computes the reference β* according to the PV array voltage and current in the GMPP from the Bat-MPPT algorithm. After that, when the Bat algorithm achieves the GMPP, the tracking is kept employing the Beta algorithm, which is capable to reach the GMPP even for small oscillations in solar irradiance and/or temperature. Experimental and simulation results using the card TMS320F28335 DSC (Texas Instruments) confirmed the overall superior performance of Bat-Beta based MPPT algorithm when compared to Bat, Bat-P&O and Bat-INC based MPPT methods for all test conditions considering either uniform solar irradiation or PSC case [68].

In addition to the previous hybrid MPPT method, we indicate to the DE-PSO method that is a hybridization of differential evolutionary (DE) algorithm and PSO. The DEPSO algorithm as discussed in [29]. Is able to avoid local optima by combining DE operator with PSO.

I.5. Analysis and qualitative comparison of MPPT Methods

We have tried ours best to provide a fair and comprehensive comparison between different Sixteen MPPT techniques including conventional , soft computing and hybrid techniques based on four important performance parameters that are common assessed. The performance criteria

considered for the study are: (1) Ability to handle shade problem (2) Tracking speed, (3) Steady state oscillation (4) level of complexity (5) Hardware cost of implementation. However, this comparison may not be a final conclusion, because it is not possible to compare the all MPPTs methods in a common platform. A detailed qualitative comparison of the most used MPPT methods is given in Table I.2

Table I.2 Detailed qualitative comparison of the most used MPPT techniques [48] [76].

N:	Name of the MPPT method	Ability to handle shade problem	tracking speed	Steady state oscillation	level of complexity	Hardware Cost of implementation
1	Perturb and observe P&O	No	Normal	High	Low	low
2	Incremental conductance	No	Normal	High	Low	low
3	Hill Climbing HC	No	Normal	High	Low	low
4	Fuzzy Logic control FLC	Yes	Average	Average	high	Moderate
5	Artificial neural network ANN	Yes	Good	Average	High	Moderate
6	Particle Swarm optimization PSO	Yes	Normal	Low	Moderate	Moderate
7	Cuckoo Search CS	Yes	Good	Low	Moderate	Moderate
8	Ant colony optimization ACO	Yes	Average	Low	high	Moderate
9	Artificial Bee colony	Yes	Good	Low	high	Moderate
10	Gray wolf optimization GWO	Yes	Very good	Low	high	high
11	Bat algorithm BA	Yes	Very good	Low	Moderate	Moderate
12	Firefly Algorithm FA	Yes	Very good	Low	Low	low
13	Flower pollination Algorithm FPA	Yes	Very good	Very low	Moderate	low
14	Hybrid DEPSO method	Yes	Good	Low	high	high
15	ABC-P&O	Yes	Good	Very low	high	high
16	Hybrid GWO-P&O	Yes	Good	Low	high	high

In overall by comparison with previous state of the art MPPT methodologies, metaheuristics are appropriate candidates for MPPT and are superior to classic MPPT strategies, FLC-based MPPT strategies and ANN-based MPPT strategies, due to the following reasons.

• Unlike classic methods such as P&O, IC and HC, metaheuristics are able to conduct global search and find global optimum in multimodal landscapes. Therefore, in partial shading conditions, where multiple local optima exist, metaheuristics are able to find global maximum power point, while classic methods may easily be trapped in false local optima.

- Unlike FLC-based MPPT strategies and ANN-based MPPT strategies which are designed based on a specific PV system, metaheuristic based MPPT strategies are not system-dependent and perform effectively for different PV systems. Unlike classic MPPT methods such as P&O, IC and HC, metaheuristic based MPPT strategies do not oscillate around maximum power point [55].

Hence, in order to obtain maximum power from the PV module under all conditions many MPPT methods are developed. Various methods are proposed in literatures to track the MPP of a PV array. The MPPT methodologies are majorly classified into three groups: Conventional methods, Soft computing methods and hybrid methods. In this section, the performances of MPPT methods are analyzed by considering various aspects including Ability to handle partial Shading, tracking speed, level of complexity, cost of hardware implementation and occurrence of oscillations near MPP and this in turn determine the efficiency of the entire PV system [6].

I.6. Conclusions

Tracking maximum power point MPPT in photovoltaic systems is an important task and represents a challenging problem. In MPPT controllers, the duty cycle of DC-DC converter is adjusted in a way that maximum achievable power is extracted. We presented in this chapter the mains factors influencing in efficiency of a photovoltaic systems, as we have seen the effectiveness of the MPPT controller plays an important role in determining the effectiveness of the PV system for this reason, we focused in this section on explaining the various MPPTs techniques that used in ancient and modern researches. The existing MPPT methods have been categorized into three main categories are conventional, soft computing and hybrid MPPTs methods and the most used methods of each category have been discussed. The analyzes of this chapter indicate that both metaheuristic techniques like CS, FA and FPA and some hybrid techniques like PO-PSO, DE-PSO, GWO-FLC and FPA-PSO despite its complexity are the best candidates for MPPT in all changing climate conditions. They are superior to all classic techniques, FLC and ANN techniques, due to its many merits such as system independency, effective performance in partial shading conditions and absence of oscillations around maximum power point.

Chapter II

Partial shading effects on both PV module and different PV Array configurations

Chapter II	Partial shading effects on both PV module and different PV array configurations

II.1. Introduction:

In the recent years, most of the countries of the world have tended to exploit the solar energy as an alternative source of the fossil energy sources, photovoltaic (PV) installations are being increasingly used in several applications. However, a major challenge in using a PV source is to tackle its nonlinear output characteristics, which vary with temperature and solar insolation. The electrical characteristics of PV modules get more complicated if the entire PV array does not receive uniform insolation, as in partially cloudy (shaded) conditions, resulting in multiple peaks. The presence of multiple peaks reduces the effectiveness of the existing maximum power point tracking (MPPT) schemes, due to their inability to discriminate between the local and global peaks [77]. In this chapter, we explain the partial shading problem and its impacts on the electrical characteristics of PV generators from PV cells inside module to different configuration of PV array. We use Matlab/Simulink software, for simulate first the partially shaded model of a series of PV cells in a PV module and secondly, we simulate the different configurations of PV array subjected to partial shading conditions (PSC). To show the negative impacts of partial shading (PS) problem on the electrical characteristics, we clearly show each simulated model in the curves of Power-Voltage (PV) and the Current-Voltage (IV).

II.2. Influence of partial shading on PV generators characteristics

In this chapter, we explain the negative impacts of the shade problem on the electrical characteristics of PV cells inside PV module and on the different topologies of PV array: series (S), parallel (P), series-parallel (SP) and Total-Cross-Tied (TCT).

II.2.1. Maximum PV power and Mismatch losses in PV system

A PV system should be designed to operate at the maximum available power under all operating conditions [78]. Unfortunately, a photovoltaic (PV) array usually produces less power than the combined capacities of the entire modules, the really extracted power can be lower

than the maximum available power, Such power losses, known as mismatch losses, have recently drawn attention in order to identify all the potential sources of power losses in PV systems [79]. Mismatch caused by non-uniform solar irradiation due to shading, dirt or non-uniform PV module orientation, but can also be caused by aging or damage to the PV module [78] the partial shading generate the nonhomogeneous illumination in PV cells, it considered one major source of mismatch losses in PV systems. In residential applications, PV cells are subject to shadows cast by both predictable surrounding objects, e.g., nearby antenna towers and power lines, and unpredictable sources, e.g., fallen leaves, dirt. In large PV plants, where PV modules are usually placed far from any surrounding obstacles, the passing clouds and the shadows of adjacent rows of modules can also contribute to partial shading conditions. In fact, partially shaded conditions are likely to take place in a variety of PV applications [79]. Series connection sets the same current for all PV modules in a string. This means that it will not be possible to individually track the maximum power point for each PV module, therefore, if the electrical parameters of the PV modules differ, mismatch will occur and a part of the available power will be lost [78]. Fig II.1, show some the situations of partially shaded PV module caused by nearby building, trees and public lighting pole.

a)   b)   c)
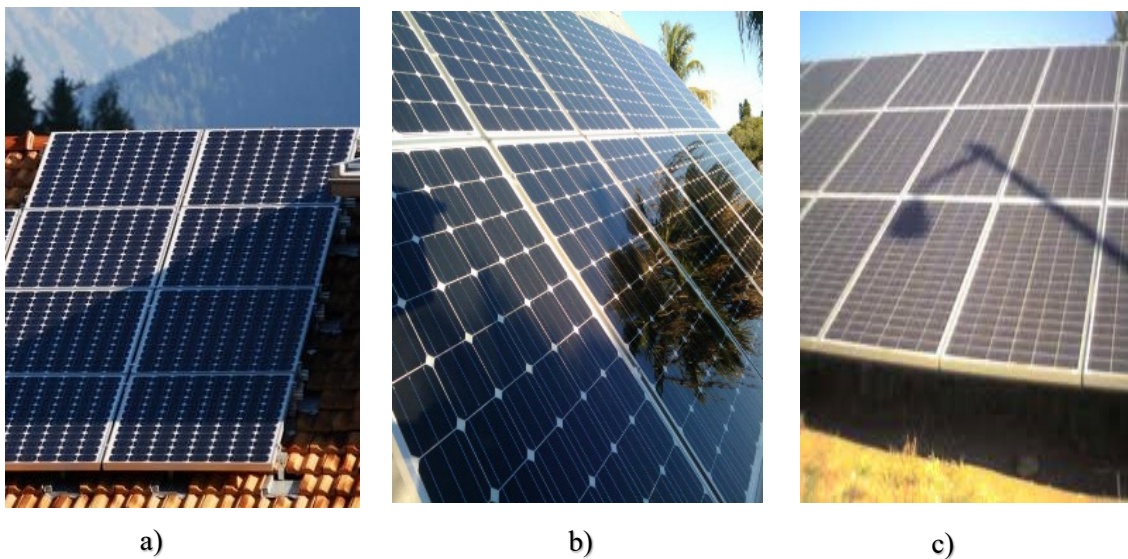
Fig.II.1. Shaded PV modules examples caused by a) nearby building elements
b) Nearby tree c) Nearby public lighting pole

II.2.2. Reverse Breakdown in Photovoltaic Cells

When a PV cell becomes reverse biased, it will sink rather than source power and heat up owing to the resulting power dissipation. Ideally, power dissipated through a reverse-biased cell

is distributed over the full cell area, but this is not always the case. As cell temperature increases, a phenomenon can occur called second breakdown or thermal breakdown .Second break down in a p-n junction is observed when the reverse voltage magnitude decreases rather than increases as current is increased and local thermal runaway is triggered. The current is driven into 1-D channels, which can result in high internal temperatures, well above 400°C. Second breakdown generally leads to permanent cell damage. Even if second breakdown does not occur, high cell temperatures can lead to secondary degradation effects. PV panels are typically rated up to 85°C, but hot spotting can push the cell temperature far above the rated temperature. If cell surface temperatures surpass 150°C, the encapsulated and isolative material surrounding the cells may be damaged. Once the encapsulated is damaged, cells are exposed to environmental elements that can cause corrosion and further damage to the cell. Hot spotting with or without second breakdown can lead to PV degradation. Thus, proper measures must be taken to prevent hot spotting in PV panels [80].

II.2.3. Reverse-Bias and Power Dissipation Levels

The amount of power dissipated in a reverse-biased PV cell depends on its I–V characteristics, which vary widely among cells; most manufacturers do not control for reverse breakdown characteristics. There are two cell categories recognized by the PV industry: Type A and Type B. Type A cells have a reverse-breakdown voltage greater in magnitude than the subpanel string's maximum power point (MPP) voltage; Type B cells have a reverse-breakdown voltage magnitude lower than the subpanel string's MPP voltage. A common subpanel string length is 24 cells, and the nominal MPP voltage for such a substring is approximately 12 V. Fig. II. Shows the I–V curve for two representative PV cells, shaded at zero irradiation (0W/m^2) and illuminated at the nominal irradiance of 1000W/m^2. Fig. II.(a), shows the forward characteristics, where an illuminated cell produces power while operating in the first quadrant with positive voltage and current. Fig.II.(b), shows the reverse characteristics, where a cell dissipates power while operating in the second quadrant with negative voltage and positive Current. Note the voltage scale difference between the plots. As shown, the sample Type A cell breaks down beyond −18V and the sample Type B cell around −8V. Both cell types will be examined under reverse-biased conditions.

Partial shading is the most common culprit behind severe mismatch that leads to hot spotting, but uneven cell degradation and temperature gradients also cause mismatch.

The bypass diode across the substring may or may not turn on when mismatch occurs in a panel substring; it depends on the I–V operating point of the string [80].
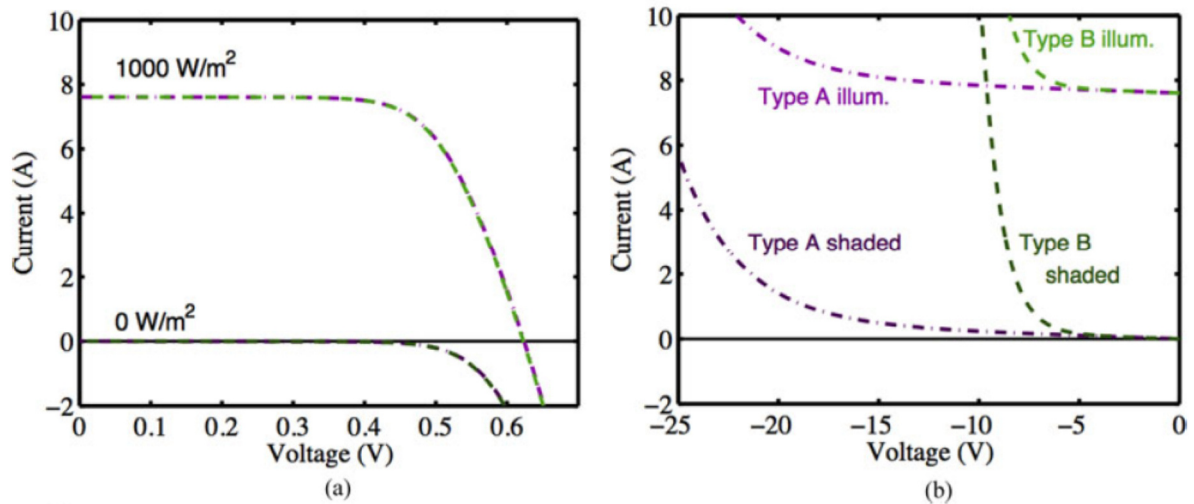
Fig. II.2. *I–V* curve in (a) forward and (b) reverse voltage region for illuminated and shaded Type A and B cells.

II.2.4. Photovoltaic hot spotting analysis

Although this hot spotting problem was identified early on 1969, it still present in PV modules where a precise hot spot definition is not well established in the PV industry. Hot spotting is defined as temperature increase above the temperature of its surroundings due to power dissipation in a reverse-biased PV cell, which can occur in the entire cell or a portion of the cell. A hot spot refers to the portion of the cell with a higher temperature due to hot spotting. The term hot spot damage is permanent damage or degradation to a PV cell as a direct result of hot spotting [80]. Hotspots are relatively frequent in current PV modules and this situation will likely persist as the PV module technology is evolving to thinner wafers, the hot spots is impact negatively on operational efficiency and lifetime of PV modules the researchers has been proposed several studies to mitigate the hot spott phenomenon in PV systems. In order to improve the output power performance of the hot spotted PV modules [81]. the researchers has been proposed several solutions in their studies to improve the output power performance of the hot spotted PV modules by mitigating the impact of hot spot phenomenon.

Among the solutions that mitigate, the hot spotting problem is a passive bypass diode that is placed in parallel with a string of PV cells. The use of bypass diodes across PV strings is standard practice that is required in crystalline silicon PV panels. Their purpose is to prevent hot spot damage that can occur in series-connected PV cells. Bypass diodes turn ON to provide

an alternative current path and attempt to prevent extreme reverse voltage bias on PV strings. The general misconception is that bypassing a string "protects" cells against hot spotting. Numerous long-term field studies on systems employing bypass diodes have found that hot spotting still occurs, which results in accelerated panel degradation. In addition, various simulation and experimental studies have shown that partial shading on a bypassed string of PV cells has the potential to dissipate substantial amounts of heat and form hot spots [80].

In addition, this approach requires a high technological cost and can be even detrimental in terms of power production when many diodes are activated because of their power consumption as discussed by Daliento et al (2007) in the paper [82]. More recently, Coppola et al. in the ref [83] suggested the distributed MPPT technique that is beneficial for mitigating the hot spot in partially shaded modules, with a temperature reduction up to 20 °C for small shadows.

The general misconception is that by passing a string protects cells against hot spotting. The "inadequateness" of the standard bypass diode, the insertion of a series-connected switch are suited to interrupt the current flow during bypass activation process. However, this solution requires a quite complex electronic board design that needs devised power supply and suitable control logic for activation the hot spot protection device [81]. A modified bypass circuit for improving the hot spot reliability of solar panels is proposed by Daliento et al (2016) in the paper [84]. The technique relies on series-connected power MOSFET that subtracts part of the reverse voltage from the shaded solar cell, thereby acting as a voltage divided, while the bypass circuit does not require either a control logic or power supply and can be subtitled to the standard bypass diodes of the PV panels [85]. As a recent solution of the hot spot problem, Dhimish et al (2018) in the paper [81] developed a new design of two hot spot mitigation techniques by using a simple, costless and reliable method that based on FLIER i5 thermal imaging camera. Several experiments have been examined during various environmental conditions, where the PV module I–V curve was evaluated in each observed test to analyze the output power performance before and after the activation of the proposed hot spot mitigation techniques. One PV module affected by hotspot was tested. The output power during high irradiance levels is increased by approximate to 1.25W after the activation of the first hot spot mitigation technique. However, the second mitigation technique guarantee an increase of the power equals to 3.96 W. Both proposed techniques ensure a decrease in the shaded PV cell temperature, thus an increase in the output-measured power [81]. Hot spot endurance tests are part of the IEC 61215 Si PV panel qualification testing standard and are meant to identify PV

panels that are susceptible to hot spotting, however many simulation and experimental studies presented here contradict the notion that current practices of bypass diodes and qualification testing are sufficient to protect against hot spotting. PV hot spotting is still a prevalent problem that limits reliability. It is also a safety concern, as hot spotting can damage panels and potentially lead to fires [80].

II.2.5. Role of Bypass and Blocking Diodes in PV module

The hot spot occurrence significantly related to the internal structure of a solar panel, the typical arrangement that is reported in Fig.II.3. of a solar panel is made by series-connected elementary cells, usually organized in multiples of about 20, forming subpanels [86][87], each equipped with an anti-paralleled bypass diode. If one or more cells are affected by shading or malfunctioning events that reduce their photo-generated current, these cells are most likely pushed into reverse-bias mode; in this case, the diode plays the following roles:

- It play a protection role, by mitigating the reverse voltage falling on them.
- It guarantees an alternative current path, thereby preventing a collapse of the power production.
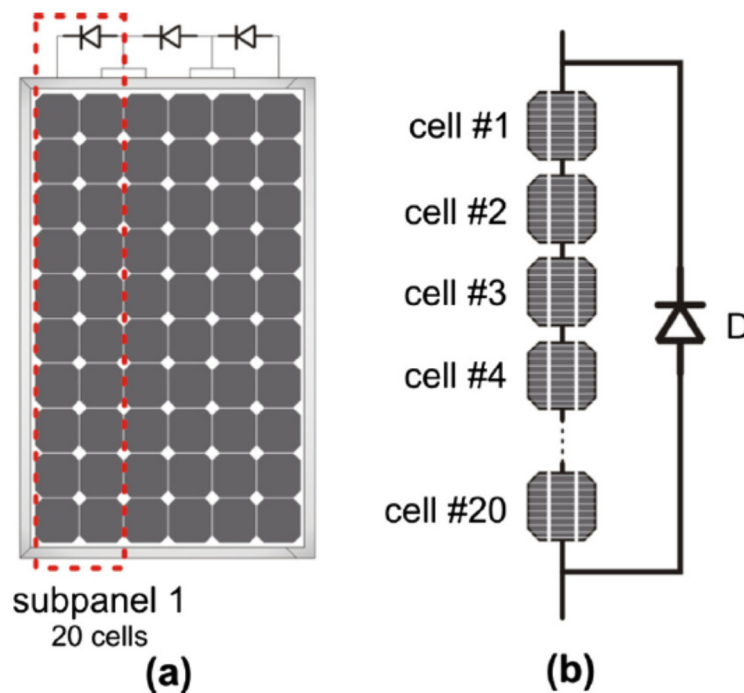
Fig. II.3. Role of diodes in PV panel (a) Sketch of a solar panel partitioned into 3x20-cell subpanels, (b) simplified representation of an individual subpanel

This scenario is schematically, illustrated in Fig. II.4, which shows the circuit representation of a subpanel, built as the series connection of one-diode cell models [88], the shunt resistances have been taken into account, because they strongly impact the operation in reverse-bias conditions, while, for the sake of simplicity, the series resistances have been neglected [84]. Whenever for some reason the current photo generated by a solar cell is less than others (in the example shown in Fig. II.4, the photo generated current corresponding to cell #1 is assumed zero) the excess current coming from other subpanels (equal to I_{string} in this case, if, in a first-order analysis, the current flow through R_{sh1} is disregarded) is forced to flow through the bypass diode D. As a consequence, the voltage across the whole subpanel coincides with the low voltage drop V_D across the forward-biased diode D (about 0.8 to 1V for silicon diodes or 0.3 to 0.5V for Schottky diodes depending on the excess current). Meanwhile, the other cells inside the subpanel cannot supply their photo-generated currents, because the series connection is broken by cell #1; hence, these currents are forced to flow through the corresponding intrinsic forward-biased diodes $D_{\#i}$, thus exhibiting a voltage drop V_F.
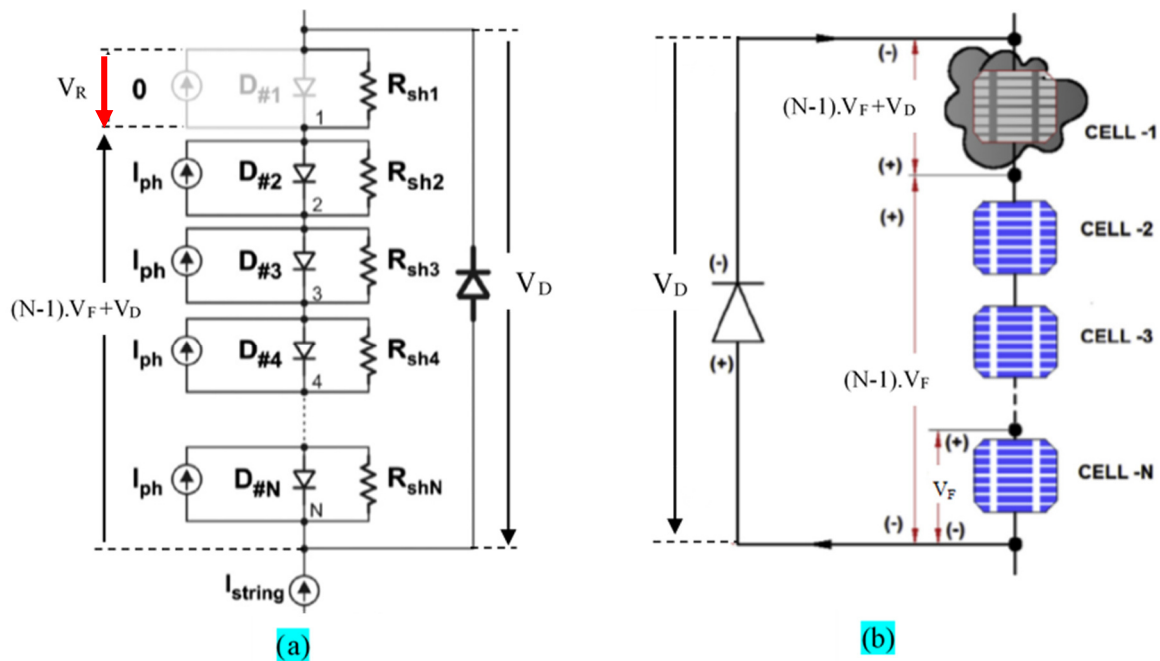
Fig. II.4. Shaded PV cells modeling (a) Equivalent circuit and (b) pictorial description of a subpanel comprising 20 cells. Cell 1 is assumed fully shaded.

As a consequence, a voltage given by $[(N - 1) * V_F]$ falls from node 1 to node N (see Fig. II.4). by applying the KLV, the reverse voltage V_R across the dark cell 1 can be evaluated as:

$$V_R = (N - 1)V_F + V_D \qquad \text{(II-1)}$$

For a reliable design the number N should be chosen low enough to prevent V_R from exceeding the breakdown voltage BV.

The above analysis has been performed by neglecting the current flow through the shunt resistance of the shaded cell; in such a hypothesis, the power dissipated by the cell would be zero (the cell does not conduct current) unless V_R approaches breakdown voltage BV. In order to quantify the power dissipation occurring in real cells ($Rsh>0\Omega$), the simple geometric construction shown in Fig.II.4, can be adopted. The I–V curve describing the series of the N-1 illuminated cells, which is also depicted as mirrored in the second quarter because, from the KLV, the positive voltage supplied by the illuminated cells appears as reverse voltage for the shaded one. Thus, the operating current of the system is given by the intercept value I^*, and the power dissipated by the shaded cell corresponds to the shaded area. It can be easily inferred that the power dissipation depends on the shunt resistance (besides depending on the shaded area, as will be shown later); in particular, a lower shunt resistance would entail a higher dissipation. A critical condition takes place when BV is lower than expected; in such a case, the reverse branch of the I–V curve may exhibit a sharp growth, thus increasing the power dissipation in fully shaded cells. Given the almost exponential shape of the I–V curve in that region, it is clear that an even small reduction in the reverse voltage could offer great benefits in terms of dissipated power [84]. Daliento et *al,* in the ref [84], confirmed by the experimental tests on two solar modules (mono-crystalline and polycrystalline, respectively) that the occurrence of low-R_{sh} cells is not rare.
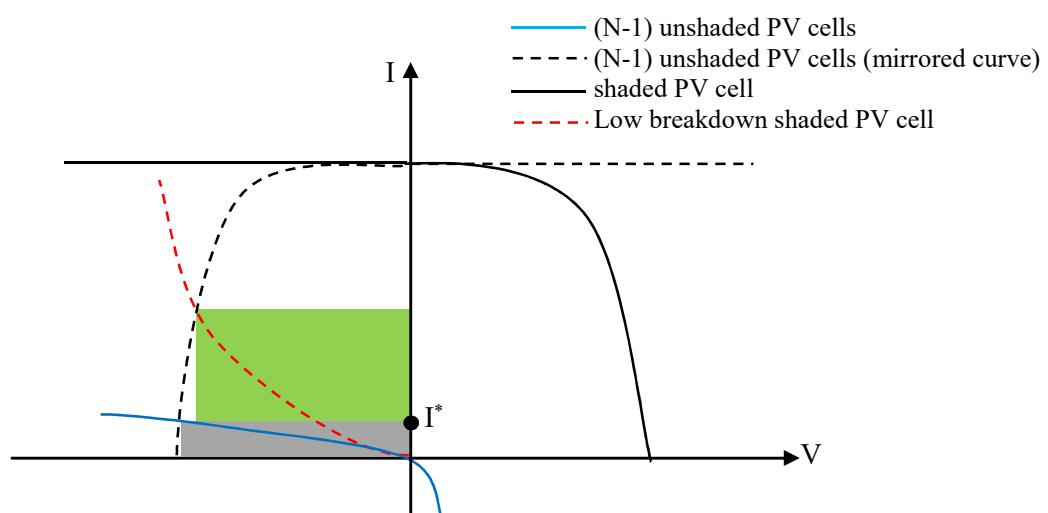
Fig. II.5. Geometric approach to determine the power dissipation in a fully shaded cell
based on the I–V curve

The geometric approach determines the operating point P_1 of a cell with a large shaded area (black dashed line) with respect to point P_0 corresponding to a fully shaded cell (black solid line). The operating point P_1 identifies the power dissipation, while I_1 is the current photo-generated by the shaded cell. By reducing the shaded area (black dash-dotted line), the power dissipation grows up to the maximum value corresponding to the operating point P_2. It is worth recalling that the qualification procedure EN 61215 identifies as ''critical'' cell the one exhibiting the highest shunt resistance; this definition originates from the fact that the dissipated power also depends on the shaded area, as schematically illustrated in Fig. II.6. [84].
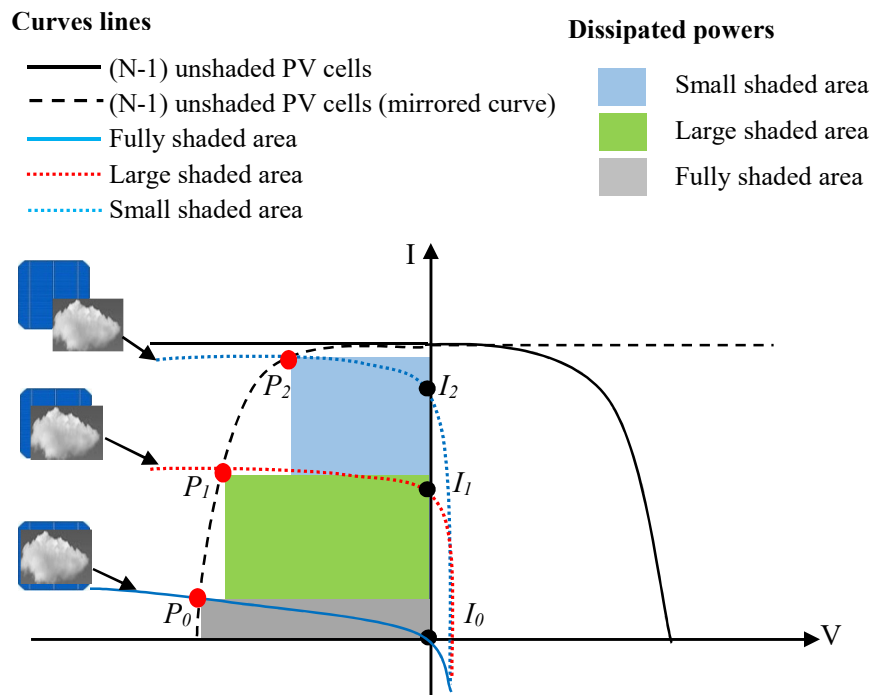
Fig. II.6. The dissipated power resulted by the shaded area in PV cells

This figure shows what happens when the shadow does not cover the entire cell so that partial photo-generation (given by current I_1) occurs. The I–V curve of the partially shaded cell can be obtained by simply translating upward the I–V curve of the dark cell. As I_1 is lower than the current supplied by fully illuminated cells, also the partially shaded cell is reverse biased and its operating point P_1 lies in the second quarter. Although the reduction of the shaded area could in principle be associated to ''better'' conditions, it is evident that the power dissipation increases with respect to the case of a fully shaded cell. By further reducing the shaded area the operating point of the shaded cell moves toward higher currents so that power dissipation increases. For each given shunt resistance a specific shaded area exists such that the maximum power producible by illuminated cells is dissipated over the shaded cell (P_2 in Fig. II.6.), an

additional decrease in the shaded area would instead reduce the power dissipation. The above description explains why a high quality cell (very high shunt resistance) can be subject to dramatically high dissipation induced by even small shadows (bird dropping, leafs, etc.). EN 61215 prescribes that in such a condition the solar panel must work for at least five hours without damages [84]. The previous analysis showed that the power dissipation over shaded cells depends on the shape of the reverse branch of I–V curves.

II.3. Simulation of PV module and different PV configurations under PSCs

The aim of this part is modeling and simulated of partially shaded PV cells inside a PV module and a different PV array configurations to show the effects of partial shading (PS) on the electrical characteristics of each one, In order to demonstrate the features of PV generators in different weather conditions. We test different PV array configurations (series, parallel and series-parallel) under uniform and PS situations. The used PV module (shell SM 55W) consists of 36 cells, connected in series and protected by anti-parallel bypass diodes, and the PV array consist of nine PV modules. The main unit of PV generators is the PV cell where a group of PV cells connected electrically and placed into a frame is called a module, which can then be grouped into larger groups of modules to form a solar array as presented Fig. II.7.

Table II.1, presents the electrical characteristics of the considered SM55W PV module, in this chapter under standard tests conditions STC ($1000W/m^2$ and $25°C$).

Table II.1. Electrical characteristics of PV module Shell SM55

Parameter	Value
Power at MPP P_{MPP}	55 W
Current at MPP I_{MPP}	3.275 A
Voltage at MPP V_{MPP}	16.5 V
Short circuit current I_{SC}	3.382 A
Open circuit voltage V_{OC}	20.5 V
Number of series cells	36

II.3.1. Simulation of partially shaded PV module

In this part we illustrate the impact of PS on PV cells inside the PV module Sell SM 55W using the graph of characteristics I-V and P-V for this module, which have 36 PV cells. This module composed of three strings, each string consist 12 series cells and each string connected in parallel with one bypass diode, that allow current flow when cells are shaded or damaged.

Fig. II.9. illustrate the interconnection of the 36 solar cells, which are organized in three strings connected in series inside the used PV module (55W). The simulation model of the PV module (SM55W), which represented previously in Fig. II.10. gives its P-V and I-V characteristics under normal conditions (1000W/m^2 and 25°C).
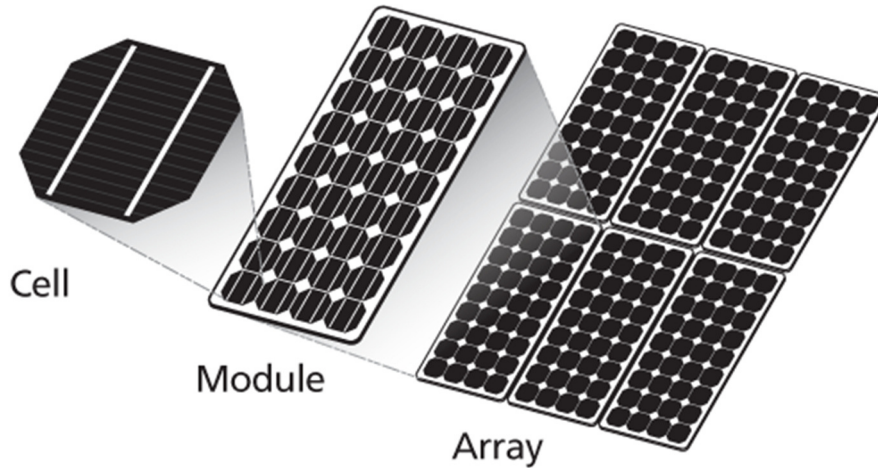
Fig. II.7. PV generator from cell to array
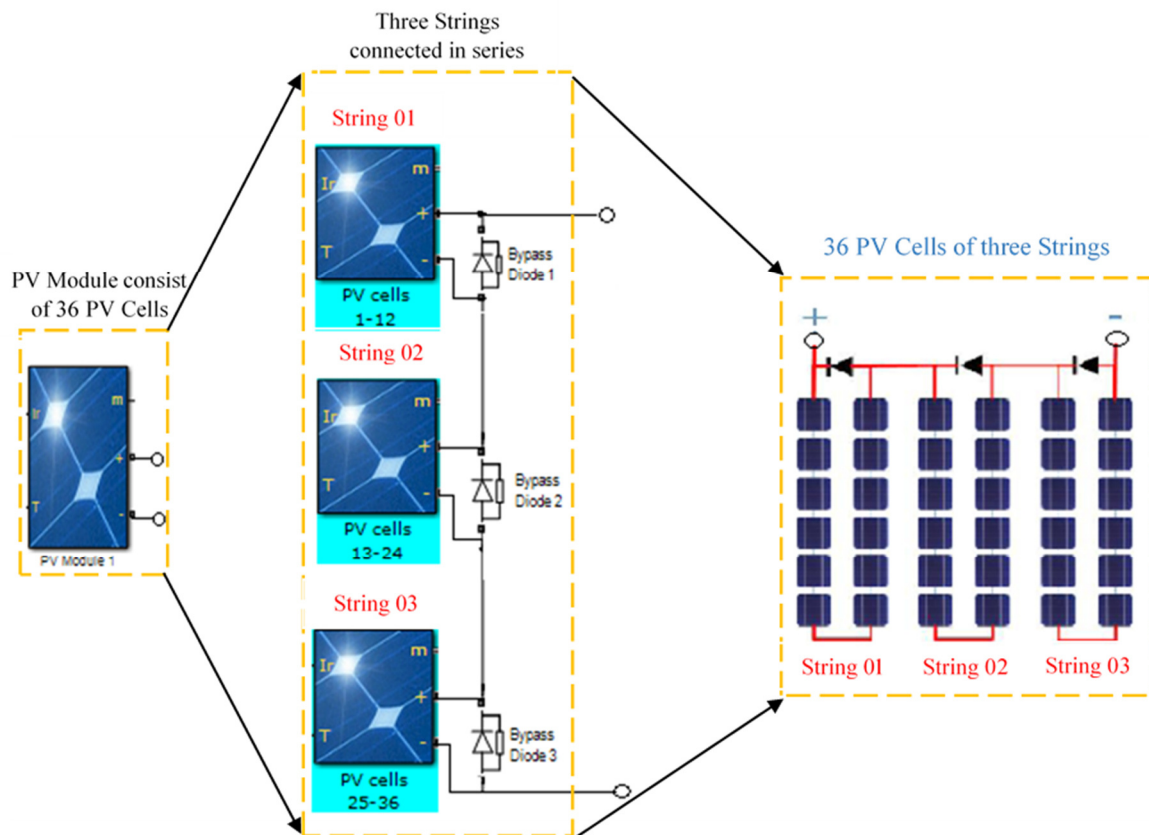
Fig. II.8. Illustrative schema for the interconnection of solar cells inside the used PV module

We note that the tested PV module (SM55W) consist of 36 cells connected in series to provide a maximum power (P) of 54.5W at a maximum voltage (V_{mpp}) of 16.51V, and maximum current (I_{mpp}) of 3.287A. Fig. II.11. shows the curves of voltage-power P-V characteristic and voltage-current I-V characteristic of the PV module (SM55W) operated under different irradiation levels. We note that the maximum output power point MPP depends on the irradiation levels, as shown Fig. II.11, whenever the solar irradiation decreases from the maximum value 1000W/m² to the minimum value 100W/m², the extracted power decreases with it.
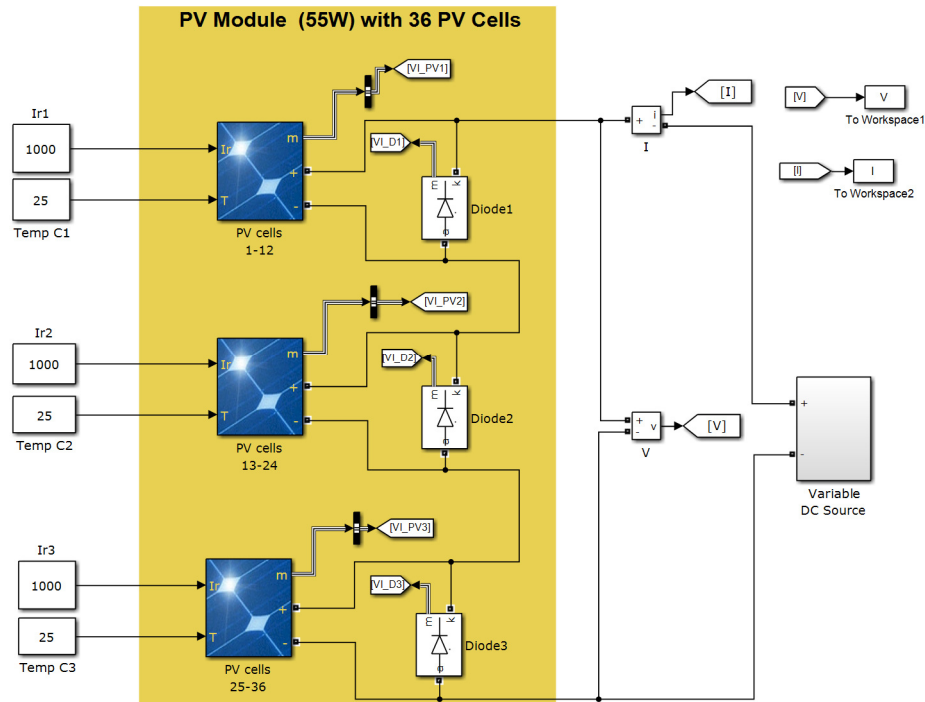
Fig. II.9. Simulated solar cells of PV module as three strings under standard test conditions STC
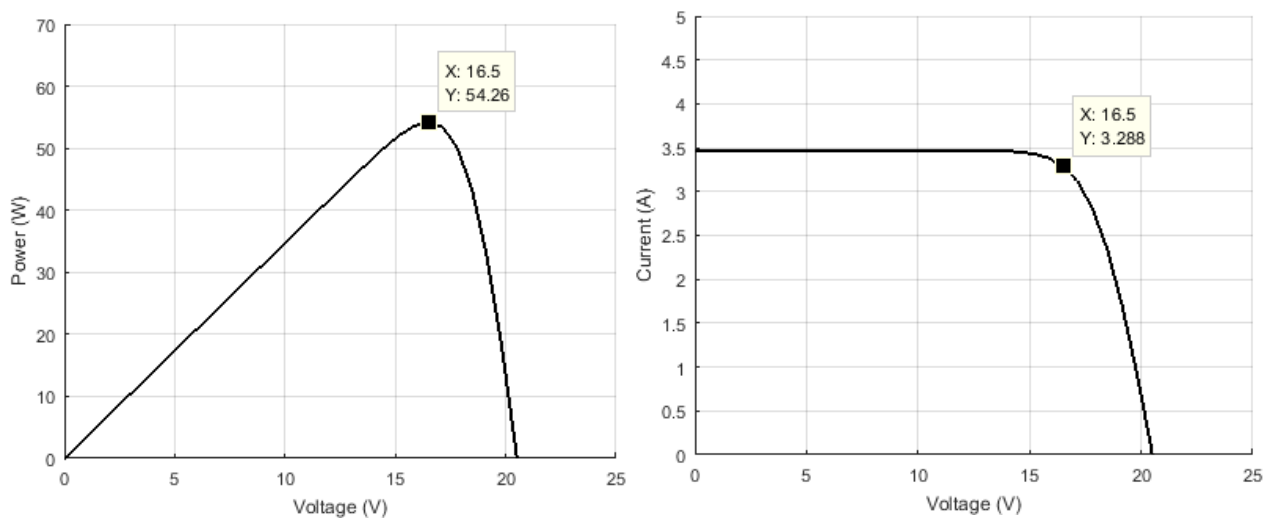
Fig. II.10. Simulated characteristics of PV module (SM55W) under standard test conditions STC
(a) P-V curve, (b) I-V curve

(a)

(b)
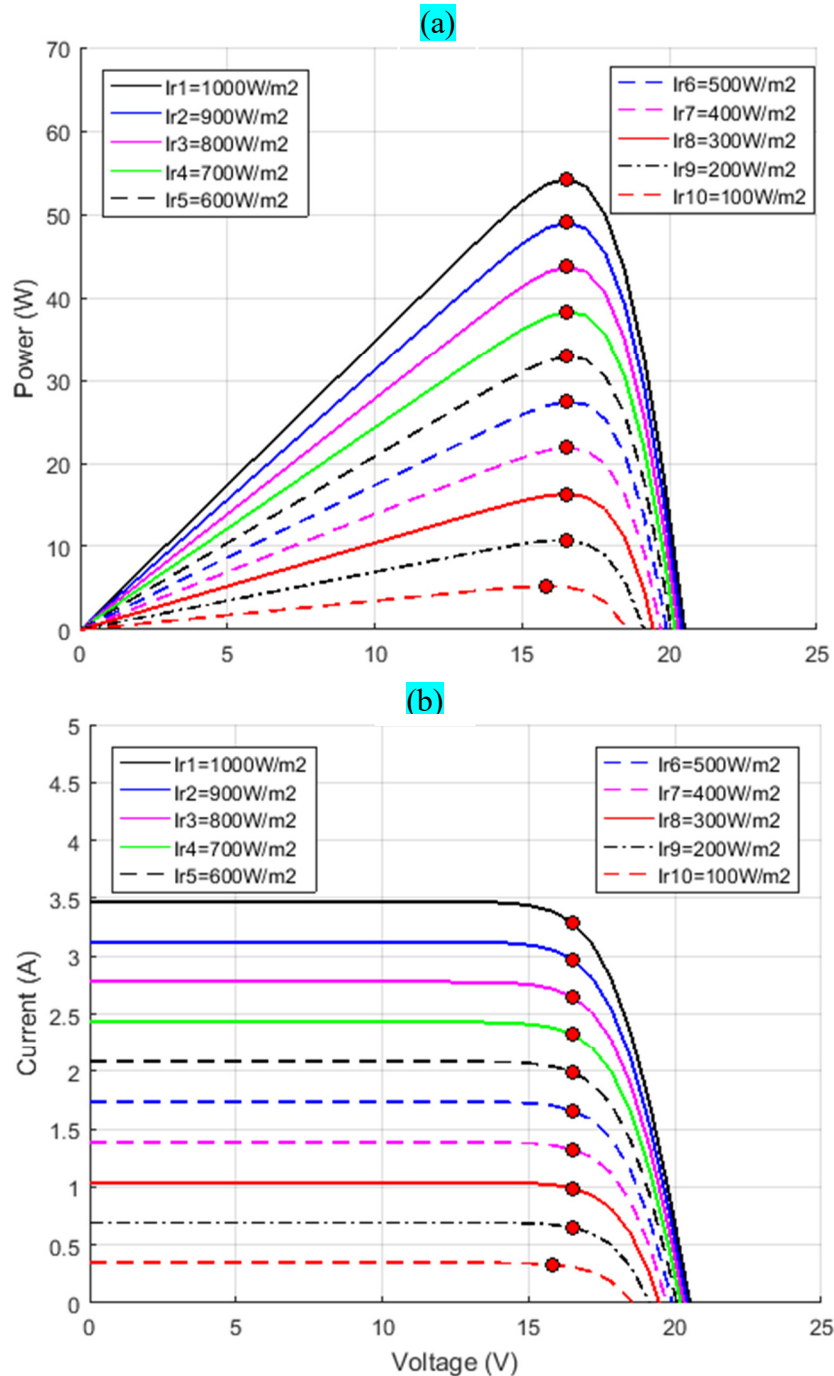
Fig. II.11. Output characteristics of PV module (SM55W) under different irradiation levels
(a) P-V characteristic, (b) I-V characteristic.

To show the effect of partial shading on the used PV module shell SM55W, we performs many simulation testes under partial shading operating conditions. Table.II.2 shows the Different tested scenarios (STC and PSC) for the used PV module 55W that consist 36 Solar cells divided to three cells strings as follow:

• String 1 consist 1-12 solar cells.

- String 2 consist 13-24 solar cells.

- String 3 consist 25-36 solar cells.

Table.II.2. The used scenarios to test the 36 solar cells of PV module Shell SM55

Strings of PV Cells	Scenario(1)	Scenario(2)	Scenario(3)	Scenario(4)
String 1: PV Cells of 1-12	1000	1000	1000	800
String 2: PV Cells of 13-24	1000	1000	800	500
String 3: PV Cells of 25-36	1000	800	600	400

Fig. II.12. Illustrate the shaded solar cells of PV module (55W) under severe shading case of the scenario 4 (800W/m^2, 600W/m^2 and 400W/m^2). Fig.II.13. illustrates the curves of the power-voltage, and the current-voltage characteristics of the three strings of the used PV module (SM55W), and three different scenarios of PSC the presented in Table.II.2.
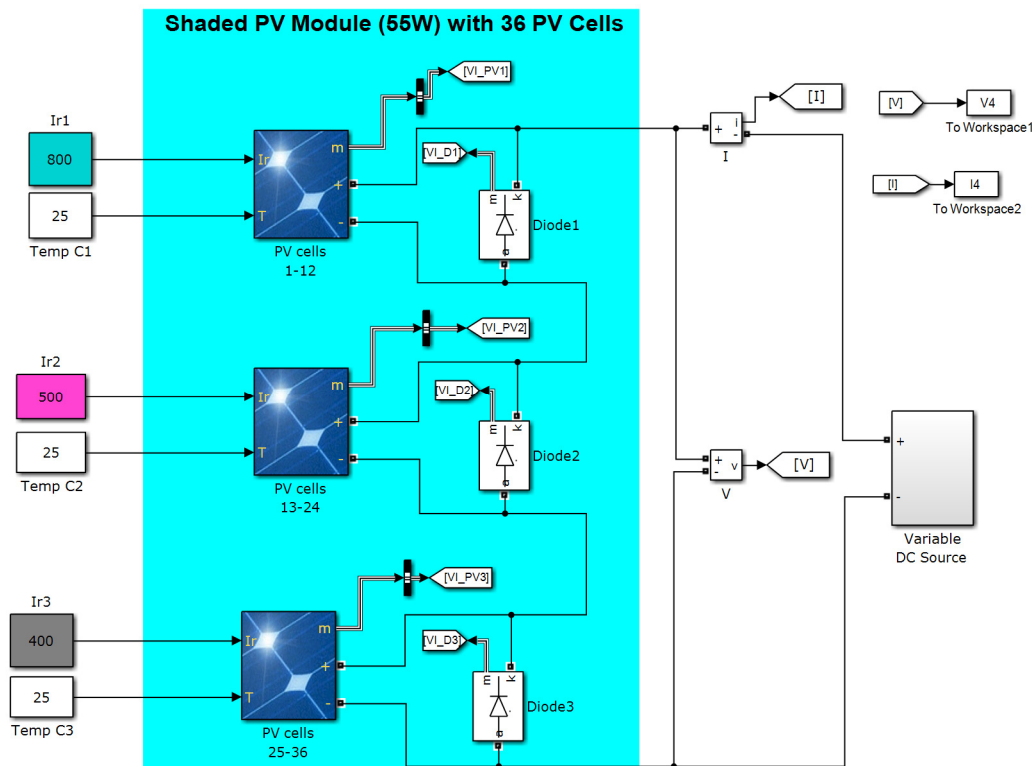
Fig. II.12. Model of partially shaded PV module cells (36 cells) under the partial shading conditions of scenario 4

The tested PV module SM55W contain three strings of 36 photovoltaic cells, which are interconnected in series as shown Fig.II.12. Under PSC, the shaded strings consumes the by current of shaded one. In order to overcome this dilemma, bypass diodes have been parallel generated power by others and dissipates heat. PSC limits the current of series connected cells
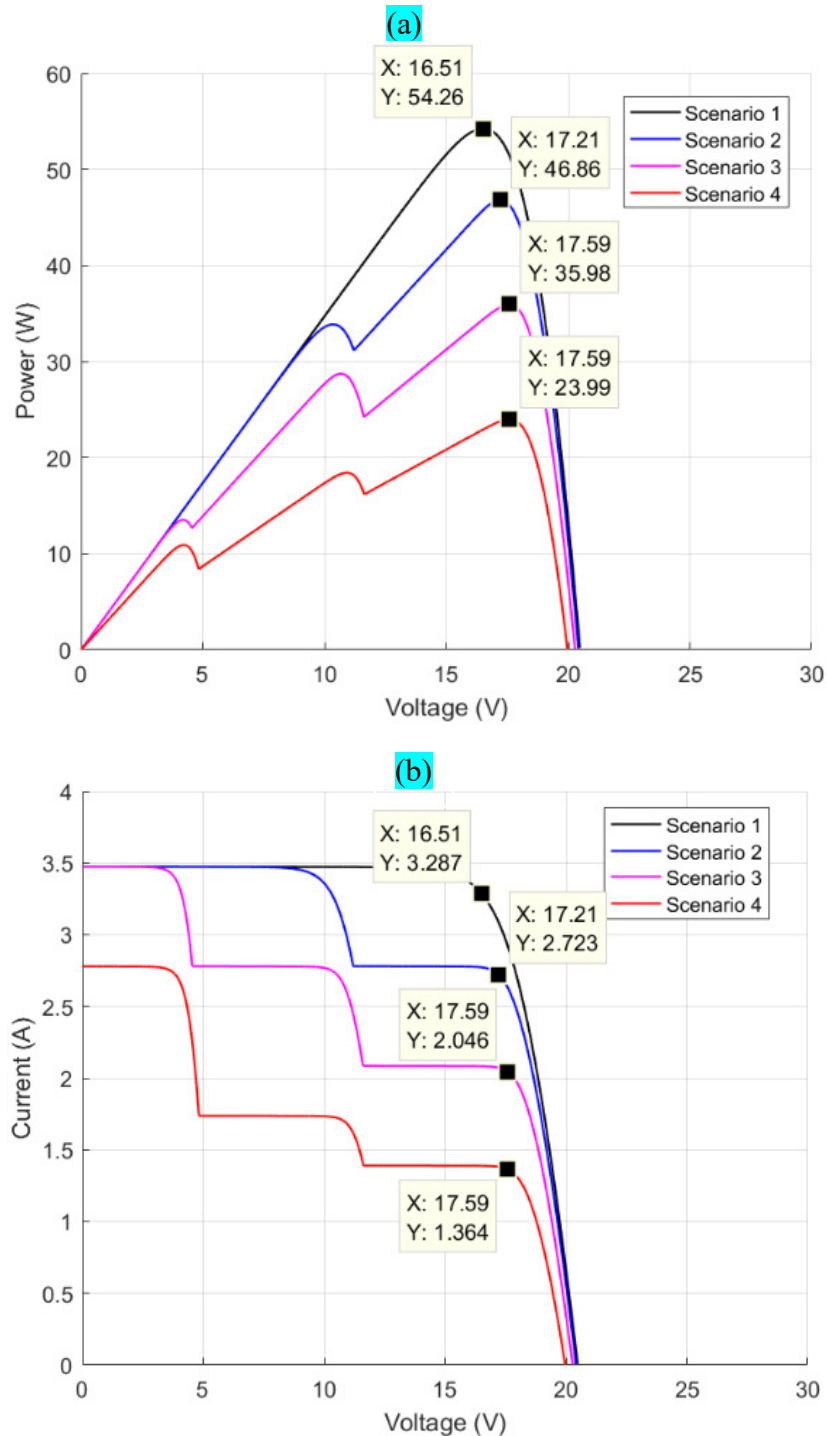
Fig. II.13. Curves of electrical characteristics for partially shaded solar cells in PV module
(a) P-V curve, (b) I-V curve

connected with each string, in this work we uses PV module contains three bypass diodes (one for each string). In normal operation, such diode is reversed and do not has any effects. Conversely, under PSC it is forward biased and carry current instead of shaded strings. From Fig.II.13, one must note that, under PSC P-V graphs contain a number of peak points, while the

I–V curve contains many steps. The number of peak points is the same as the number of different irradiance levels incident on PV strings inside the PV module. Referring to Fig.II.13 (P–V curve), the black peaks indicated by the values of the power and voltage are called the global maximum power points GMPPs while the others peacks is called local maximum power points LMPPs. it is important to operate the PV module in GMPP.

II.3.2. Simulation of different partially shaded PV array configurations

Solar arrays of photovoltaic systems use various configuration to achieve desired voltage and currents. Among these configurations, we can point to series (S), parallel (P), series-parallel (SP) total-cross-tied (TCT), Honey-comp (HC) and Bridge linked (BL) configuration [89]. Fig. II.14. represent some PV configurations simulated in this chapter.

(a)   (b)   (c)   (d)
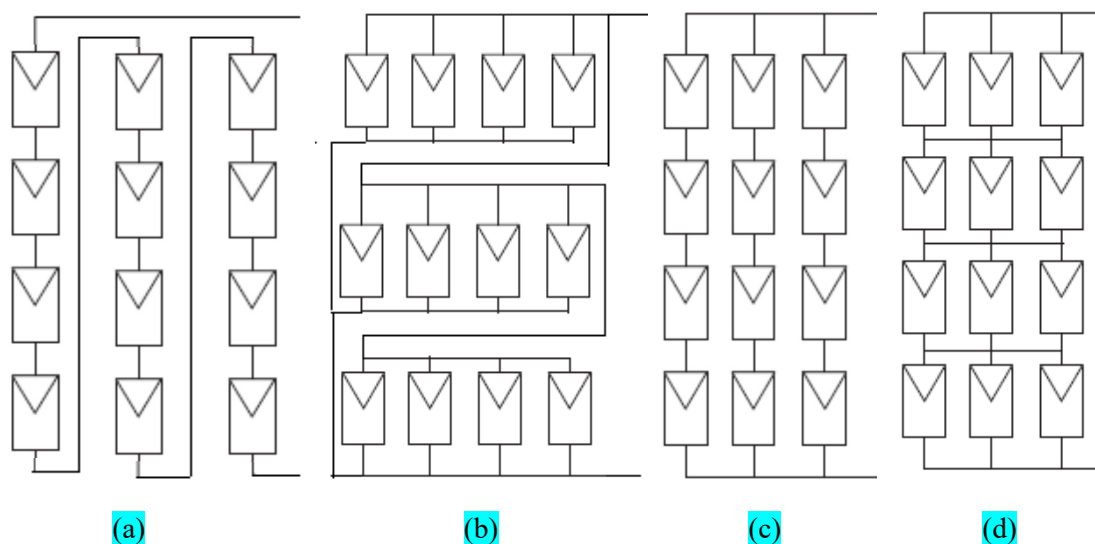
Fig. II.14. PV array configurations (a) series S, (b) parallel P, (c) Series-Parallel S-P
(d) Total-Cross-Tied TCT

In order to evaluate the behavior of each PV configuration under non-uniform irradiance conditions, which are produced by the phenomenon of partial shading and in order to show the impact of these conditions on the electrical characteristics of each of the tested topologies.

To choose the most optimal configuration that provides that highest performance. Different irradiance levels for each one PV array configuration are used to describes the partial shading in this work we applied four scenarios for each PV configuration these scenarios contain the current of shaded one. In order to overcome this dilemma, bypass diodes have been parallel generated power by others and dissipates heat. PSC limits the current of series connected cells

uniform irradiance and non-uniform irradiance (PSC) with a fixed temperature 25°C. All the used scenarios are illustrated in Table.II.3

Table. II. 3. The used scenarios for different PV configurations (W/m^2) with fixed temperature 25°C

Modules PV	Scenario (1)	Scenario (2)	Scenario (3)	Scenario (4)
PV Module 1	1000	1000	1000	1000
PV Module 2	1000	1000	1000	800
PV Module 3	1000	1000	1000	900
PV Module 4	1000	1000	900	400
PV Module 5	1000	1000	800	500
PV Module 6	1000	1000	1000	600
PV Module 7	1000	1000	800	800
PV Module 8	1000	900	700	300
PV Module 9	1000	800	400	200

II.3.2.1. PV configuration Series (9S) under PSCs

Series configuration is the simple and basic configuration and it is shown in Fig. II.15. While output voltage of this configuration is high, but output current is low. We simulated four different scenarios as shown in Table. II. 3, for showing the characteristics P-V and I-V of series configuration (9S), that is presented in Fig. II.15.
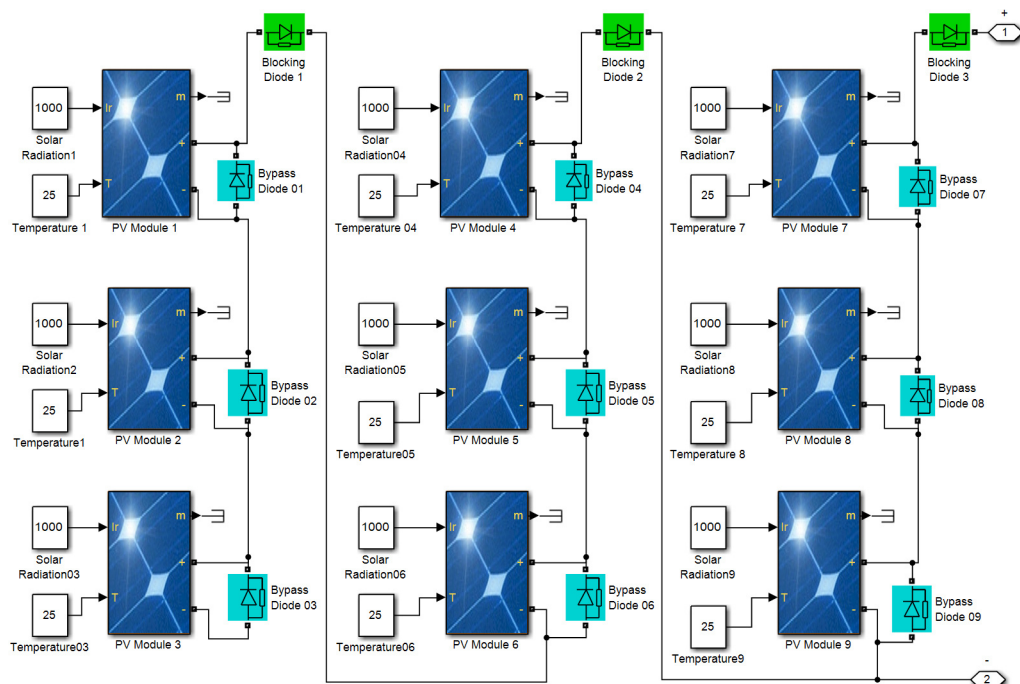
Fig. II.15. Simulink model of the PV configuration series (9S) under STC

The first scenario represent the uniform irradiation case. All PV modules of PV array receives the same solar irradiance is 1000W/m^2 that produces one global maximum power point

GMPP$_1$= 488.3W, while the others scenarios represent the partial shading cases, where the solar irradiances stroked each PV module are changing. The characteristics graphs P-V and I-V are showed in Fig. II.16. (a) and (b), gives four global maximum power points GMPPs and the local maximum power points LMPPs for the four adopted scenarios, where the GMPPs of 9S configuration for each scenario are 488.3W, 434.2W, 399.4W and 182.4W.
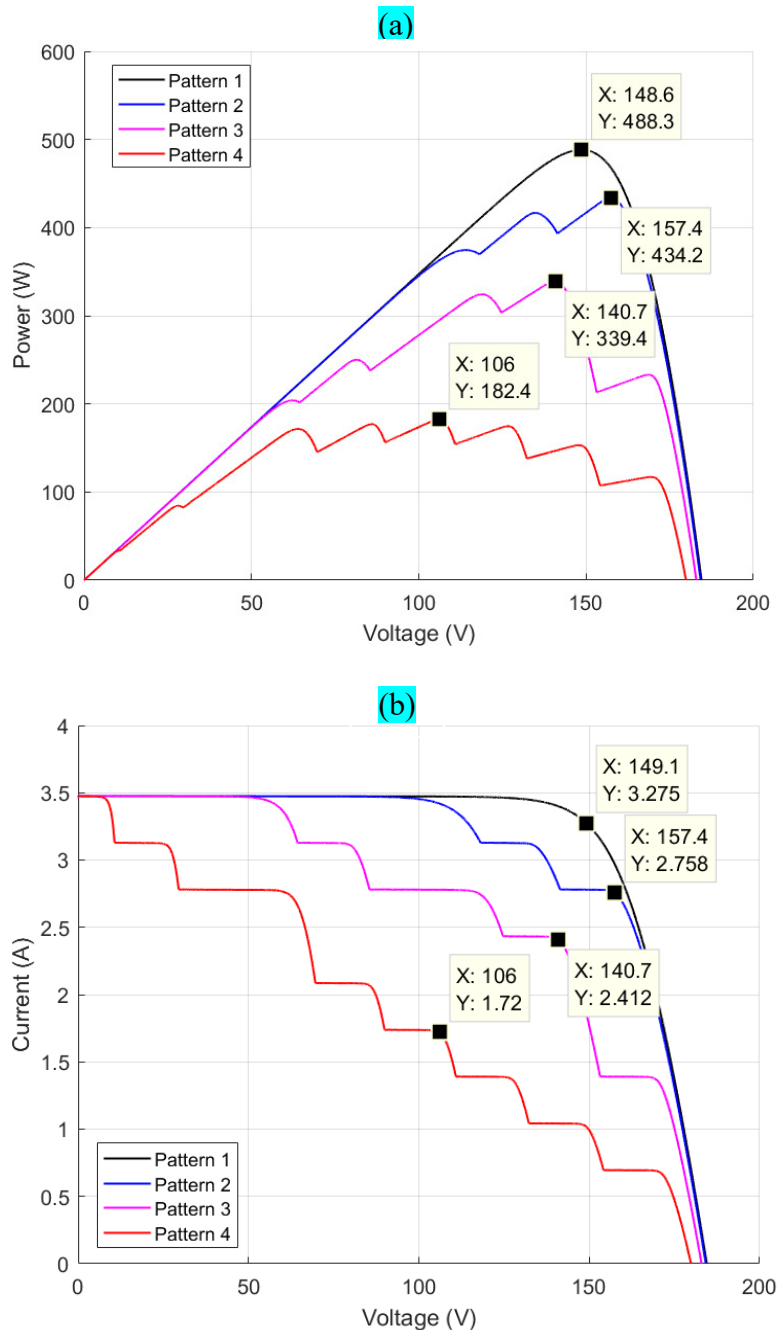
Fig. II.16. Curves of electrical characteristics for series PV configuration (9S) under the conditions of the four scenarios tested (a) P-V curve, (b) I-V curve

II.3.2.2. PV configuration parallel (9P) under PSCs

The Simulink model of a parallel configuration (9P) of the used PV array is presented in Fig.III.17, The P–V and I–V characteristics curves under uniform and partial shading conditions for parallel configuration are shown in Fig.III.18. In parallel connection, array voltage is same as module voltage and the array current is equivalent to sum of the currents of the individual PV modules. In this configuration, the voltage at MPP of non-shaded and shaded PV modules is almost constant and is uniform throughout the entire PV array. While the current generated from each PV module flows without any limit with respect to the irradiance level. Therefore, parallel interconnected PV system operates more effectively under rapidly varying solar irradiance levels. Under PSCs, parallel PV array topology produces more power than series PV array topology due to high currents and low voltages that are do not vary significantly. However, due to higher currents, power losses and voltage drops are generally higher [90].
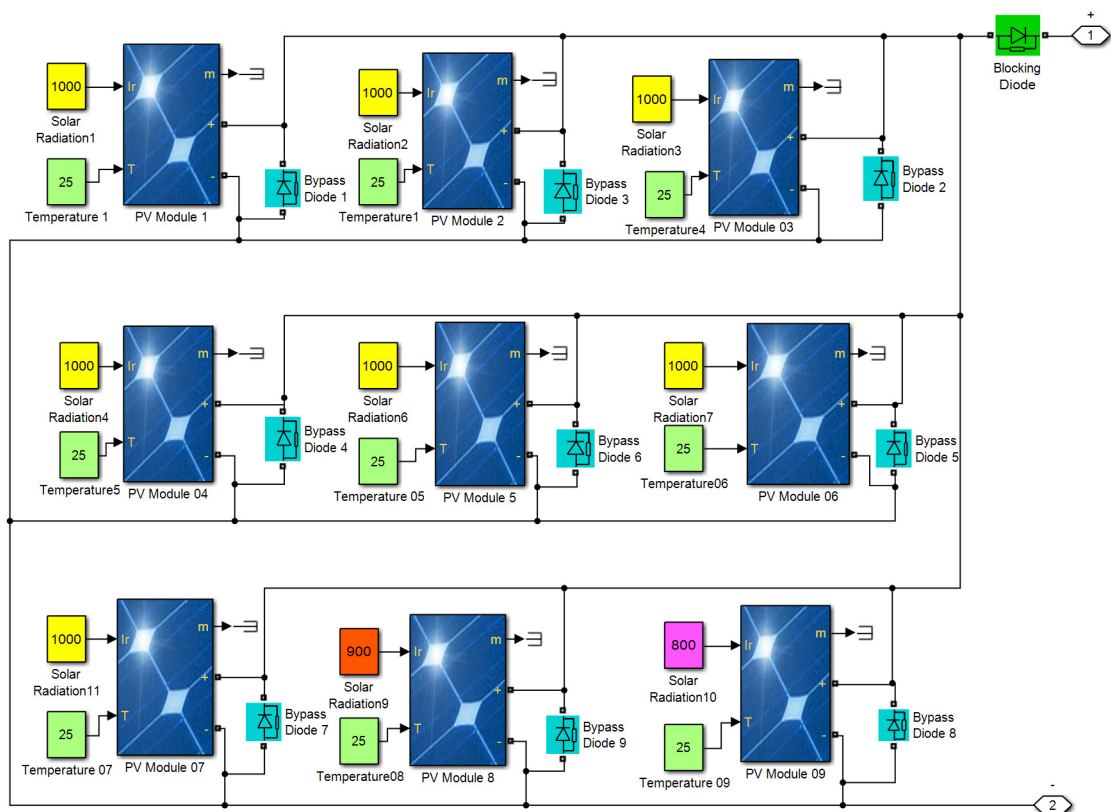
Fig. II.17. Simulink model of the PV configuration parallel (9P) under PSC

The simulated output characteristics of parallel PV array topology under various shading scenarios are shown in Fig. II.18. From these characteristics, we examined that under PSCs it

generated a single power peak and the effect of bypass diodes is ignored and output characteristics represent a single MPP similar to uniform irradiance condition.

However, due to its low voltage and high current make this topology is not suitable for many PV system applications and, also for the performance assessment of PV array topologies this configuration is not considered.
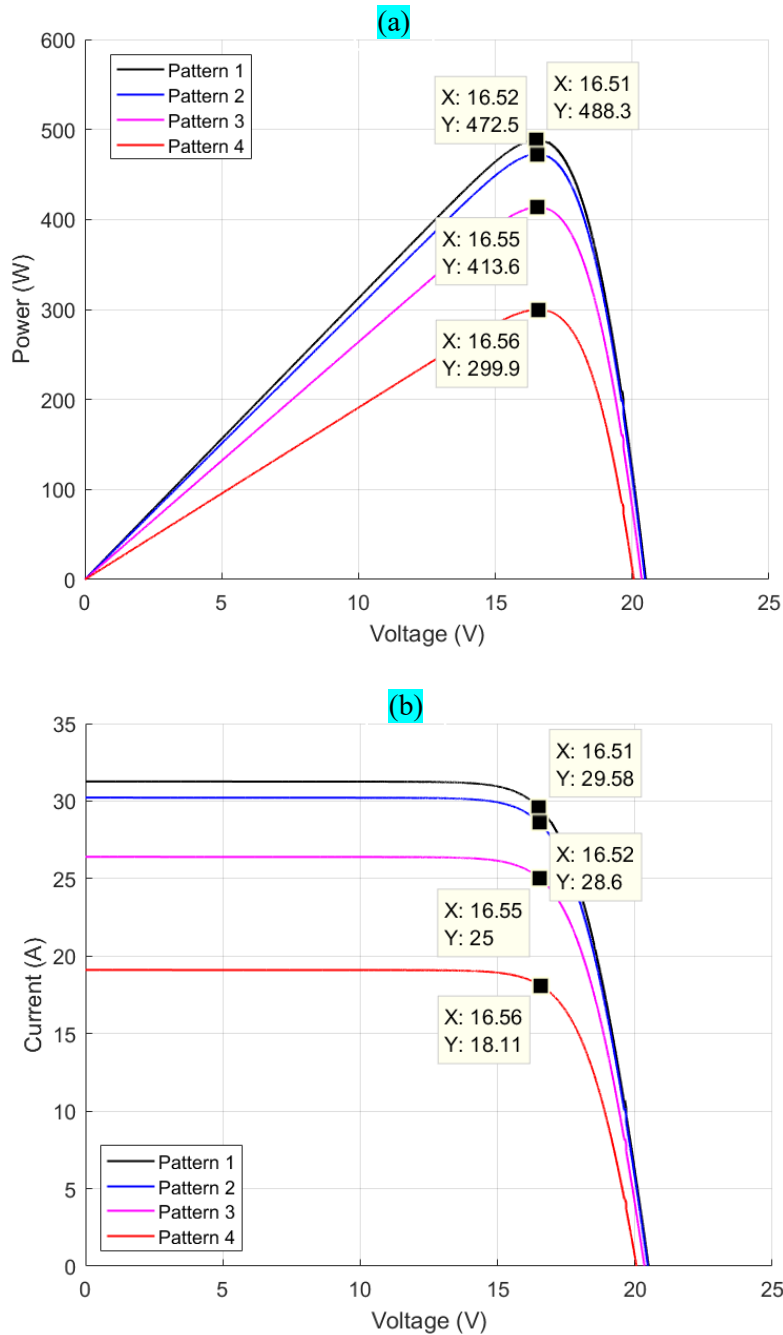
Fig. II.18. Curves of electrical characteristics of the PV configuration parallel (9P) under the conditions of the four scenarios tested (a) P-V curve, (b) I -V Curve

II.3.2.3. PV configuration Series–Parallel (S-P) under PSCs

The configuration (3S3P) of tested PV array is shown in Fig. II.19. In order to get desired Output voltage, all modules are first connected in series form and then these series connection are connected in parallel. In this section, the procedure used to obtain the I-V characteristics of shaded PV arrays is described. An illustrative example explains the behavior of a PV array composed of three parallel-connected strings, while each string composed of three series connected modules is presented. The irradiance levels received by each module in this configuration is given in Table II.3.
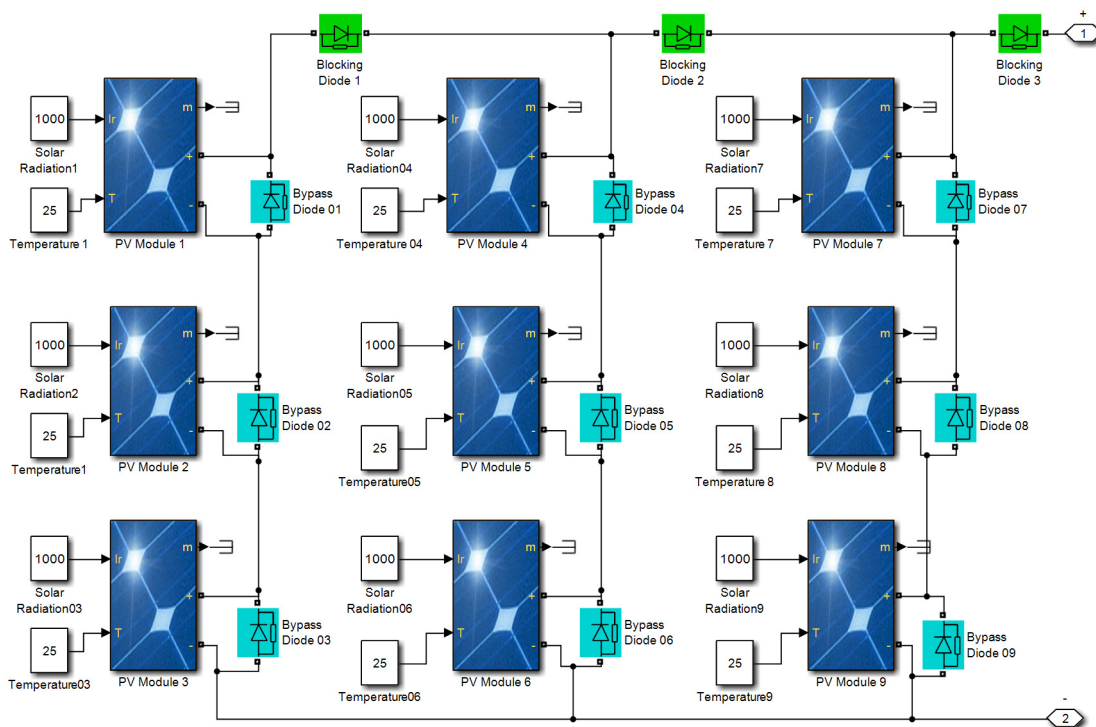
Fig. II.19. Simulink model of PV configuration Series-Parallel (3S3P) under STC

The series-parallel PV array topology is most commonly used PV array topology because it is easy to construct, economical and there are no redundant connections.

 The PV modules in this topology are divided into three rows and three strings and each string consists of three series connected modules. The PV array current is the sum of the three string currents and the array voltage is equal to the sum of module voltages in a string. In addition, bypass and blocking diodes are also connected in series (see Fig. II.19) to protect each PV string from severe PSCs or short circuit conditions. These diodes blocks backflow of string current into another string, due to the potential difference between the strings under PSCs.

 In standalone PV systems, blocking diodes are preferred to block reverse flow of currents from the storage battery to PV array under PSCs or at night times.

The simulated output characteristics of 3S2P topology under various shading patterns are shown in Fig. II.20. the 3S2P configuration produced fours global various shading patterns are shown
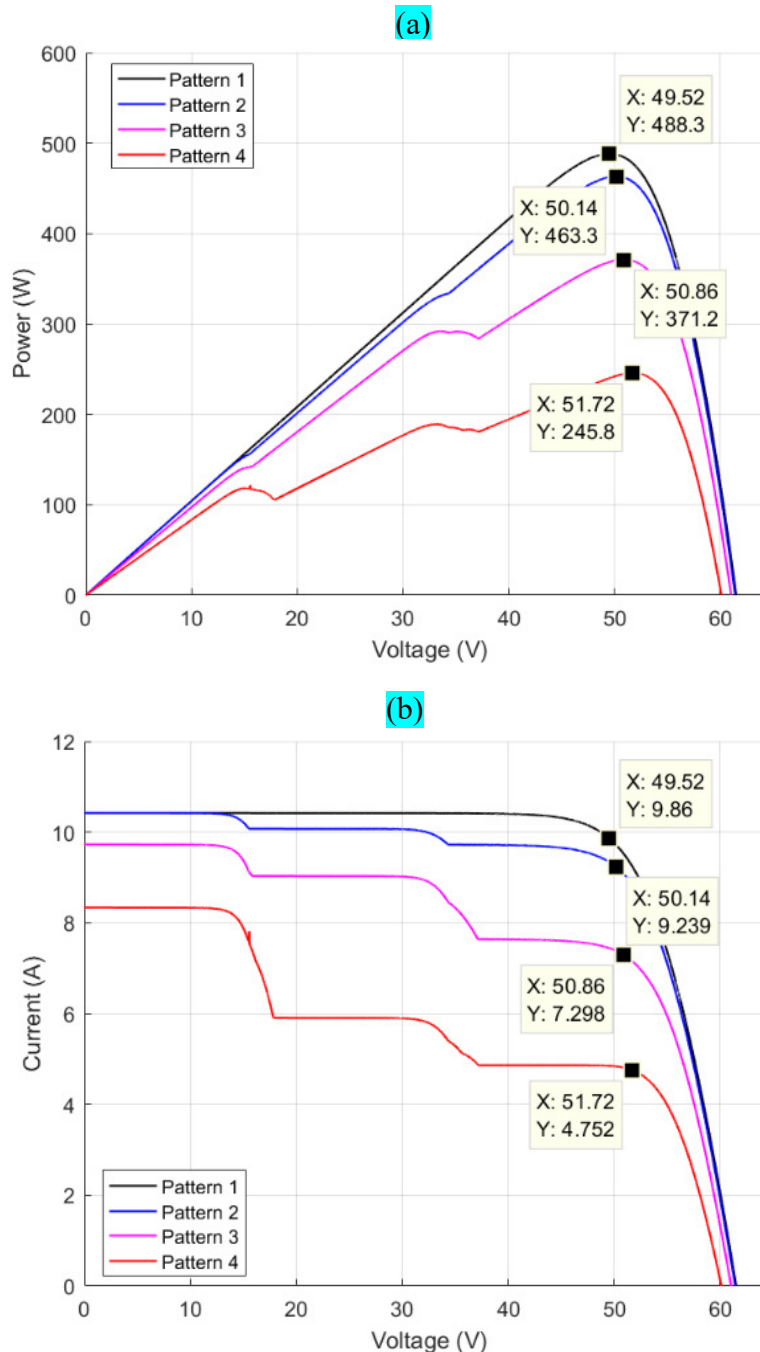
Fig. II.20. Simulated characteristics of PV array configuration (3S3P) under four used scenarios (a) P–V curve (b) I–V curve

In Fig. II.20. the 3S2P configuration produced fours global peaks representing the global maximum power points GMPPs which are 448.3W, 463.3W, 371.2W and 245.8W for the four adopted scenarios also respectively. Due to more number of series connections in strings the mismatching losses are more but less than series array topology.

II.3.2.4. PV configuration Total-Cross-Tied (TCT) under PSCs

Total-Cross-Tied (TCT) configuration is formed by connecting all nodes of rows in SP configuration. In TCT configuration, the voltages of all nodes and also the sum of currents in different junctions are equal, this configuration can resolve the disadvantages of S-P configuration. There have been many studies conducted on comparison between different solar array configurations (SP), Honey-comp (HC), Bridge-linked (BL), and TCT) under partial shading conditions and in every study (references [91], [92] and [93]) the superiority of TCT configuration under partial shading conditions is proved through simulation [89]. TCT topology modeled as first, all PV modules are connected in parallel as rows and then rows are connected in series. The Simulink model of 3×3 TCT PV array topology shown in Fig. II.21, in TCT configuration, the voltage across each row is equal to open-circuit voltage of single PV module and the array or desired output voltage is equal to sum of voltages across all the rows.
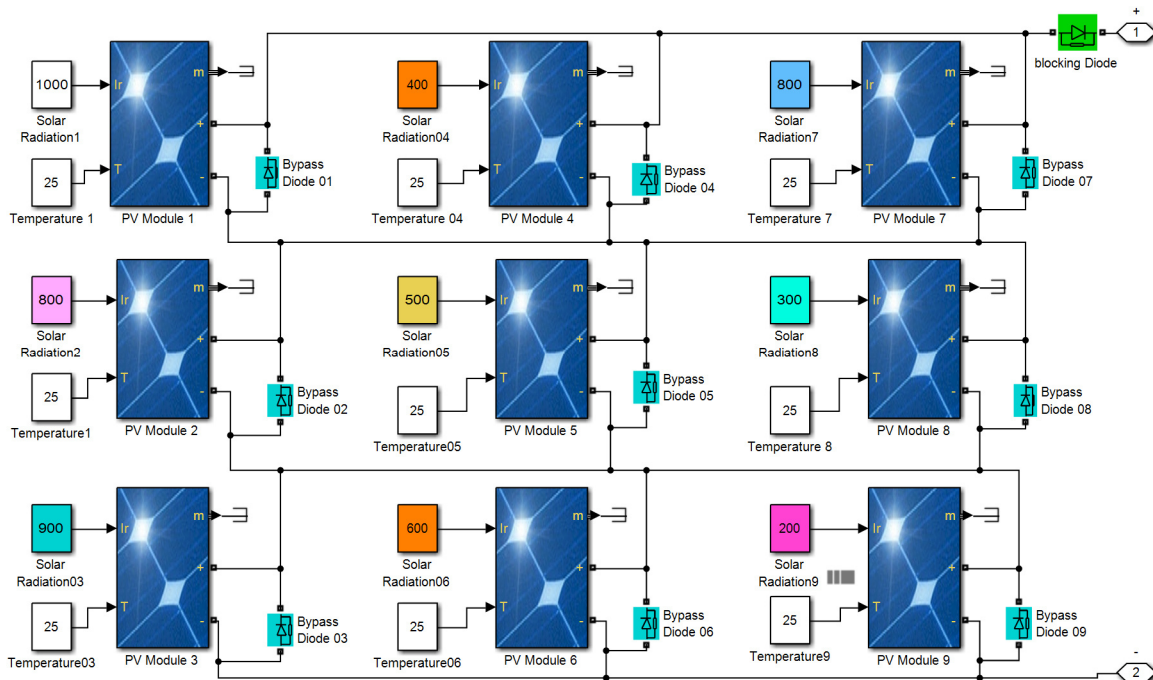
Fig. II.21. Simulink model of partially shaded PV configuration TCT for scenario 4

In TCT configuration, the total array current is the sum of currents generated from all the PV modules in a row. Since PV array configuration has higher number of electrical connections when compared to other topologies.
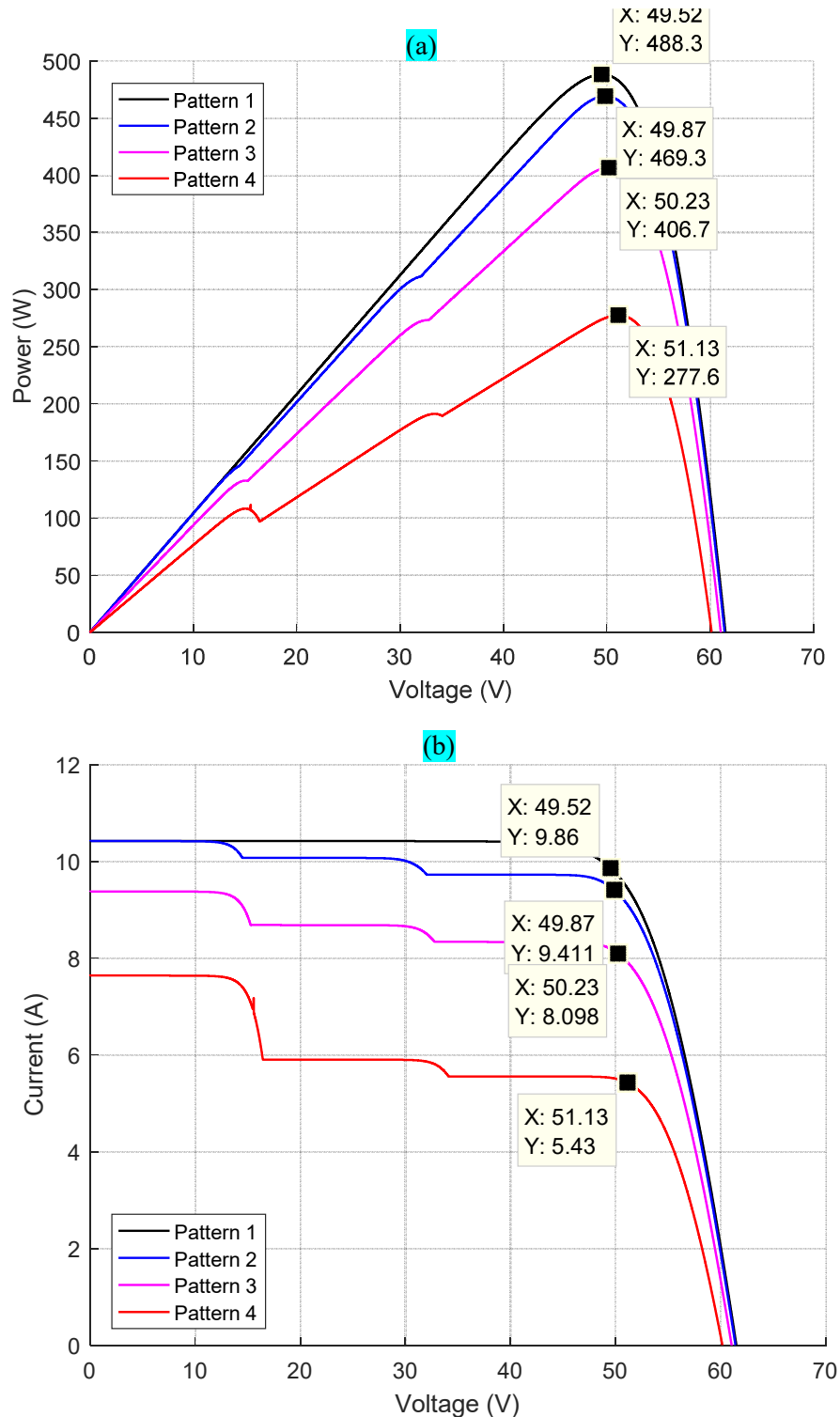
Fig. II.22. Simulated characteristics of PV configuration 3x3 TCT under four used scenarios
(a) P-V curve (b) I-V curve

The curves of the electrical characteristics P-V and I-V of the simulated TCT configuration that tested for STC and PSCs conditions are shown in Fig. II.22 (a) and (b). As shown in Fig.II.22.(b), the PV array in TCT configuration generated four global peaks which represent the global maximum power points GMPPs, which are 470.6W, 452.6W, 391.9W and 267.9W these points correspond to four adopted scenarios respectively.

II.3.2.5. Analysis and discussion

Firstly, we summarizes in the Table.II.2, all global maximum power GMPPs values obtained from the simulation for each proposed PV array configurations in all tested cases.

Table II.2. Global Maximum power GMPP (W) for all PV array configurations for a 3×3 array

Configuration	GMPP (W) For Scenario (1)	GMPP (W) for Scenario(2)	GMPP (W) for Scenario(3)	GMPP (W) for Scenario(4)
Series (S)	**488.3**	434.2	339.4	182.4
Parallel (P)	**488.3**	**472.5**	**413.6**	**299.9**
Series- Parallel (S-P)	**488.3**	463.3	371.2	245.8
Total-Cross-Tied (TCT)	**488.3**	**469.3**	**406.7**	**277.6**

According to those data the configurations S, P, SP and TCT gives the same maximum power at the first scenario (STC case) where in this case all the PV modules in each PV array topologies are subjects to the uniform irradiance 1000 W/m². From the simulated output characteristics of PV topologies S, P, S-P and TCT, that shown in Figs.II.16, 18, 20 and 22, respectively all the PV array topologies generates the maximum power of 488.3W and produces a single MPP on output characteristics, which is referred to as GMPP. Under this condition, the S, P, S-P and TCT PV array topologies generates the same voltage and current at GMPP. In STC case the mismatching power losses of all these topologies is almost equal to zero and the function of bypass diodes is ignored since all these diodes are operates under reverse bias condition only. The fourth scenario, represent critical case of partial shading where the parallel (P) configuration gives the highest maximum power (299.9W), then the TCT configuration has second best maximum power (277.6W), the series-parallel (S-P) configuration has third best maximum power (245.8W) but series configuration (9S) has the lowest maximum power (182.4W).

As a result, of the previous simulations results, we noted that the parallel (P) and Total-Cross-Tied (TCT) configurations has the highest output power during all examined scenarios,

comparing to all other examined configurations, whereas the series (S) configuration has lowest output power.

II.4. Conclusions

In this chapter, we have studied, with precise analysis, the effects of partial shading on the I-V and P-V characteristics of PV cells and different configurations of PV panels, are series (S), parallel (P), series-parallel (S-P), Total-Cross-Tied (T-C-T). All the simulated PV configurations consist of nine PV modules. As we noted in the simulation results that the partial shading problem reduced the generation efficiency of a solar cells in PV module or PV array, or even cause hot spot phenomena. Based on simulation results we conclude that parallel (P) and Total-Cross-Tied (TCT) configurations has the highest output power during all examined PS conditions comparing to all other tested configurations, whereas the series (S) configuration has the lowest output power. The parallel and TCT configurations confirm their superiorities in comparison to other configurations in terms of maximum output power and power dissipation for different shading scenarios. This better performance is due to more internal connections of parallel and TCT configurations in comparison to series (S) and series-parallel (SP) configurations, which provides more current paths for these configurations and prevents the reduction of current because of current reduction in other branches. As a result, efficiency of PV array strongly depends on the PV array configuration. Furthermore, the partial shading problem greatly affects the efficiency of any PV array configuration.

Chapter III

Simulation of metaheuristic MPPT methods under changing weather conditions

| Chapter III | Simulation of metaheuristic MPPT methods under changing weather conditions |

III.1. Introduction:

The production of electric energy from photovoltaic (PV) has a lot of applications as in space satellites and orbital stations, solar vehicles, power supply for loads in remote areas, street lighting systems, and generation of electric power in central power stations. PV is environmental friendly and has no emission of harmful gasses as the emission associated with conventional electricity generation [50]. In recent years, there is a great attention in the development of renewable energy sources due to the depletion of fossil fuels and burning of those fuels causes the environment pollution. Renewable energy sources are pollution free energies and they contribute to reduce the greenhouse effects. Solar, Wind, Tidal, biomass are the different types of renewable energy sources utilized to generate electricity. Out of these four sources, solar energy is one of the most prominent alternative sources of energy because of surplus amount of energy from the sun and the financial support provided by the governments and in recent times solar panel costs are drastically decreased, which will lead to the for reduction per unit electricity generated. Furthermore, solar energy considered the best solution for many rural area applications such as communication systems, water pumping, or small house appliances [49]. By forcing, the PV array to work at the voltage corresponding to MPP will substantially increase the energy produced. This increase in the energy production can be translated into cost reduction of the PV power system, which shows the importance of MPP tracker, maximum power point tracking (MPPT). Tracking MPP needs a fast and smart controller system to counteract the fast change in weather data or load changes [50]. In order to achieve MPP in PV systems, a power controller is needed to implement one of MPPT algorithms. Many scholarly methods to reach the maximum power effectively. We found in recent studies, three main classes of MPPT methods, are conventional MPPT class (P&O, INC, HC…etc.), soft computing (SC) class (FLC, ANN, and meta-heuristic methods), and hybrid MPPT class. The conventional methods failed to locate MPP (LMPP) and have continuous fluctuation to power oscillations at MPP, which reduce the extracted power by the PV array. Hence, to alleviate this problem, recent researchers have proposed a variety of metaheuristic optimization algorithms such algorithms contain: Cuckoo Search (CS), Particle Swarm Optimization (PSO), Ant Colony Optimization (ACO), Artificial Bee Colony (ABC) and

Firefly Algorithm (FA) and Teaching Learning Based Optimization (TLBO) [94]. Recent various studies, on soft computing algorithms are attracted the attention of researchers, because many of SC algorithms proved their high effectiveness, better convergence and robustness for a lot of optimization problem. This encourages us for propose soft computing algorithms to dealing with tracking global MPP in partially shaded PV systems [8].

This chapter aims to verify the performance of some MPPT methods that are Perturb and Observe (P&O), Particle Swarm Optimization (PSO) and Cuckoo Search technique (CS) for a standalone PV system with boost *DC-DC* converter, under different changing weather conditions. In addition, we presents in this chapter a quantitative comparison between the simulated MPPT methods P&O, PSO and CS.

III.2. Overview of simulated MPPT techniques

As a reminder, we present in this section a brief overview of each proposed MPPT methods P&O, PSO and CS, that we will test in this chapter using simulations in Matlab/Simulink. Knowing that these methods are presented with explanations in chapter two.

III.2.1. Overview of P&O-MPPT method

As it presented in chapter II, the perturb and observe P&O algorithm is based on the concept that on the power-voltage curve, the change in the PV array output power is equal to zero ($\Delta P_{PV} = 0$) on the top of the P-V curve. The P&O operates by periodically perturbing (incrementing or decrementing) the PV array terminal voltage or current and comparing the corresponding output power of PV array with that at the previous perturbation. If the perturbation in terminal voltage leads to increase in the PV power ($\Delta P_{PV} > 0$) the perturbation should be kept in the same direction, otherwise the perturbation is moved to the opposite direction. The perturbation cycle is repeated until reaching the maximum power at ($\Delta P_{PV} = 0$). There are two different ways to implement the P&O algorithm.

- In the conventional way a reference voltage is used as a perturbation parameter, therefore a PI controller is needed to adjust the duty ratio.
- The second way is that, the duty ratio is directly perturbed and the power is measured every PWM cycle [95].

The crucial aspect of this algorithm is to determine the step size. If step size is large, the convergence is fast but that causes large fluctuation in the steady state power and vice versa. Whatever the case, the oscillation causes undesirable losses of PV power during steady state [21]. the advantages of this technique are simplicity, ease of implementation and it does not require a previous knowledge of the PV array [95].

III.2.2. Overview of PSO-MPPT method

PSO is a soft computing method that is used to solve the several optimization problems, it has been recently applied for MPPT application, originated from observing the behavior of the bird flocks, which and is used, and in PSO particles, each particle represents a potential solution, which is corresponding to a fitness values based on fitness function. Assuming in a space, there are N particles, among them, the velocity and position of ith particle are respectively [96]. In the start, the optimization process is initialized by the duty cycle vector, which serve as the initial particles in the first iteration. Consequently all particles move towards their local best position P_{best}. Among these particles, one of them is the global best G_{best}. It gives the best power value (fitness). After calculating the velocity, which serves as a perturbation to the duty cycle, a new position of the duty cycle is found. Through successive iteration all particles move towards global best position. As the particles approach the MPP, they get closer to the G_{best} position that represent GMPP. Eventually a zero velocity is achieved and the duty cycle position remains almost unchanged. Under this condition, the PV system reaches at GMPP [21].

III.2.3. Overview of CS-MPPT method

This swarm optimization technique is derived from the behavior of cuckoo, which is based on the reproduction strategy of some species of cuckoo bird which are reported to lay their eggs in the nests of other birds and destroy the host bird eggs to get more food for its own species. Intelligence of bird Cuckoo during hatching is applied for MPP tracking where the step size of the CS is based on Lévy flight and is a population-based algorithm. The birds lay their eggs in some other birds (host bird) nest. [64]. At the starting, the number and values of duty cycles is randomly selected. Then, all initial values of duty cycles are sent to dc-dc converter of PV system. The system current and voltage are measured in order to estimate extracted PV power P_{pv}. Such power represents the fitness value. The duty cycle related to best fitness function has been selected as current best nest (d_{best}). Next, Lévy flight is applied in order to generate new nests. New finesses values P_{pv} are tested through the PV system. Afterward, the worst nest is randomly destroyed, and this process simulates the behavior of the host bird discovering the cuckoo's eggs and destroying them. The fitness P_{pv} is measured and the current best nest is selected. When the stopping criterion is achieved, CS-based tracker stopped and gives optimal duty cycle which corresponds to global power GMPP [61].

III.3. Simulation results of metaheuristic MPPTs methods:

In this section, we aim to check the tracking performance of GMPP for three MPPT

methods which contain two metaheuristic techniques are PSO and Cuckoo search (CS) and one conventional technique is P&O. We evaluate these MPPT techniques by a Matlab/Simulink simulation for an isolated PV system subjected to four different cases, including changing weather scenarios, which represent, the both variations of irradiation levels and temperature, in all tested cases we use the configuration series-parallel (3S2P) of PV array that illustrated in Fig.III.2. The proposed MPPT controllers feeding the boost converter with suitable duty cycle for studying and comparing dynamic response of PV system during the different tests cases, which presented in Table. III.1.

Table.III.1 Operating conditions of four tested cases

Tested cases	Atmospheric conditions
case 01	Standard test conditions (STC), characterized by: irradiation and temperature are constants
case 02	Constant irradiation and high temperature
case 03	Partial shading case (PSC), characterized by: Non-uniform irradiation and constant temperature
case 04	uniform irradiation and variable temperature

All parameters of each proposed MPPT methods are detailed in the Table.III.2 where:

- P&O method contained the initial duty cycle D_0 and the step size ΔD.

- PSO algorithm included the maximum and minimum inertia weight (w_{max}, w_{min}) and the acceleration factors c_1 and c_2.

- CS method included the Lévy multiplying coefficient $k_{Lévy}$, the variance $Beta$, the normal distribution σ_v where $v \approx N\left(0, \ \sigma_v^2\right)$ and the probability of discovered P_a.

Table.III.2 Tuning parameters of the utilized MPPT methods

P&O	PSO	CS
$D_0 = 0.85$	$w_{min} = 0.4$	$Beta = 1.5$
$\Delta D = 0.005$	$w_{max} = 1$	$k_{Lévy} = 0.6$
	$c_1 = 1.4$	$\sigma_v = 1$
	$c_2 = 1.6$	$P_a = 0.25$

The DC-DC converter used is a Boost converter. It is designed for continuous conduction current mode with the specifications that detailed in Table.III.3.

Table.III.3 Boost converter specifications

Parameter	Value
Frequency f_s	50kHz
Inductor (L, r)	$500\mu H$, 0.23Ω
Capacitor C_1	$100\mu F$
Capacitor C_2	$100\mu F$
Load R_L	$200 \ \Omega$

III.3.1. Characteristics of PV Array configured in Series-Parallel (3S2P)

In this part, PV array of six PV modules has been used and configured in Series-Parallel (3S2P), as shown in Fig.III.2, two chains connected in parallel, where each chain consists of three photovoltaic modules connected in series. In this chapter, all simulation tests are performed by using the PV module Shell SM55W, which construct the adopted configuration 3S2P of PV array. The data specifications of the PV module Shell SM55W used for simulation are given in Fig.III.1, for standard test conditions (STC). In these conditions all PV modules of PV array (3S2P), receiving similar irradiance G =1000W/m^2, and the PV system operate in the fixed temperature T = 25°C in this case the PV system will continue operating at optimal efficiency.

Module data		
Module:	Shell SM 55W	
Maximum Power (W) 54.945	Cells per module (Ncell) 36	
Open circuit voltage Voc (V) 20.5	Short-circuit current Isc (A) 3.382	
Voltage at maximum power point Vmp (V) 16.5	Current at maximum power point Imp (A) 3.33	
Temperature coefficient of Voc (%/deg.C) -0.35602	Temperature coefficient of Isc (%/deg.C) 0.07	
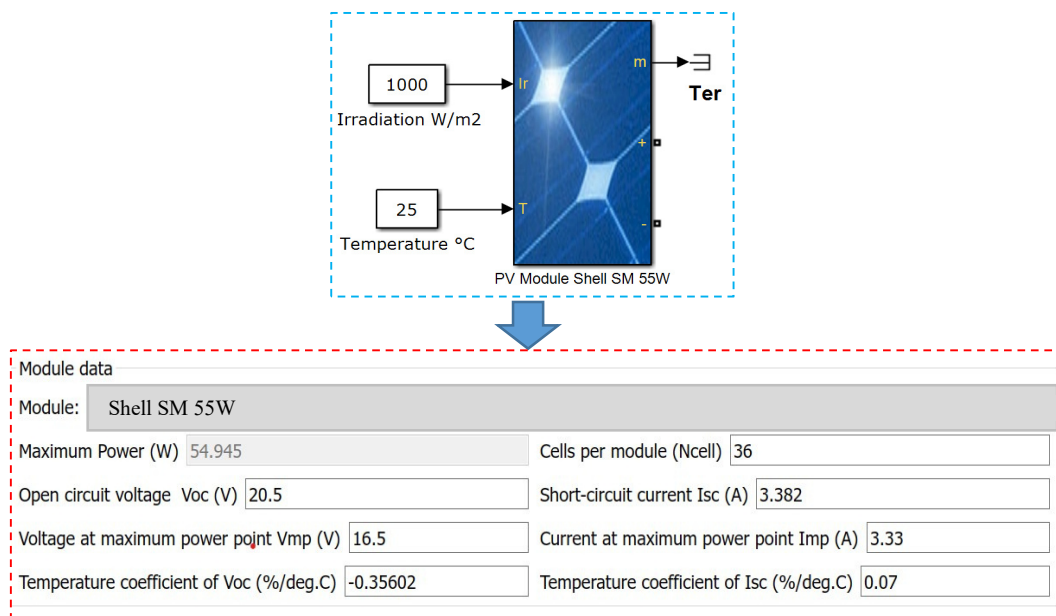
Fig. III.1. Electrical specifications data of the used PV module Shell SM 55W for STC conditions

We simulated the PV array 3S2P in Matlab/Simulink at standard test conditions (STC) as shown in Fig.III.2, the STC conditions are:

- Irradiance 1000 W/m^2 spectrum AM 1.5 G
- PV module temperature 25°C

Fig.III.3. display the electrical characteristics Power-Voltage (P-V) and Current-Voltage (I-V) curves of the tested PV array 3S2P under STC conditions (1000W/m^2 and 25°C). The tested PV array 3S2P produces only one global peak in the characteristics curve power- voltage (P-V) this global peak represent the global maximum power point GMPP at P_{gmpp} = 325,5W in the maximum voltage V_{gmpp} = 49.55V, and maximum current I_{gmpp} = 6.56A, as illustrated in the characteristics curve current-voltage (I-V) in Fig. III.3.b.
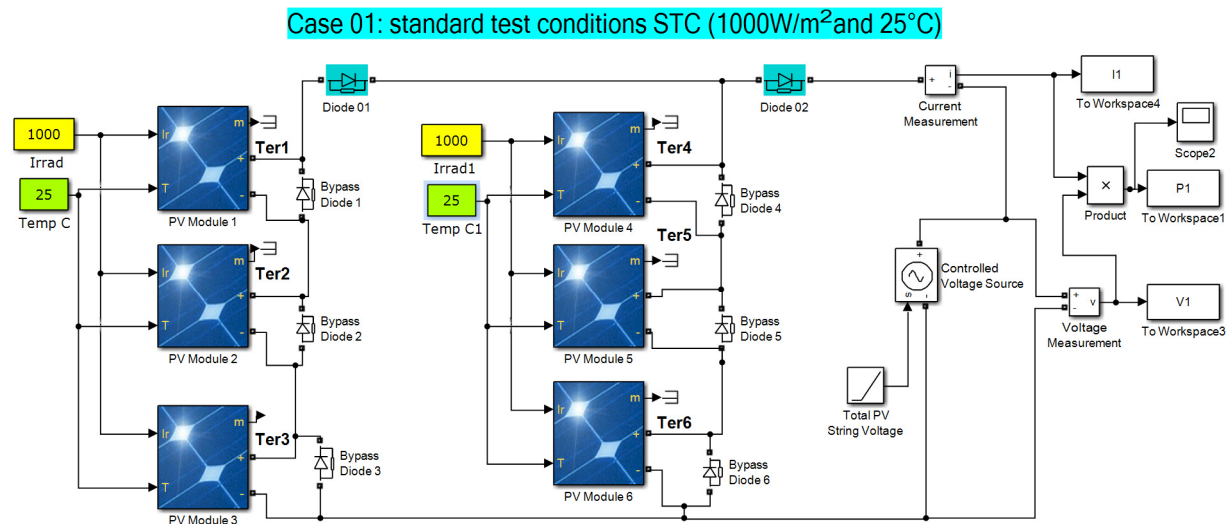
Fig.III.2. Simulink model of the tested PV array configuration (3S2P) for case 01 (STC)
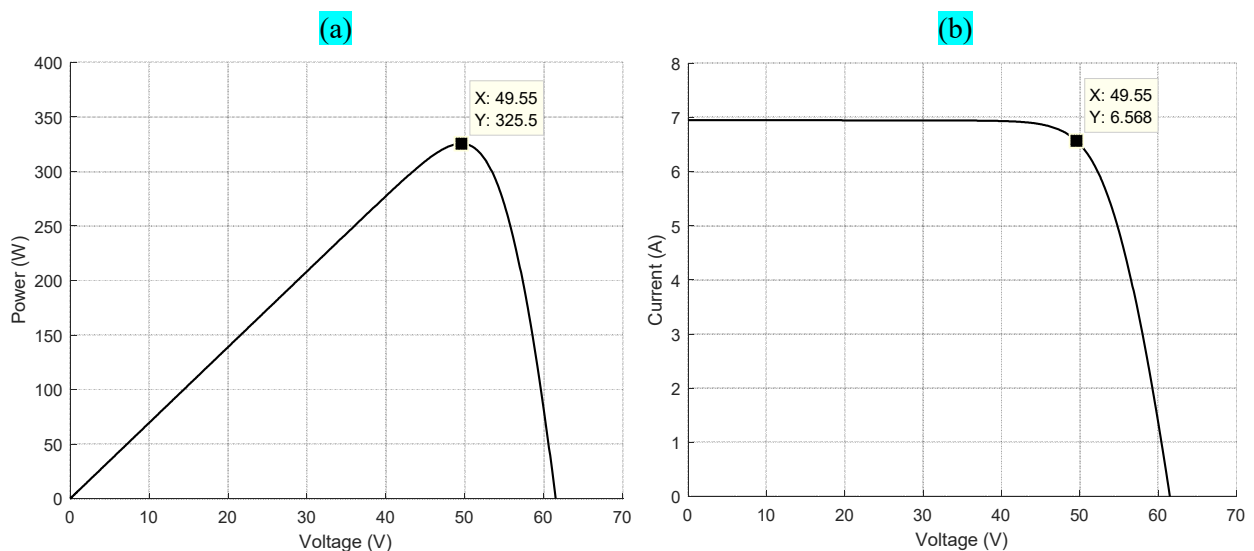
Fig.III.3. Characteristics curves of PV array 3S2P under standard test conditions STC
(a) P-V curve, (b) I-V curve

When the environmental condition changes, both solar irradiation insolation as well as ambient temperature do change now, the temperature is maintained constant at 25°C and the radiation level is varied uniformly for all the PV modules in the 3S2P configuration, the used insolation levels are 1000W/m², 800W/m², 600W/m², 400W/m² and 200W/m². The P-V and I-V curves shown in Fig.III.4. (a). (b) As shown in this figure, each curve from the P-V characteristic has a unique peak for certain radiation and temperature, clearly this figure show that, PV output power reduces significantly when there is a decline in the insolation level.

III.3.1.2. Effect of temperature on PV array 3S2P

The characteristics curves P-V and I-V of the PV generator varies when there is a change in temperature and solar irradiation. To demonstrate this, 3S2P configuration that shown in
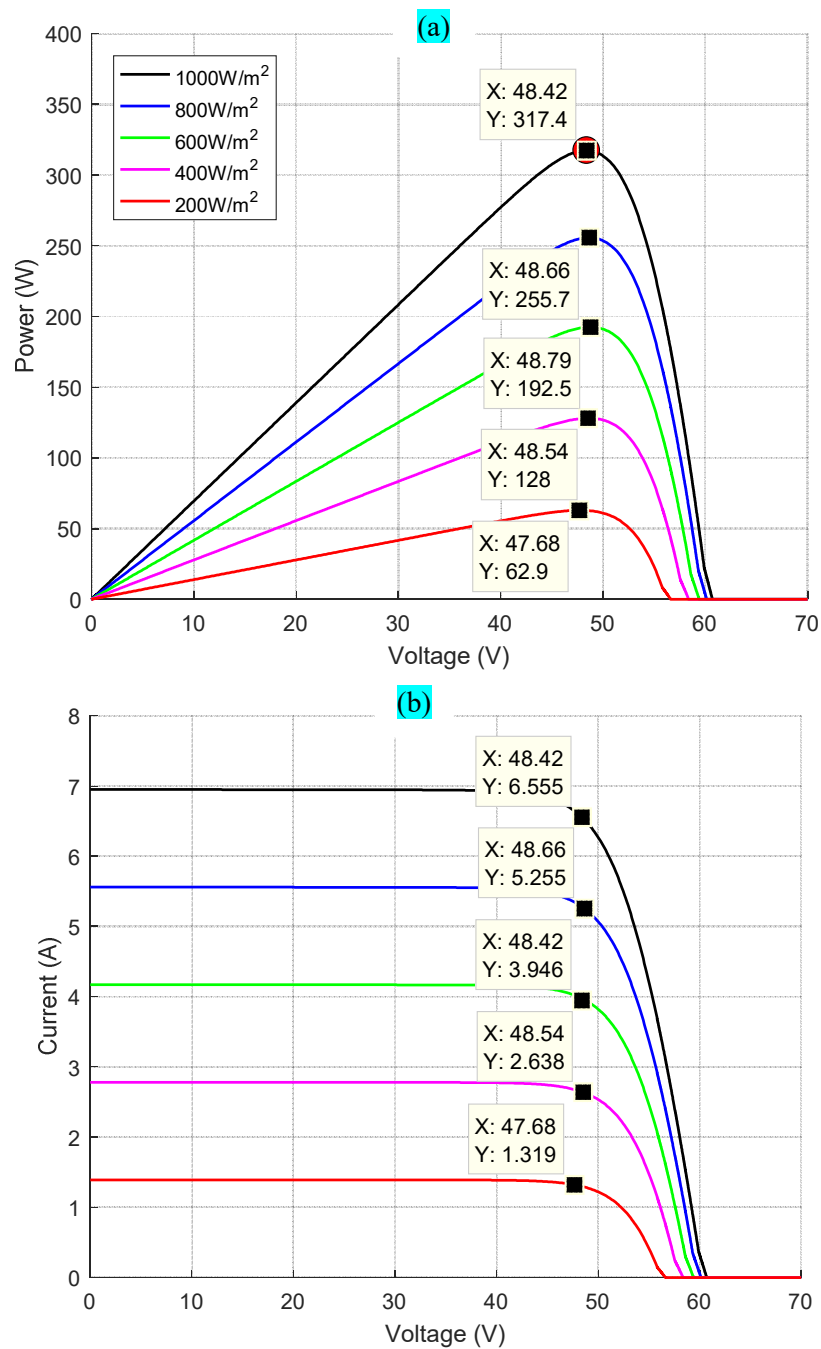
Fig.III.4. Characteristics curves of PV array 3S2P under different irradiation levels and constant temperature 25°C, (a) P-V curve, (b) I-V curve

Fig.III.2 with temperature changes from 25°C, 35°C, 45°C, 55°C and 60°C. for an uniform standard insolation 1000W/m^2 and these changing temperature, the characteristics P-V and I-V curves of PV array configuration 3S2P are displayed in Fig.III.5.(a).(b). It can be seen from this figure that as the temperature increases the peak power of PV system decreases, thereby reducing the efficiency. The peak power of PV system decreases by 0.5% for an increase of 1°C of temperature [7]. The PV output power thus depends on the operating temperature of the PV module. The dependency of PV output power on temperature is because of the dependency of and on the temperature V_{oc}, V_{sc}.
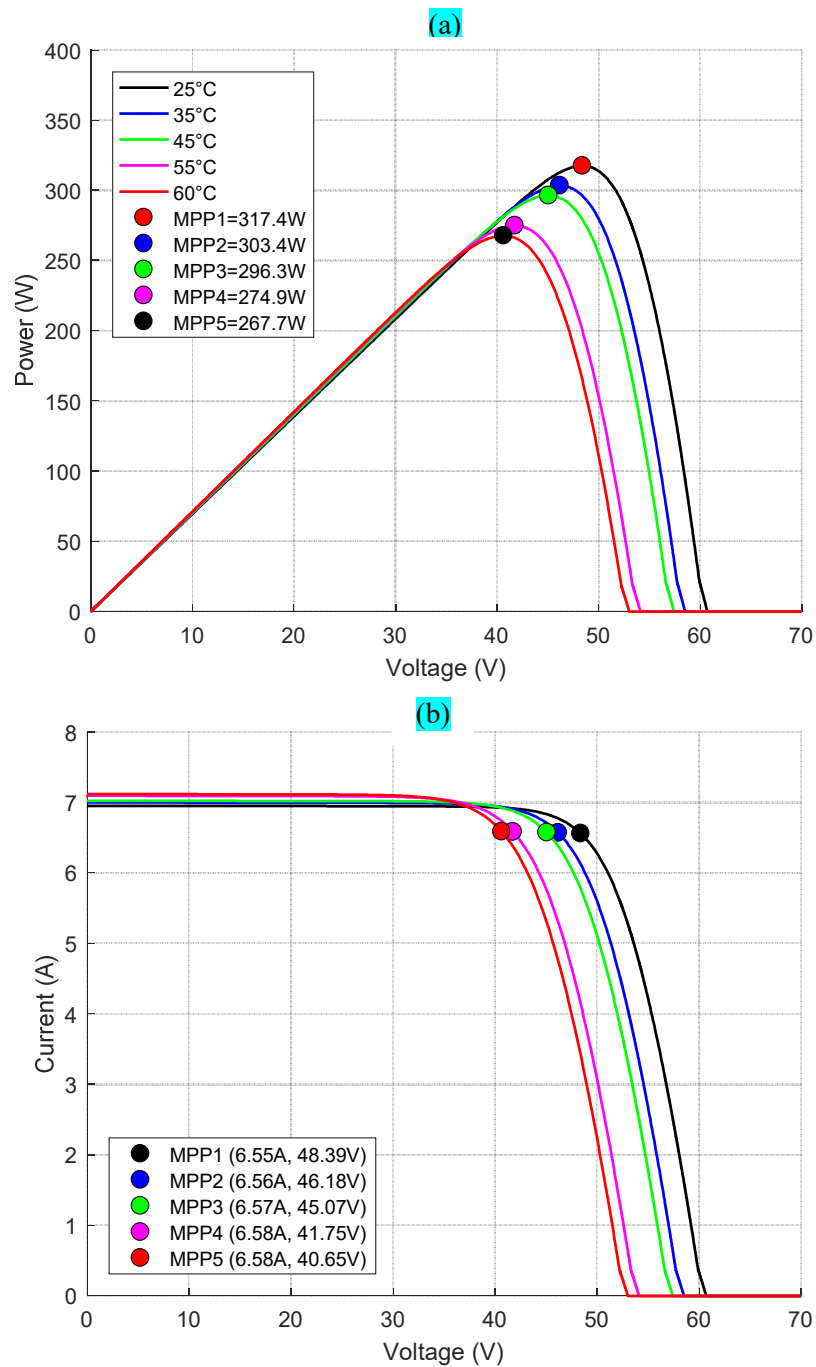
Fig.III.5. Curves of PV characteristics of PV array 3S2P under constant irradiation 1000W/m² and variable temperature (a) P-V curve, (b) I-V curve

III.3.2.Performance of simulated MPPT Methods

To verify the effectiveness of the proposed MPPT methods, a photovoltaic system is simulated on Matlab/Simulink. The different blocks constituting the model are shown in Fig.III.6. The photovoltaic array used consists of six shell SM55 photovoltaic modules connected in series-parallel (3S2P). In this part we studies the performance of the proposed MPPT methods Perturb and Observation (P&O), Particle Swarm Optimization (PSO) and Cuckoo Search algorithm (CS) under four different atmospheric cases presented in Table.III.1.

III.3.2.1. Case 01: Standard test conditions (STC)

Initially, we verify the functionality and performance of simulated MPPT methods using PV Array configured in 3S2P and a boost converter operate in frequency f =50Khz, and resistive load R 200Ω. Fig.III.6. showed the used PV system using P&O-MPPT controller under STC.
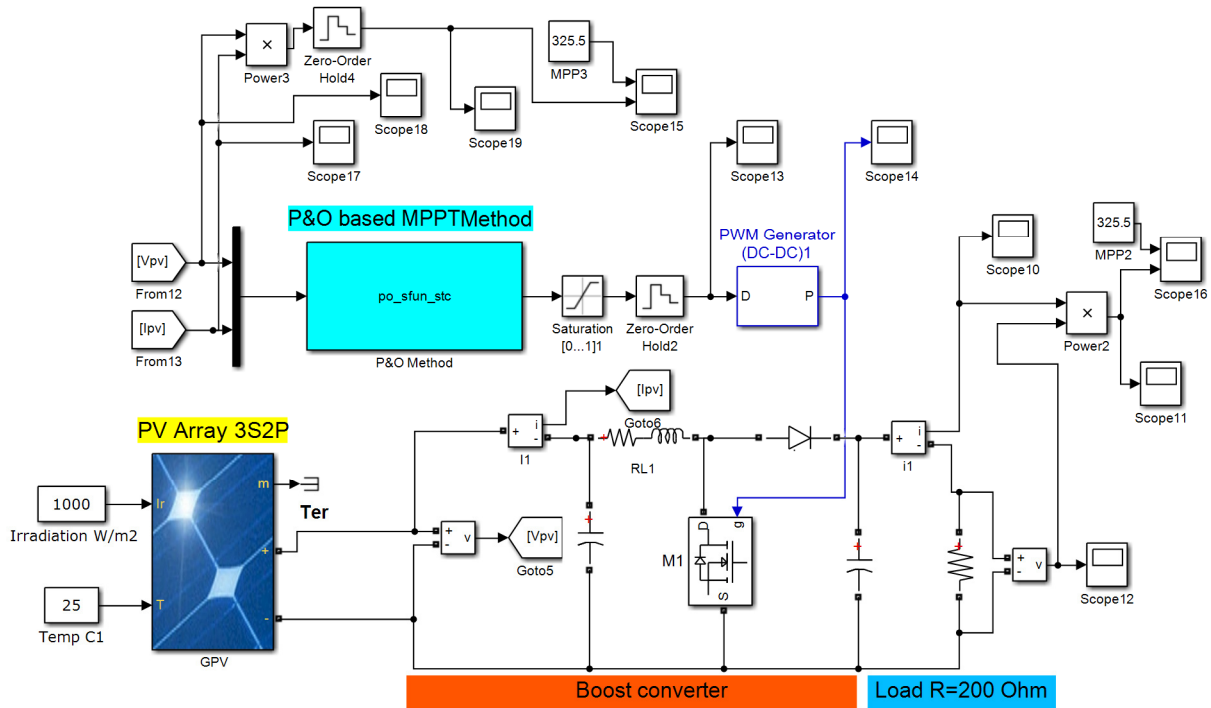
Fig.III.6. Simulink model of standalone PV system with P&O Based MPPT controller under STC

Table.III.4, summarize the quantitative data of obtained results for three proposed MPPT methods CS, PSO and P&O under the standard test conditions (STC) of the second case.

Table.III.4 Summarize of obtained results of CS, PSO and P&O methods for case 01 STC

Tested case	Method	Optimal Power of P-V curve (W)	Extracted PV power (W)	Efficiency (%)	Convergence time (Sec)	Optimal Duty Cycle
Case (1) STC	CS		325.5	100	0.523	0.804
	PSO	325.5	325.5	100	0.602	0.804
	P&O		324	99.53	0. 375	0.810

III.3.2.1.1. Analysis and discussion of case 01 (STC) results

In order to evaluate the tracking performances of two metaheuristics MPPT methods CS and PSO based MPPT and compare them with the conventional one, P&O technique, MATLAB simulation tests under four different cases have been performed. Shell SM 55W PV module is employed in the simulation model. The tested PV system illustrated by Fig. III. 6, consists of six PV modules configured in 3S2P with DC/DC boost converter and resistive load 200 Ω.
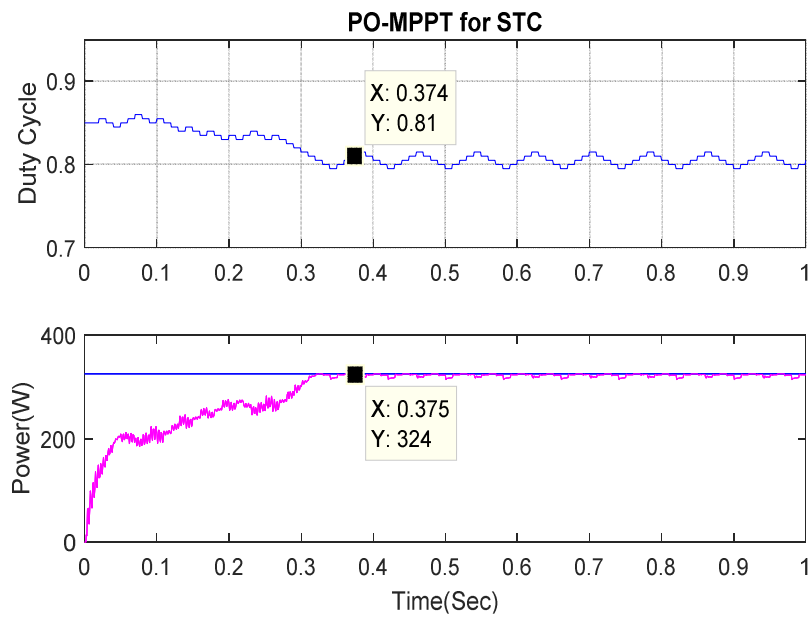
Fig.III.7. Duty cycle and PV power responses using P&O based MPPT technique for STC case
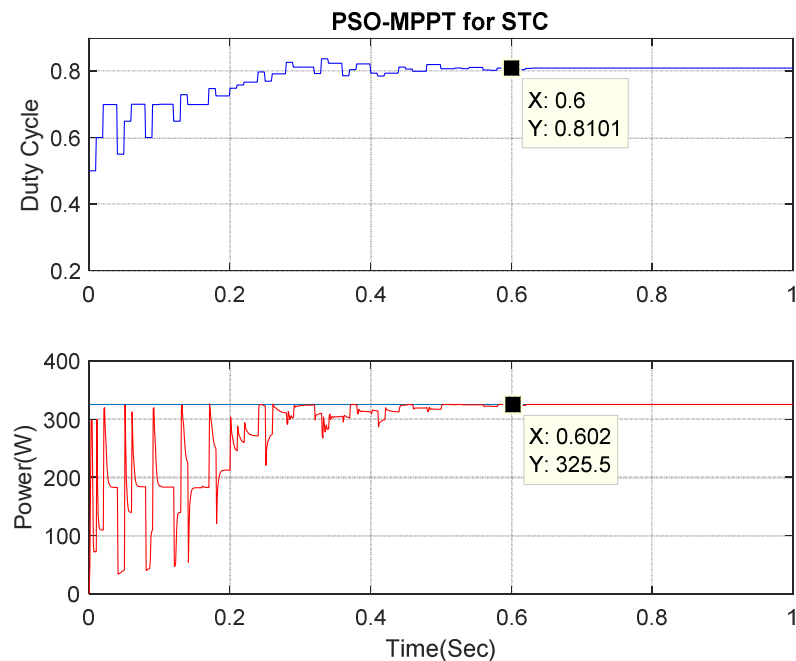
Fig.III.8. Duty cycle and PV power responses using PSO based MPPT technique for STC case

In order to evaluate the three proposed MPPT techniques P&O, PSO and CS, the PV system of Fig.III.6, is tested under standard test condition STC (G = 1000 W/m², T = 25 °C). The duty cycle and output PV power graphs produced by using P&O, PSO and CS based MPPT for PV system under uniform irradiance are illustrated in Figs.III.7, 8 and 9 respectively. . From these figures, it can be seen that, all adopted MPPT techniques reached the GMPP with a small difference in the final values of GMPP and the required convergence time, where Fig.III.7, showed that P&O technique reached the maximum power point of 324W after the convergence time 0.375s. While both metaheuristic methods PSO and CS attained the same optimal value at

GMPP = 325.5W, after convergence time 0.6s for PSO and 0.52s for CS, as shown in Figs.III.8 and 9. This means that using CS based tracker decreases the tracking time by 13.33% compared with PSO for uniform irradiance.
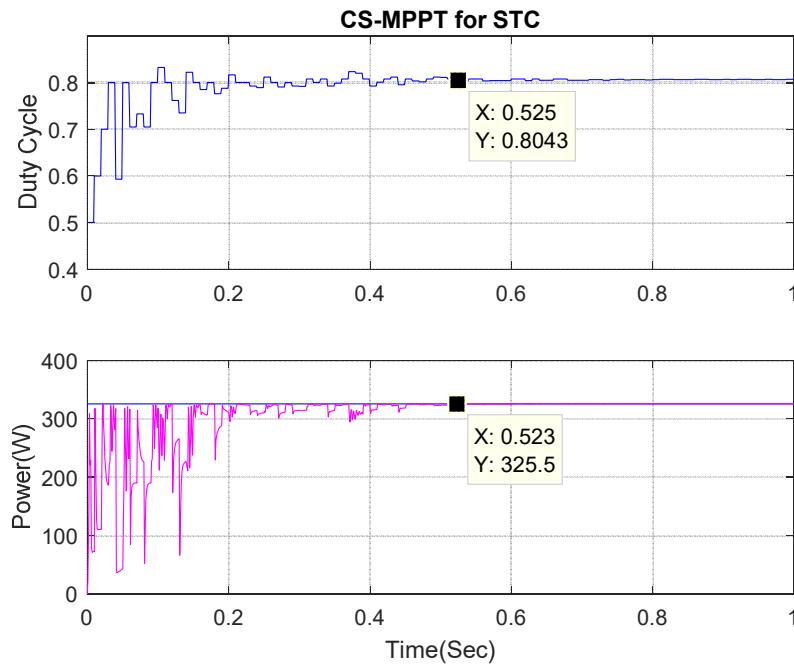
Fig.III.9. Duty cycle and PV power responses using CS based MPPT technique for STC case

III.3.2.2. Case 02: Partial shading case (PSC) with constant temperature

Partial shading condition (PSC) has a bad effect not only on the shaded PV modules/arrays itself but also on the output power generated from the partially shaded photovoltaic generator. As it presented in chapter II, PSC reduces the output power generated from the PV generator and contributes in hot spot problem that may lead to thermal breakdown of shaded PV modules. Under PSC, multiple peaks, one global peak (GP) and many other local peaks (LPs) are generated in the P–V curve [65]. For PSC case the PV modules of PV array 3S2P receives a non-uniform irradiation levels with a constant temperature at 25°C. The used irradiation levels for each PV module are detailed in Table.III.5.

Table.III.5 Operating conditions of case 03 partial shading case (PSC)

PV Modules	Temperature (°C)	Irradiation (W/m^2)
PV Module 1	25	1000
PV Module 2	25	1000
PV Module 3	25	800
PV Module 4	25	1000
PV Module 5	25	600
PV Module 6	25	400

III.3.2.2.1. Characteristics of PV array 3S2P for case 02:

In order to clarify the characteristics of PV array configuration 3S2P under case 02 (PSC) that represent the critical weather conditions, we tested the Simulink model of 3S2P configuration under PSC as shown in Fig. III.10.
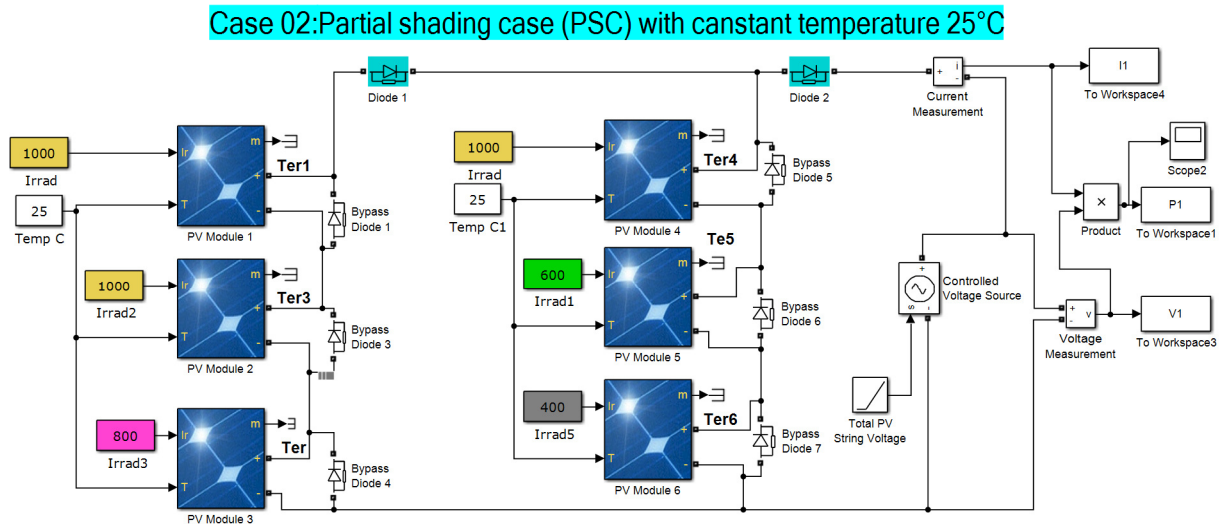
Fig. III.10. Simulink model of the tested PV array 3S2P under case 02 partial shading case (PSC)

The Fig.III.11. (a). shows the produced local and global MPP of PV Array 3S2P for critical PSC case where, the number of peaks equals the number of parts (modules) in series having different irradiances. There are four peaks includes one global peak that represent the global maximum power point GMPP = 212.5W three local maximum power points LMPPs. As showed in Fig.III.11. (b) this GMPP corresponding to the point V_{mpp} = 52.14W, I_{mpp} = 4.075A.

III.3.2.2.2. Performance of MPPTs Methods for case 02 (PSC):

Partial shading case (PSC) is considered a condition when a part or the whole solar panel exposed a non-uniform irradiance, due to the series configuration of solar cell in the panel, cells subject to shadow; have to operate in the reverse bias voltage region for providing the current equal to that flowing in the unshaded cells. Operating in such conditions has an inverse impact on the efficiency of entire PV panel and may cause hotspots in solar cells. In order to overcome that problem, bypass diodes have been interconnected in parallel with each panel as presented in Fig. III.10 [97].

We summarize in Table.III.6, the obtained results of three proposed MPPT methods CS, PSO and P&O under the second case, which represented the partial shading case (PSC).
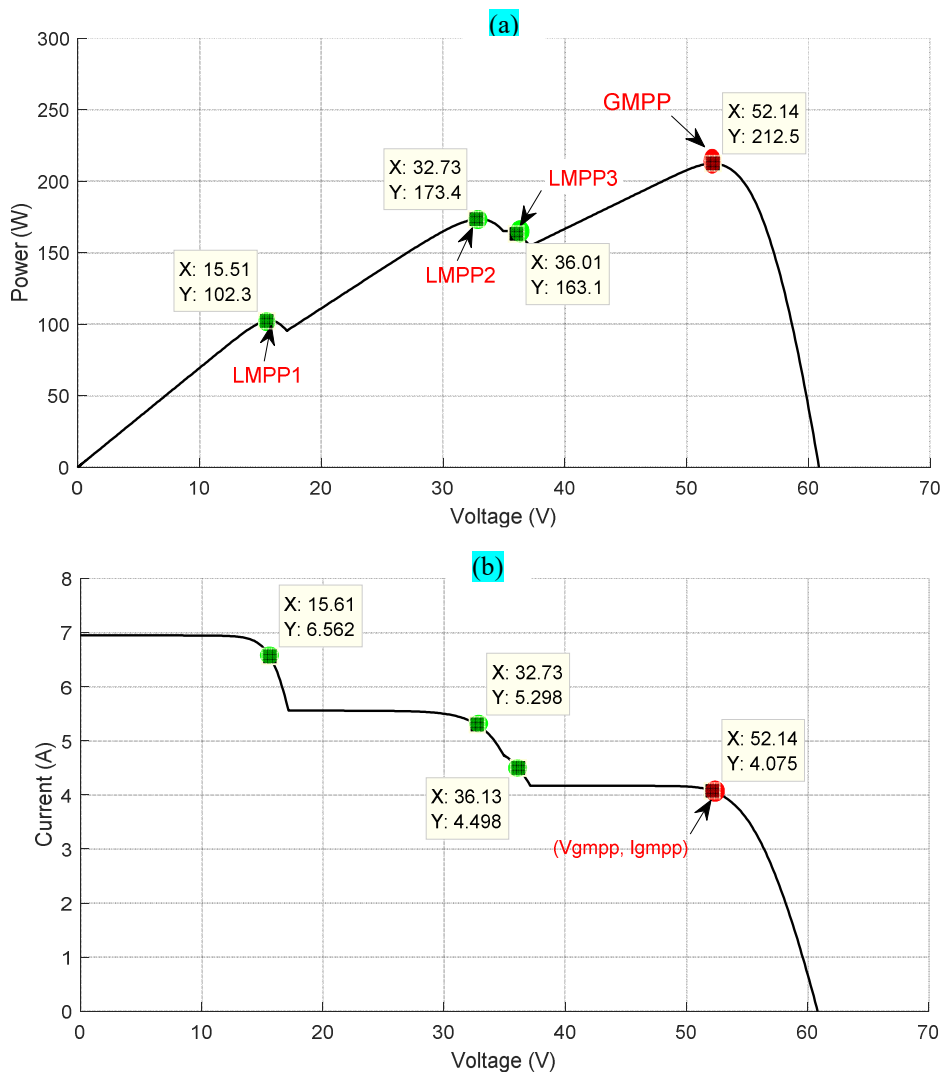
Fig.III.11. Characteristics curves of PV array 3S2P under PSC (a) P-V curve (b) I-V curve

**Table.III.6** Summarize of obtained results of CS, PSO and P&O methods for case 02 PSC

Tested case	Method	Optimal GMPP of P-V curve (W)	Extracted PV power (W)	Efficiency (%)	Convergence time (Sec)	Optimal Duty Cycle
Case (2) PSC with 25°C	CS	212.5	212.5	100	0.542	0.742
	PSO		212.1	99.81	0.673	0.747
	P&O		150.7	70.91	0. 40	0.815

III.3.2.2.1 Analysis and discussion of case 02 (PSC) results

For the second case which represent the partial shading case (PSC) the used solar irradiances levels are $1.0\,\text{kW/m}^2$, $1.0\,\text{kW/m}^2$, $0.8\,\text{kW/m}^2$, $1.0\,\text{kW/m}^2$, $0.6\,\text{kW/m}^2$, and $0.4\,\text{kW/m}^2$. As shown in Table.III.5, from this case, it is clear that there exist four different irradiations changes, hence four peaks occur in the power-voltage P-V characteristics of PV array 3S2P as shown in Fig.III.11.(a). The global peak value in this case is GMPP = 225.5W and the remaining three local peaks are located at LMPP1 = 102.3W, LMPP2 = 173.4.W and LMPP3 = 163.1W.

Figs.III.10, 11 and 12, illustrated the obtained duty cycle and PV power graphs of the tested PV system with 3S2P configuration for PSC case.

The analysis of the simulation results for each proposed MPPT techniques depends on the final obtained PV power and also on the convergence time to catch the final GMPP. As shown in Figs.III.10, 11 and 12, for PSC case the final GMPP obtained by CS method is 212.5W after convergence time 0.54s, while PSO method given the final value GMPP = 212.1W, after a convergence time 0.67s. However the conventional P&O method cannot reach the GMPP.

Fig.III.10. Duty cycle and PV power responses using P&O based MPPT technique for case 02 (PSC)
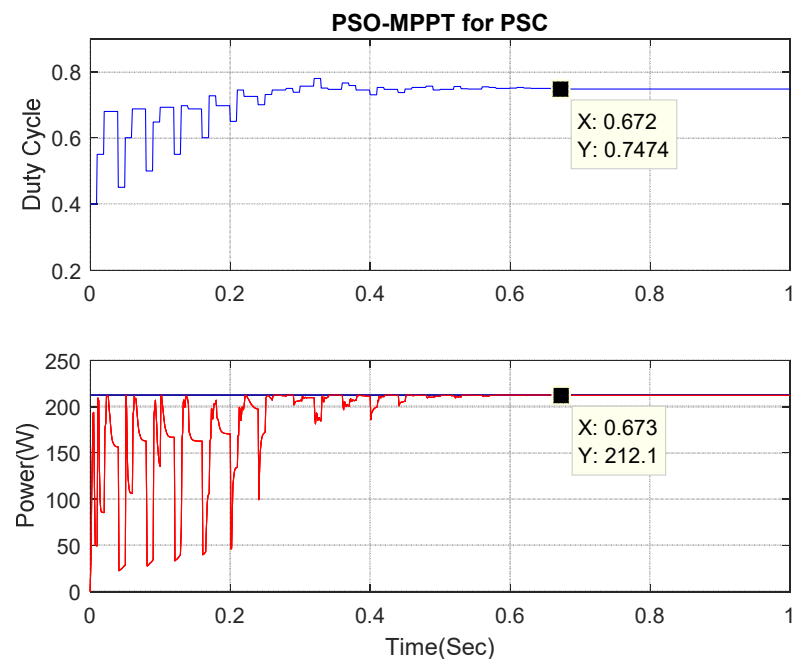
Fig.III.11. Duty cycle and PV power responses using PSO based MPPT technique for case 02 (PSC)
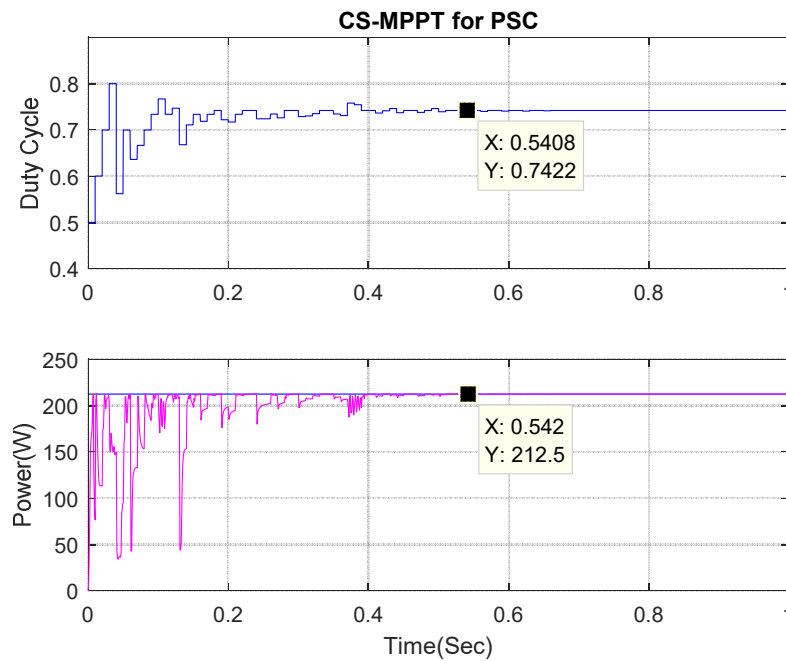
Fig.III.12. Duty cycle and PV power responses using CS based MPPT technique for case 02 (PSC)

However, it is content with getting to the weakest maximum power point MPP = 150.7W compared to CS and PSO, with convergence time 0.4s as presented in Fig.III.10. P&O converges to final MPP but does not settle at GMPP due to oscillations produced by continuous perturbation and observation. We can therefore say that the P&O method is incompetent to converge to GMPP. It is easy to check the matching between GMPP corresponding to the irradiance level, those results are obtained by using PSO and CS based MPPT methods. The obtained PV power by PSO and CS is almost very close to the global maximum power produced by the PV array.

According to previous results, we can conclude that the two metaheuristic methods PSO and CS succeed in rapidly tracking the optimal power point GMPP with a very high efficiency and zero oscillation around GMPP in steady state. However, the CS based tracker has the priority of the speed to reach the GMPP than the PSO and P&O based trackers. Therefore, the better performance of the CS-based MPPT technique can reduce the power loss and save the implementation cost and the processing time.

III.3.2.3. Case 03: Constant irradiation with high temperature 55°C

We use in this case, a constant uniform irradiation 1000W/m² for all PV modules of PV array 3S2P with a high temperature 55°C as shown Table.III.7. In order to present, the influence of high temperature on performance of the three used MPPT controllers P&O, PSO and CS.

Table.III.7 Operating sonditions of case 03

PV Modules	Temperature (°C)	Irradiation (W/m²)
All PV Modules PV1 to PV6	55	1000

III.3.2.3.1. Characteristics of PV array 3S2P for case 03

The Simulink model of PV array configured in 3S2P under case 03 (1000W/m^2 and 55°C) is illustrated in Fig. III.13.
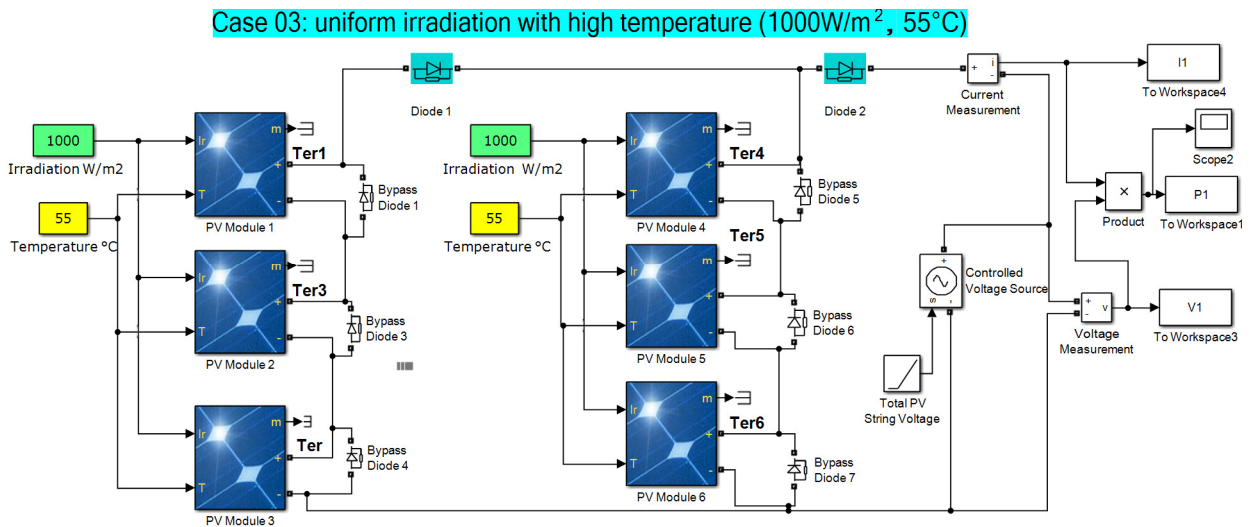
Fig.III.13. Simulink model of the tested PV array 3S2P under case 03 (1000W/m^2 and 55°C)

Fig.III.14, display the optimal point GMPP that corresponding to P_{gmpp}, I_{gmpp} and V_{gmpp} of the configuration 3S2P in the characteristics curves of P-V and I-V under case 03 (1000W/m^2 and 55°C). From the graphs data we extract the optimal values of power, current and voltage of optimal point GMPP as follow: $P_{gmpp} = 283$W, $I_{gmpp} = 6.608$A, and $V_{gmpp} = 42.82$V.
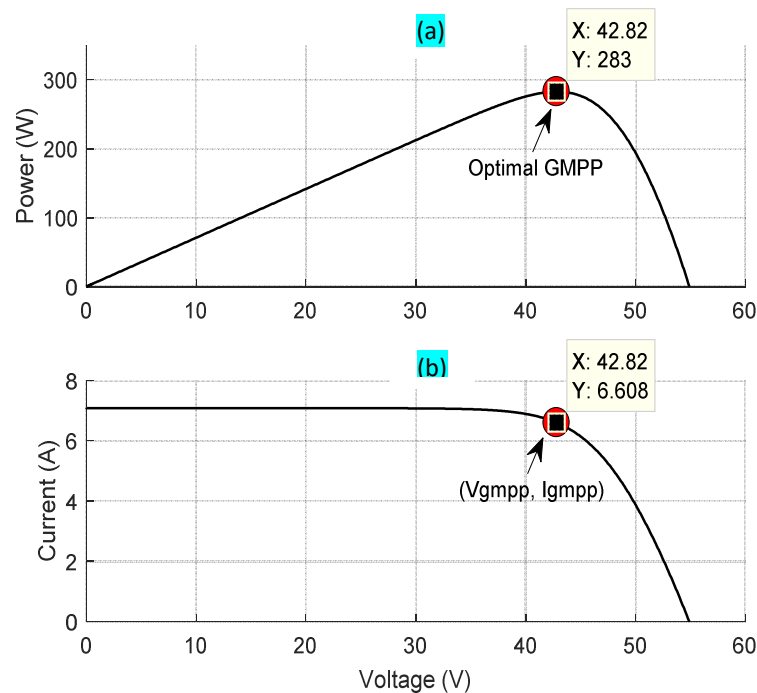
Fig.III.14. Characteristics curves of PV array 3S2P under case 03 (1000W/m^2 and 55°C)
(a) P-V curve, (b) I-V curve

III.3.2.3.2. Performance of MPPTs methods for case 03:

In this subsection we verifies the performances of MPPT controllers P&O, PSO and CS using the Simulink model of standalone PV system similar to the previous model of Fig.III.6, but in this case the simulated PV system subject to operating conditions of third case, that are uniform irradiation 1000W/m^2 and high temperature 55°C. For this case, the simulation results are illustrated in Figs.III.15, 16 and 17.
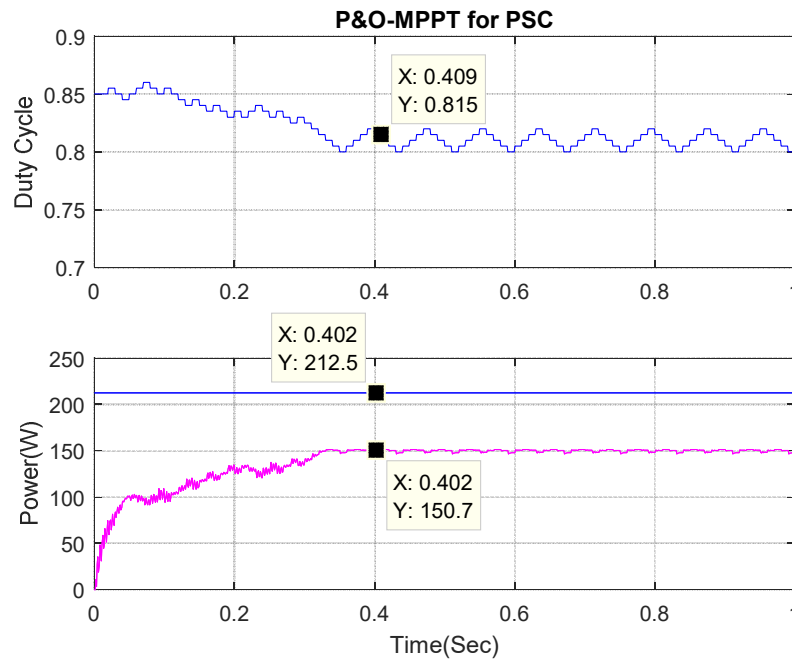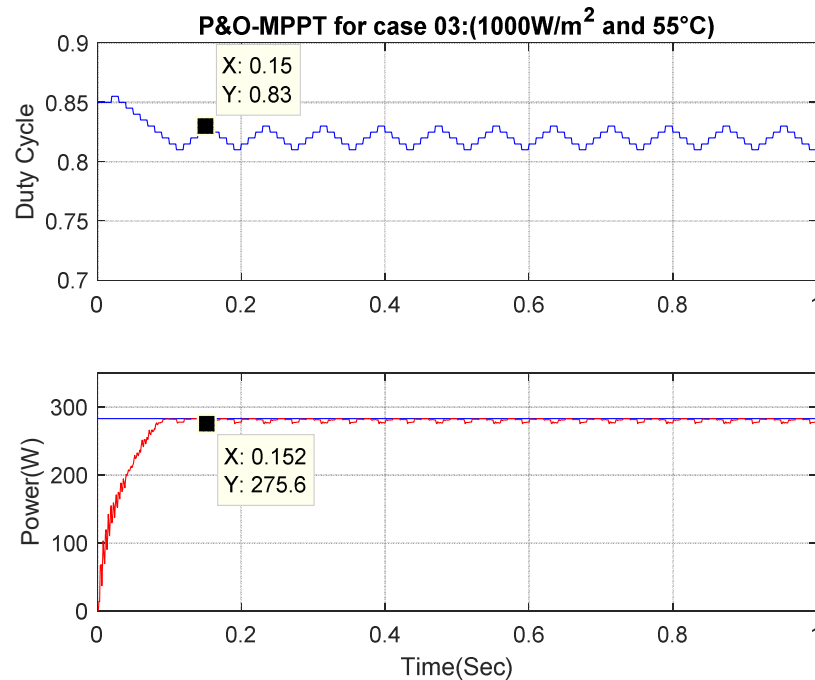

Fig.III.15. Duty cycle and PV power responses using P&O based MPPT technique for case 03 (1000W/m^2, 55°C)
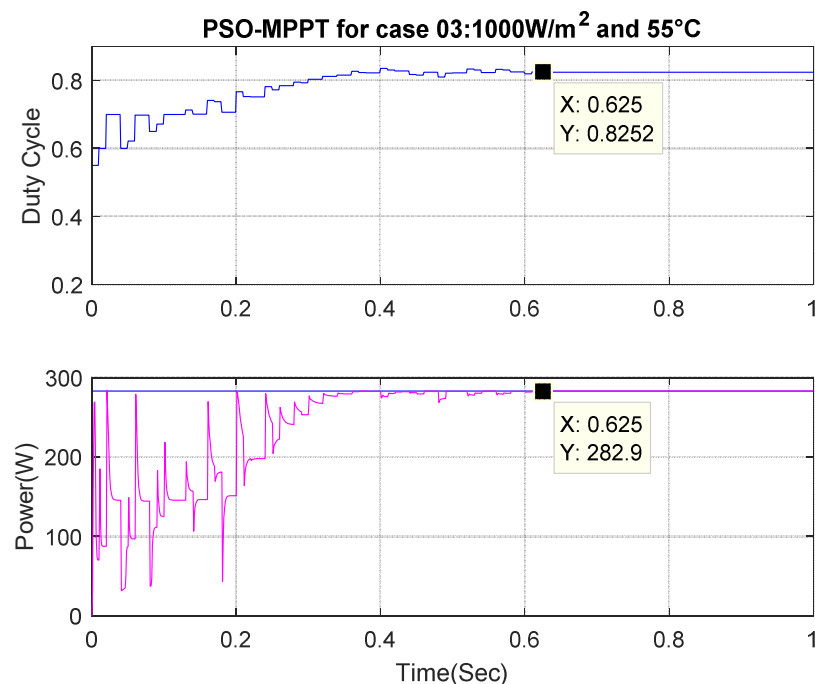
Fig.III.16. Duty cycle and PV power responses using PSO based MPPT technique for case 03 (1000W/m^2, 55°C)
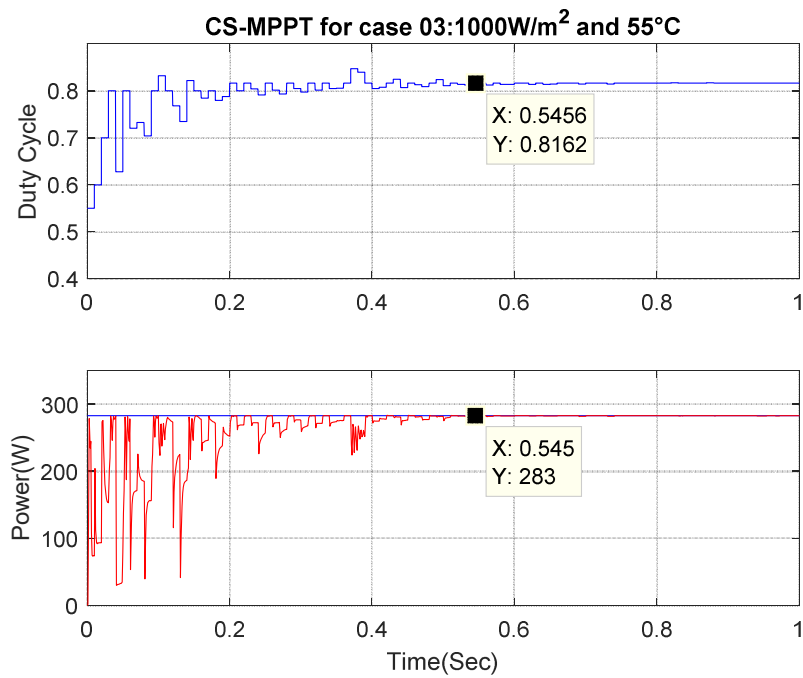
Fig.III.17. Duty cycle and PV power responses using CS based MPPT technique for case 03
(1000W/m² and 55°C)

We summarize in Table III.8, the obtained simulation results of case 03 which are shown in Figs.III.15, 16 and 17, in addition we performs an accurate quantitative comparison between CS, PSO and P&O methods based on the following performance criteria: extracted PV power efficiency and convergence time.

Table.III.8 Summarize of obtained results for case 03 using CS, PSO and P&O methods

Tested case	MPPT Method	GMPP of P-V curve (W)	Extracted PV power (W)	Efficiency (%)	Convergence time (Sec)	Optimal Duty cycle
Case (3) 1000W/m² and 55°C	CS		283.0	100	0.31	0.816
	PSO	283	282.9	99.96	0.68	0.825
	P&O		275.6	97.38	0.15	0.830

III.3.2.4. Case 04: constant irradiation 1000W/m² with variable temperature

The operating conditions of the fourth case are presented in Table III.9, which use variable temperature and constant standard irradiation 1000W/m².

Table.III.9 Operating conditions of case 04

PV Modules	Temperature (°C)	Irradiation (W/m²)
PV Module 1	25	1000
PV Module 2	45	1000
PV Module 3	55	1000
PV Module 4	50	1000
PV Module 5	60	1000
PV Module 6	55	1000

III.3.2.4.1. Characteristics of PV array 3S2P for case 04

The Simulink model illustrated in Fig. III.18, describe the tested PV array configured 3S2P under the operating conditions of fourth case, which presented in Table III.9.
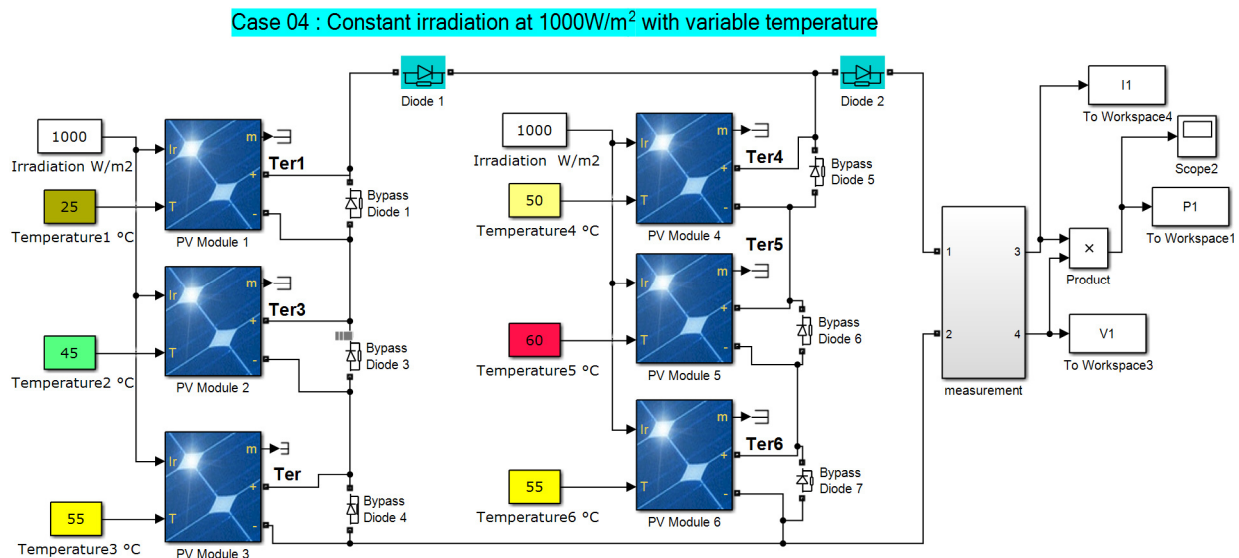
Fig.III.18. Simulink model of PV array configuration 3S2P for case 04
(1000W/m² with variable temperature)
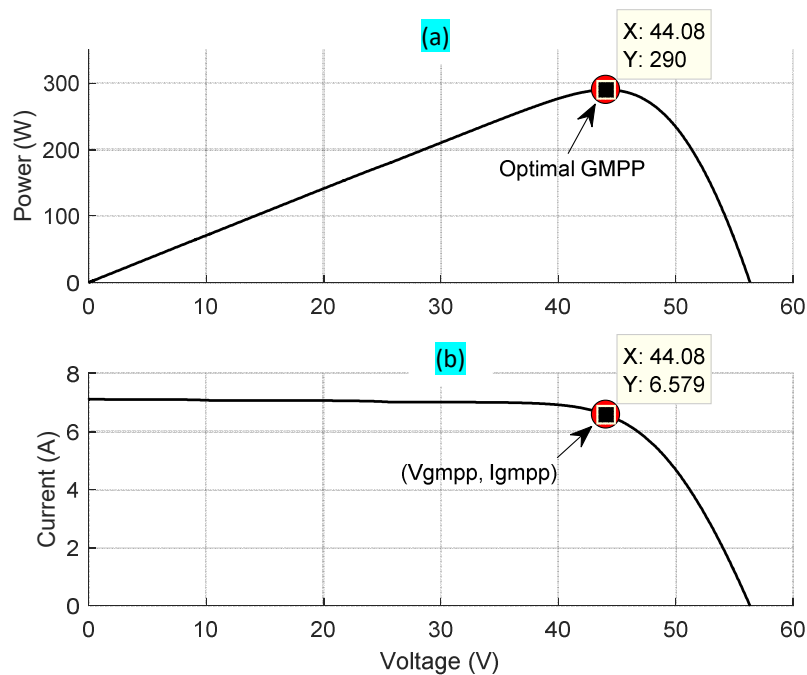
Fig.III.19. Characteristics curves of PV array 3S2P for case 04 (1000W/m² and variable temperature)
(a) P-V curve, (b) I-V curve

III.3.4.2. Performance of MPPTs methods for case 04

For the purpose of evaluate the performance of P&O, PSO and CS techniques, we used the Simulink model of the tested PV system under the conditions of case 04 which are constant irradiation and variable temperature. Fig.III.20, showed the used PV system using MPPT

controller under the conditions of case 04. Table III.10, summarize the obtained data from simulation results of case 04, moreover, this table presents a quantitative comparison between the performances of CS, PSO and P&O methods.
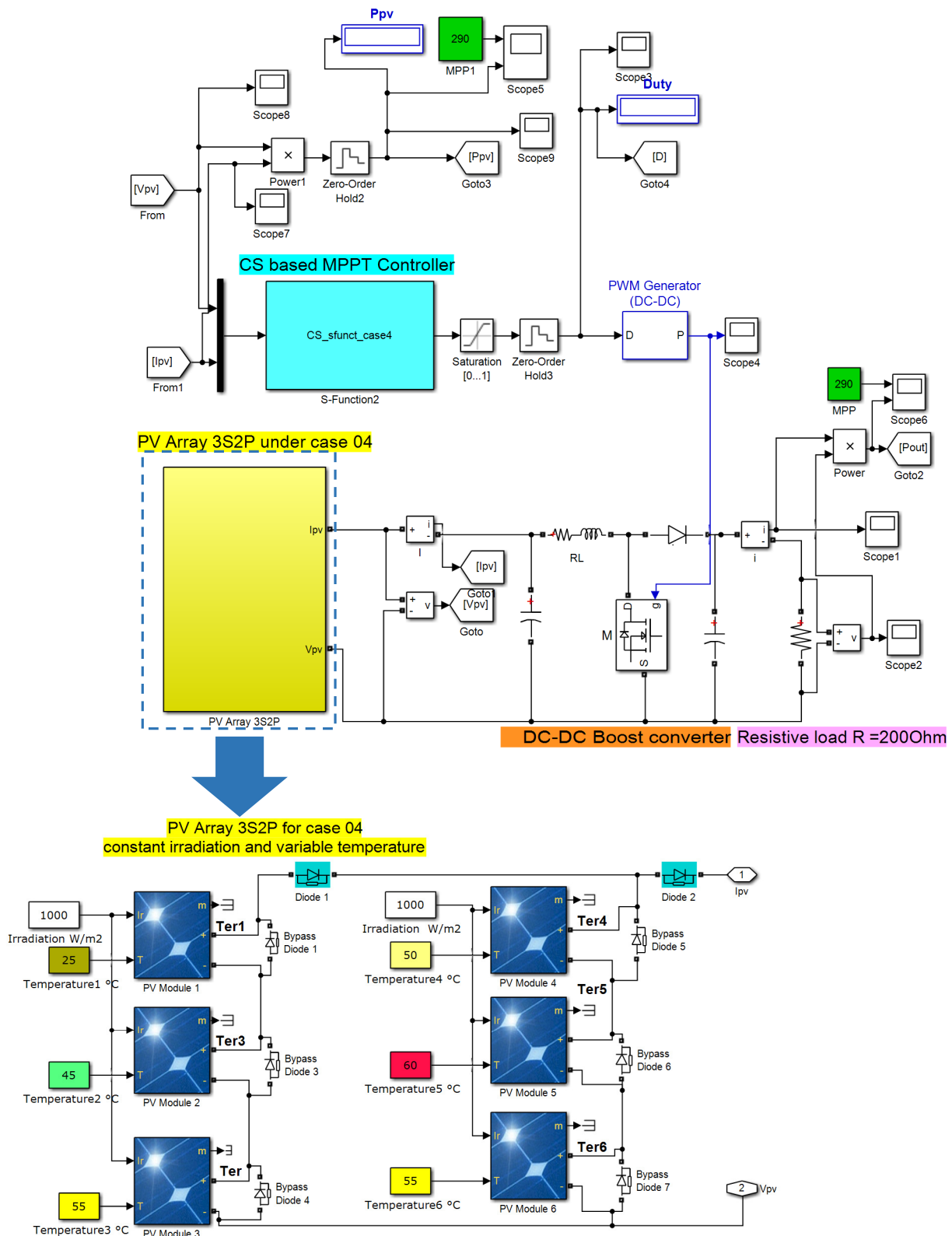
Fig.III.20. Simulink model of PV system with 3S2P configuration and CS-MPPT controller under Conditions of case 04 (Constant irradiation with variable temperature)

P&O-MPPT for case 04

X: 0.15
Y: 0.82

X: 0.15
Y: 285.8
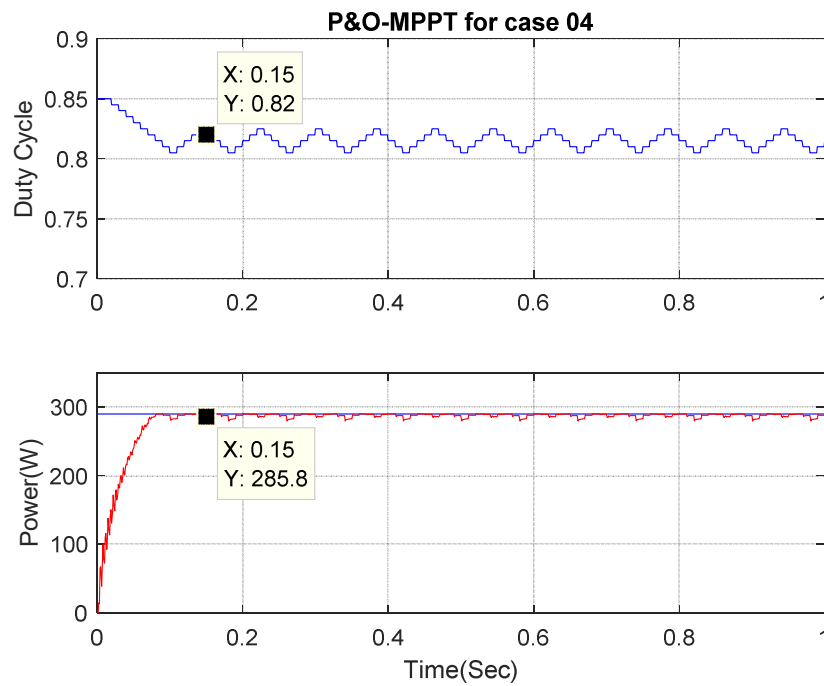
Fig.III.21. Duty cycle and PV power responses using P&O based MPPT technique
Under case 04 (constant irradiation at 1000W/m^2 and variable temperature)

PSO-MPPT for case 04 (1000W/m^2 and Variable Temperature)

X: 0.682
Y: 0.8254

X: 0.682
Y: 288.9
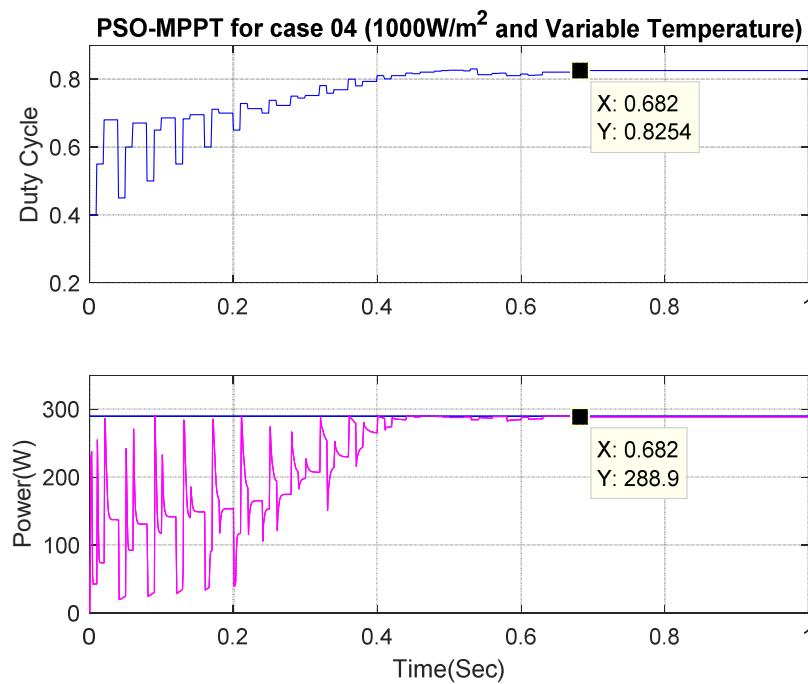
Fig.III.22. Duty cycle and PV power responses using PSO based MPPT technique
Under case 04 (constant irradiation 1000W/m^2 and variable temperature)

Table.III.10 Summary of obtained results for case 04 using CS, PSO and P&O methods

Tested case	MPPT Method	GMPP of P-V curve (W)	Extracted PV power (W)	Efficiency (%)	Convergence time (Sec)	Optimal Duty cycle
Case (4) 1000W/m^2 with Variable temperature	CS		289.8	99.93	0.544	0.816
	PSO	290	288.9	99.62	0.682	0.825
	P&O		285.8	98.55	0.142	0.820
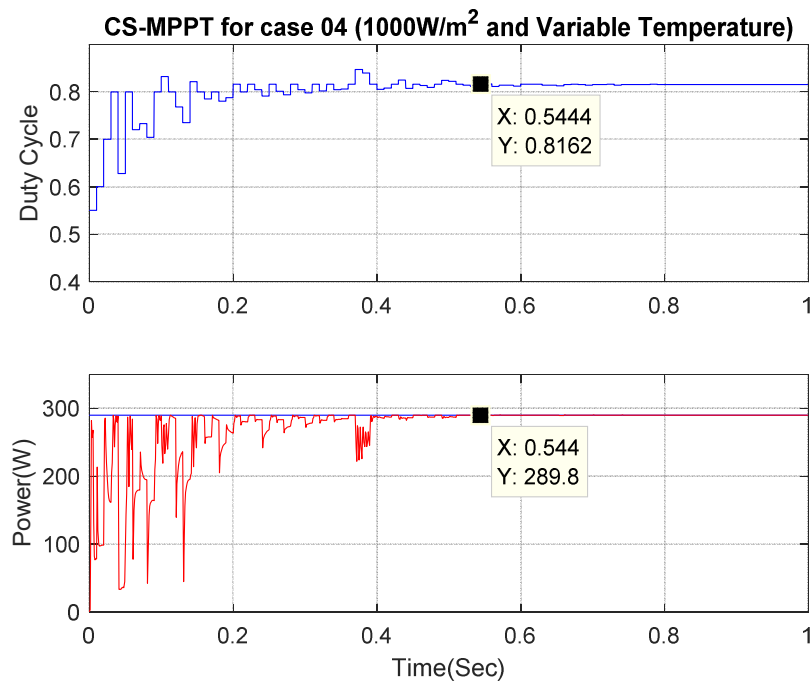
Fig.III.23. Duty cycle and PV power responses using PSO based MPPT technique
Under case 04 (constant irradiation 1000W/m² with variable temperature)

III.3.4.3. Analysis and discussion of case 04 results

The simulation results for duty cycle and extracted PV power using three proposed MPPT method P&O, PSO and CS, are shown in Figs.III.21, 22 and 23, respectively, under the case 4 that use variable temperature and fixed standard irradiation. The simulation results of P&O based MPPT are displayed in Fig.III.21, in this case P&O extract the GMPP = 285.8W for best duty cycle D_{best} = 0.82, with tracking time 0.14s. The graphs of obtained PV power, shows the high oscillation in steady state around the final value of maximum power. Fig.III.22. shows the obtained duty cycle and PV power graphs of the PSO based MPPT technique. The results indicate that this method has some defects compared to CS in the slow convergence speed of the particles and significant oscillations during the searching process. After about 0.68s searching, this algorithm found the best duty cycle D_{best} = 0.825, and the best global maximum power GMPP = 288.9W. Fig.III.23 illustrates duty cycle and PV power graphs of CS based MPPT method. It can be seen from these graphs, that CS based MPPT found the best duty cycle D_{best} = 0.816. After about 0.544s searching, and the best power (fitness) GMPP = 289.9W. compared with the optimal power value of PV array 3S2P GMPP = 290W which is illustrated in P-V characteristic curve, as shown Fig.III.19.a, CS method gives a very good GMPP value, which is very close in short time to the optimal value GMPP. Despite the large variation between the temperature tested in case 4, the CS method proved to be effective in rapid tracking of maximum power GMPP, as we have seen the simulation results confirm that CS technique

is superior in the convergence speed and the output stability under all different changing case of the complex environment conditions. This method can locate the precise GMPP, reduce the oscillation, decrease convergence time and increase the output power effectively. Based on previous analyze results, we can confirm that CS technique has the advantage of the fast convergence speed and the reduction of the power oscillations during the searching process which is beneficial to reduce power losses and increase system efficiency.

III.4. Conclusion

This chapter proposed an evaluation of the performances of some most used MPPT methods includes one conventional method is perturb and observe (P&O) and two metaheuristics methods are particle swarm optimization (PSO) and search cuckoo algorithm (CS), for stand-alone photovoltaic system subject to four atmospheric cases that contain changes in irradiation and temperature. By using simulation tests, the feasibility and availability of proposed MPPT techniques have been verified, and its tracking performance has been analyzed and evaluated for different weather conditions. The tested cases in this chapter are denotes as, case 01 is the case of standard tests condition (STC) where the irradiation and temperature are fixed in (1000W/m^2 and 25°C) respectively, case 02 represent the critical partial shading case PSC, we used in this case different irradiation levels and fixed temperature at 25°C. In case 03 we tested the atmospherics, conditions of fixed uniform irradiation at 1000W/m^2 and high temperature 55°C. Finally in case 04, we used of fixed standard irradiation and pattern of variable temperature (25, 45, 50, 55 and 60) °C for each PV module. The tested PV system includes PV array configured in 3S2P, boost converter and resistive load. Based on the obtained simulation results in all tested cases, the oscillation in the steady state are reduced significantly by using CS and PSO based MPPT techniques, while P&O performs with high fluctuation in the steady state. On the base of speed of tracking, CS is better than PSO and P&O techniques in all tested cases. The results demonstrate that CS technique outperform the others PSO and P&O, in term of convergence speed, less fluctuation in the steady state, robustness, accuracy, power efficiency and less power loss under all changing weather situations.

Chapter IV

Simple and Efficient metaheuristic technique to control the maximum power of autonomous PV system

| Chapter IV | Simple and Efficient metaheuristic technique to control the maximum power of autonomous PV system |

IV.1. Introduction:

The field of research in maximum power point tracking (MPPT) methods is experiencing great progress with a wide range of techniques being suggested, ranging from simple but ineffective methods to more effective but complex ones. Therefore, it is very important to propose a strategy that is both simple and effective in controlling the global maximum power point (GMPP) for a photovoltaic (PV) system under changing weather conditions, especially in partial shading cases (PSCs). In order to improve the tracking performances of a MPPT controller in an autonomous PV system. We proposes in this chapter a new control design based on metaheuristic optimization technique called Crow Search Algorithm (CSA), which proposed by Houam et al in the paper [94], where we purpose via this modern study to attenuate the undesirable effects of partial shading on the tracking performances of standalone PV system. CSA is a nature-inspired method based on the intelligent skills of the crow in the search process of hidden food places. CSA technique combines efficiency and simplicity using only two tuning parameters. The stability analysis of the proposed system is performed using Lyapunov function. Among the most important metaheuristic methods, Askarzadeh in ref [98] developed Crow Search Algorithm (CSA) to solve some global optimization problem. The Crows have an intelligent behavior in flock, which based on the thievery of hidden food [99]. CSA is a simple and interesting technique for global optimization. The promising results have encouraged its utilization in solving real nonlinear and multimodal optimization problems in various engineering fields, where CSA offers good trade-off between diversification and intensification in the search process. Due to its tuning parameters, it ensures successful convergence to a global optimal solution without ever being trapped into a single local solution. In an attempt to attenuate the demerits of the above mentioned MPPT techniques, this paper proposes a new control strategy of global maximum power for isolated PV systems using metaheuristic Crow Search Algorithm to mitigate the adverse effects of partial shading on the tracking performances of a GMPPT controller. Our study focused on PV isolated systems, given its great importance, the latter is used in many clean energy

extraction systems such as PV water pumping systems in agricultural rural areas, electricity domestic rural, streetlights, electric cars, space system, etc. In comparison with previous MPPT techniques. CSA requires setting only a few parameters to obtain a good performance. This is the main contribution of our work, which combines good performances of GMPPT controller on the one hand and the simplicity of algorithm processes with few tuning parameters (only two) on the other hand. Additionally, it decreases the difficulties and the cost of implementation, and reduces the calculation time. A large number of tuning parameters (four to seven parameters) in many MPPT methods increase the computational load and require a high-end microcontroller. We reformulate the problem of tracking of the global maximum power point as a global optimization problem in partially shaded PV system using CSA, to ensure good performances: fast convergence towards GMPP, high efficiency in extracting of maximum power from a PV panel and robustness in all changing atmospheric conditions.

We proposes in this chapter an implementation of simple and efficient metaheuristic optimization technique, called Crow Search Algorithm (CSA) for MPPT. Moreover, we confirm by simulation results using Matlab/Simulink, the best performances of CSA-MPPT to track the global maximum power point GMPP for standalone PV system subject to critical operating weather conditions, compared to others MPPT methods.

IV.2. PV array characteristics under shading conditions

PV systems frequently installed near urban areas, where buildings, trees and lot of objects naturally form shadows, which can also be produced by clouds. Fig.IV.1. shows the partial shading generated from an adjacent building. Thus, the same PV module becomes partially shaded. PV characteristic curves, Power-Voltage (P-V) and Current-Voltage (I-V)

Fig.IV.1. PV array subject to shading conditions from an adjacent building [100]

Chapter IV
Simple and efficient metaheuristic technique to control
the maximum power of autonomous PV system

extremely influenced by the phenomenon of partial shading [41], which creates steps in the I-V characteristic curve, and several maximum power point peaks (MPPs) in the P-V characteristic curve, including multi-local peaks (LMPPs), and one global peak (GMPP) [35]. Due to the low irradiation received by the PV module. Consequently, the extracted PV power is significantly reduced. In this chapter, six PV modules connected in series (6S), as illustrated in Fig.IV.2 are tested under three different shading cases in order to assess the impact of partial shading on the obtained PV power (as shown in Fig.IV.2). The adopted cases are:

- Case (1) corresponds to zero shading; all PV modules are subject to the same constant irradiation of 1000 W/m^2.

- Case (2) represents a weak shading, where the PV modules are exposed to two different
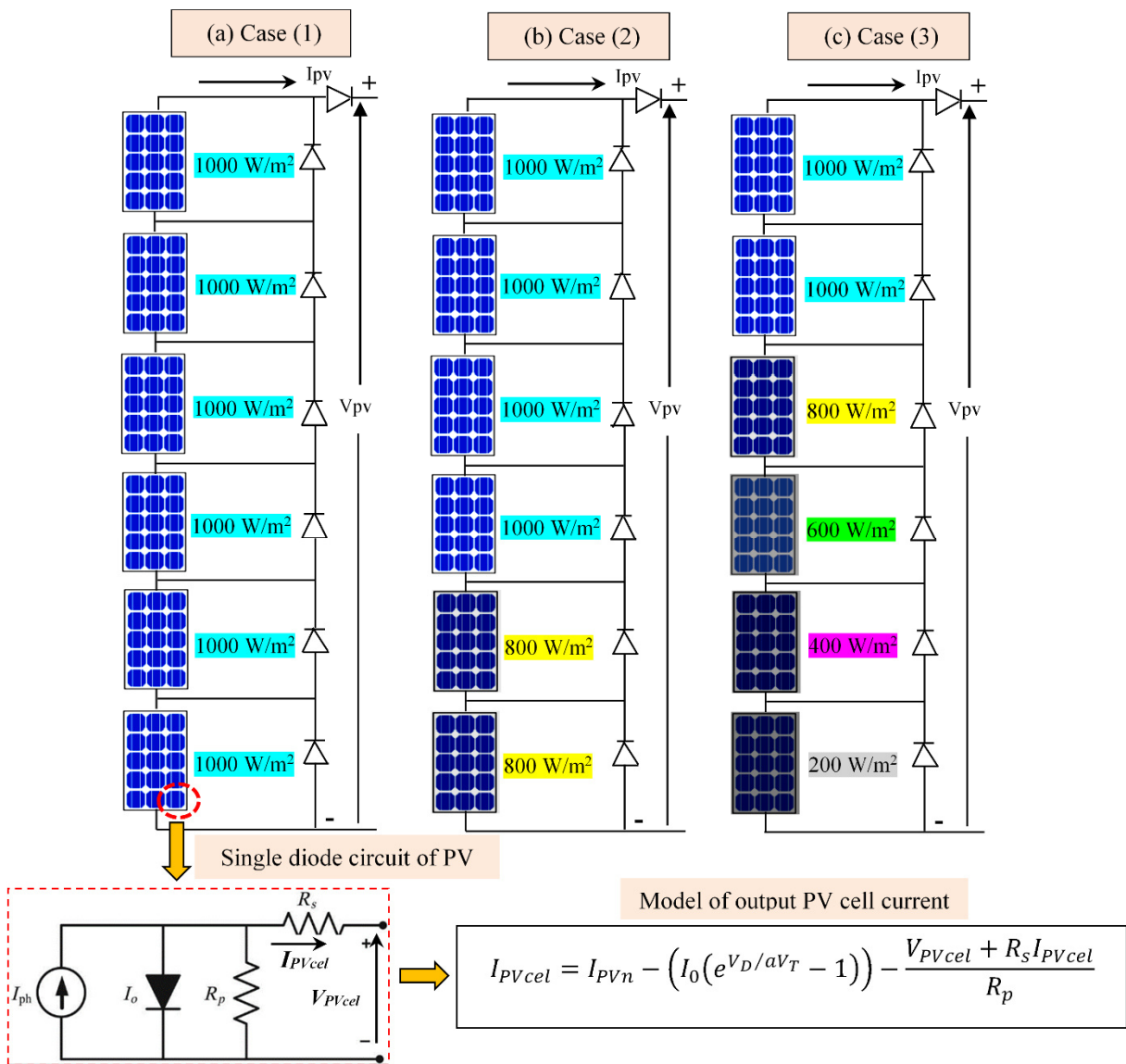
Fig.IV.2. PV modules configuration (6S) under tested partial shading cases with the equivalent single diode circuit of the PV cell

Values of irradiation: 1000 W/m^2 and 800 W/m^2.

- Case (3) is the case of severe shading with four different values of irradiation: 1000W/m^2, 800W/m^2, 600W/m^2 and 200W/m^2.

The impact of shading on P-V and I-V characteristics curves, shown in Figs.IV.3 and 4, respectively.
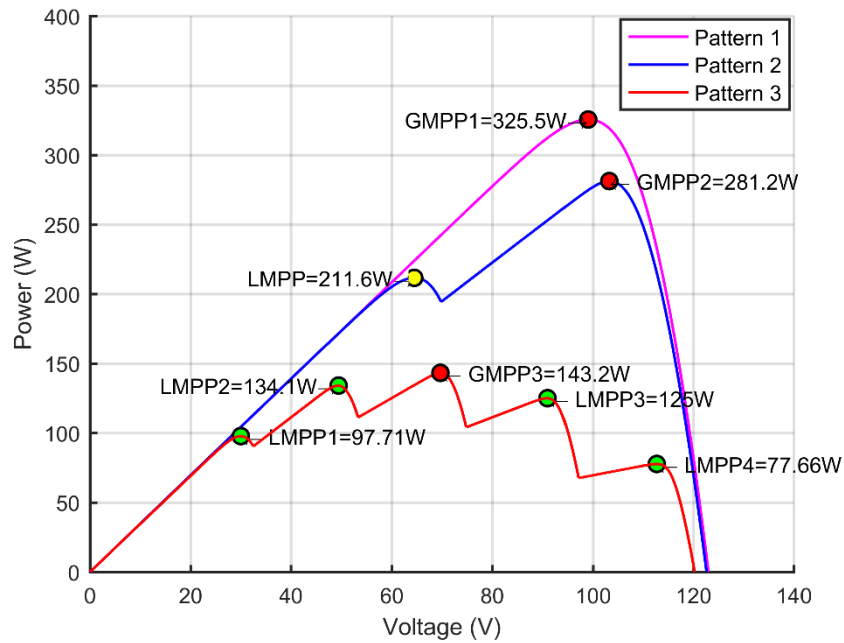
Fig.IV.3. Curve of power-voltage (P-V) characteristics for different partial shading cases
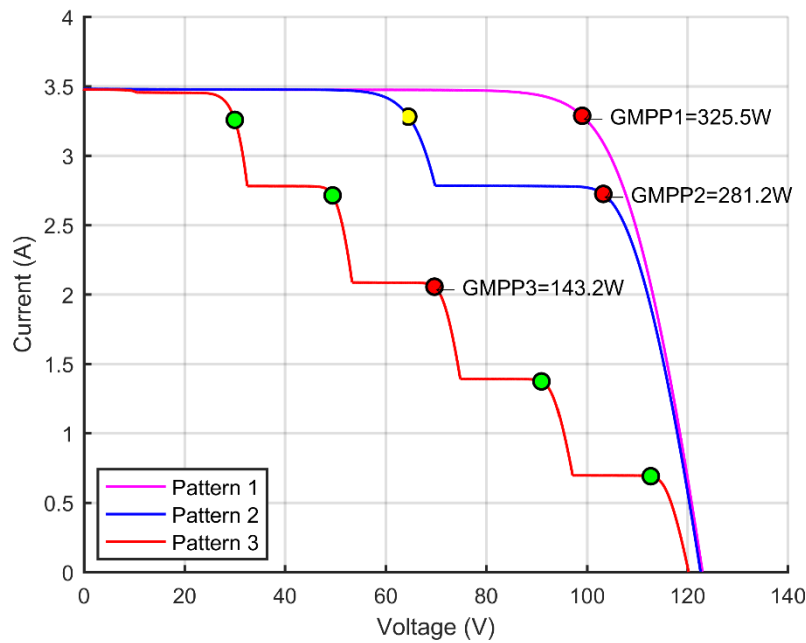
Fig.IV.4. Curve of current-voltage (I-V) characteristics for different partial shading cases

As indicated in Fig. IV.4, in case (1), which corresponds to a uniform irradiation, the shading generated several LMPPs and one GMPP. While in case (2) the shading created only one LMPP and one GMPP because there are two different irradiation rates. Case (3) includes five different irradiation rates, where the shading produced four LMPPs and one GMPP.

Table IV.1 describes the different cases of partial shading tested in this work.

Table IV.1. Irradiation levels for three tested cases (W/m^2)

PV Modules	Case (1) zero Shading	Case (2) weak Shading	Case (3) severe Shading
PV$_1$	1000	1000	1000
PV$_2$	1000	1000	1000
PV$_3$	1000	1000	800
PV$_4$	1000	1000	600
PV$_5$	1000	800	400
PV$_6$	1000	800	200

IV.3. Modeling of the PV system

For the sake of simplicity, the authors adopted the single diode model that simulates the equivalent electrical circuit of a solar PV cell as shown in Fig.IV.2, where the parameters of the model of the PV cell and PV module: I_{PVcel} and V_{PVcel} refer to the output current and voltage of the PV cell respectively. I_{ph} represents the solar-generated current. R_S and R_P are the series and parallel resistance respectively. I_0 stands for the diode saturation current. A is the diode ideality factor, k is the Boltzmann constant ($k=1.3806503\times10^{-19}$ J/K). q represents the electron charge ($q=1.60217646\times10^{-19}$ C). T is the operating temperature. The output current of PV module formulated by following equation:

$$I_{PV} = I_{ph} - I_0 \left[\exp\left(\frac{q(V_{PV} + I_{PV}R_s)}{AKTN_s} \right) - 1 \right] - \frac{V_{PV} + I_{PV}R_sN_s}{R_pN_s}$$

(IV-1)

Where I_{PV} and V_{PV} denote the output current and the output voltage of the PV module respectively. Ns all the cells in the PV module [29]. In this chapter, we use a series configuration (6S) of PV modules, thus Ns is equal to the total number of cells in the PV panel. The PV module utilized in this part is shell SM55, its electrical specifications under standard test condition STC (1000W/m^2, 25°C) are $P_{MPP}=55W$, $I_{MPP}=3.275A$, $V_{MPP}=16.5V$.

IV.3.1. Modelling of the DC-DC boost converter

A *DC-DC* power converter is connected in order to adjust the PV array output voltage V$_{pv}$ to maximize the solar power generation P$_{pv}$. Circuit topology of the DC-DC boost

converter is presented in Fig. IV.5. Where V_{pv} is the input voltage, Vs is the output voltage and i_L is the inductor current. The components R, L and C_s are respectively the resistive load, the inductor, and the output capacitor. In order to simplify design process of the MPPT controller, the input capacitor filter can be eliminated, which is in parallel with PV generator, consequently the inductor current is equal to the PV current ($I_L = I_{PV}$).
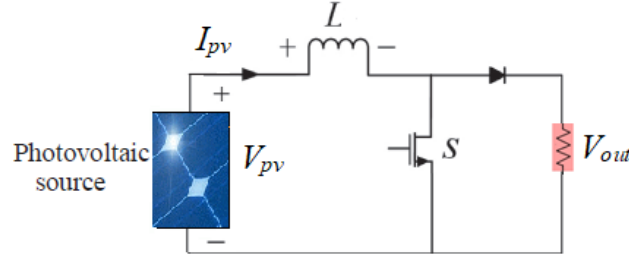
Fig. IV.5. Topology circuit of DC-DC boost converter

Depending on the switch state (S), we can be formulated the model of the boost converter in two switching modes with taking into consideration the continuous conduction only.

Based on the schematic in Fig. IV.5, the system dynamics can be derived as follow

On-state dynamics: The switch is ON (S = 1), the dynamics of V_{out} and I_{pv} are given by

$$\begin{cases} \dfrac{dI_{pv}}{dt} = \dfrac{V_{pv}}{L} \\ \dfrac{dV_{out}}{dt} = \dfrac{-V_{out}}{RC} \end{cases} \tag{IV-2}$$

Off-state dynamics: The switch is OFF (S = 0), the state space equations of the converter can be given by:

$$\begin{cases} \dfrac{dI_{pv}}{dt} = \dfrac{V_{pv} - V_{out}}{L} \\ \dfrac{dV_{out}}{dt} = \dfrac{I_{pv}}{C} - \dfrac{V_{out}}{RC} \end{cases} \tag{IV-3}$$

The general form of the nonlinear time invariant system as follow:

$$\dot{X} = f(X) + g(X)u \tag{IV-4}$$

$X = [x_1 \ x_2 \ ... x_n]^T$ is the vector of state space and $u \in [0 \ 1]$.

We can formulate the model of DC-DC boost converter as the form of Eq. (IV-4). By multiplying Eq. (IV-2) in the duty cycle D and Eq. (IV-3) in (1 - D) and using the state

space averaged technique where $X = [I_{pv} \ V_{out}]^T$, and $D \in [0 \ 1]$ [101]. The model of DC-DC
boost converter in continuous is presented as follows:

$$\begin{cases} \dfrac{dI_{pv}}{dt} = \dfrac{V_{pv}}{L} - \dfrac{V_{out}}{L}(1-D) \\ \dfrac{dV_{out}}{dt} = \dfrac{-V_{out}}{RC} + \dfrac{I_{pv}}{C}(1-D) \end{cases} \tag{IV-5}$$

IV.4. Implementation of MPPT methods for optimization problem

IV.4.1. Formulation of the optimization problem based MPPT

The MPPT application always aiming to maximize the extracted PV power from PV
generator, we can define the general formulation of the optimization problem for MPPT as
follows:

$$\text{Maximize } P_{pv}(D) \tag{IV-6}$$
$$\text{Subject to } D_{min} \leq D \leq D_{max}$$

Where P_{pv} is the extracted PV power from the PV panel, which represents the objective function
(fitness) of the optimization problem. D is the decision variable of the optimization problem,
that is represented in MPPT implementation by the duty cycle which is limited by the minimum
and maximum values $[D_{min} \ D_{max}]$ in this work we took the duty cycle $D \in [0.1 \ 0.95]$ [7].

IV.4.2. Perturb and observe (P&O) method based MPPT

The P&O is the most widely used MPPT algorithm. It measures periodically the voltage
and current and calculates the PV power. Then, it provides the steps of perturbation ΔV in the
operating voltage based on the change of power, through a change of the duty cycle of the DC–
DC converter, for each iteration compares the module output power with that of the previous
step to assess the change of power ΔP. The incrementing or decrementing processes of the duty
cycle is directed by the sign $(\Delta P/\Delta V)$, which determines the sign of the voltage perturbation ΔV
[102] The crucial aspect of this algorithm is to determine the step size of perturbation. If it large,
the convergence is fast but causes large oscillation in the steady state power and vice versa, and
this oscillation causes unwanted losses of PV power [7].

IV.4.3. Particle Swarm Optimization (PSO) based MPPT

PSO is a swarm intelligence based meta-heuristic approach inspired from the intelligent
social movement of birds in flock [103]. PSO search process starts by a chosen random

population. Each particle (solution) moves in n-dimensional space depending on their adjusted direction called velocity. This intelligent movement is subject to a flying rule, which states that every particle tracks the best global position of swarm, and moves to the best personal optimal position found by the particle itself, i.e., the local solution. Next, after sufficient iterations, each particle advances to an agreeable neighborhood of the global optimal position that corresponds to the global solution [104]. For PSO based MPPT problem, the position of a particle represents the duty cycle and the objective function represents the output PV power, and can be defined by the particle position D_i and the velocity v_i for $k+1$ iteration that detailed in chapter one [61].

IV.4.4. Crow Search Algorithm (CSA)

Crows (Corvids family) are among the most intelligent animals, and scientific experiments have proven its intelligent behavior. What sets the crow apart from the other animals is its capacity to remember faces and the places of their hidden food, up to several months later. Additionally, it has sophisticated communication with other crows and can use tools to perform some tasks [98]. Furthermore, a crow observes other crows or birds to uncover the locations of their hidden food, to steal it. On the other hand, a crow changes its place to deceive other crows if aware of being tracked [105].

CSA is designed based on the following features of the crow:

- Crows live in flocks.
- Crows hide their food in secret locations and remember it when needed.
- Each crow tracks other crows to steal their hidden food.
- Each crow deceives the others by random movements to protect its hidden food from potential thieves [106].

At iteration *iter* crow *i* tries to track crow *j* to get closer to its secret location of food. At this moment, *k* can find two states related to the value of the *AP* parameter, which embodies the extent of crow *j* awareness that crow *i* is following it or not. These two states update the places of crows as follows:

State 1: $r \geq AP$ Where *r* is a random number it values between [0 1]. *AP* represents the Awareness Probability parameter. This condition means that crow *j* is unaware that crow *i* is tracking it. The vector x_i^{iter} represents the values of the position of crows in flock at iteration (*iter*) $x_i^{iter} = [x_1^{iter} x_2^{iter} x_3^{iter}]^t$. Where the *d*-dimensional environment $d = 1$. For this condition, crow *i* moves to approach the hidden food location of crow *j* according to the following equation:

$$x_i^{iter+1} = x_i^{iter} + r \times fl \times (m_j^{iter} - x_i^{iter}) \qquad\qquad (IV-9)$$

Where x_i^{iter+1} is the position of crow i at iteration ($iter+1$). m_j^{iter} is the memory vector of crow j at the iteration ($iter$) at which it stores the the hidden food where $m_i^{iter} = [m_1^{iter} \ m_2^{iter} \ m_3^{iter}]^t$.

fl is the flight length parameter.

State 2: $r < AP$

This condition means that the crow j is aware that crow i is tracking it. In this state, crow j will try to deceive crow i by moving to a random location of the search space, hence, the location of crow i also changes randomly according to the following formula.

$$x_i^{iter+1} = a \ random \ \ location \qquad\qquad (IV-10)$$

The movements of the crows in the search space are illustrated in Fig. IV.6.
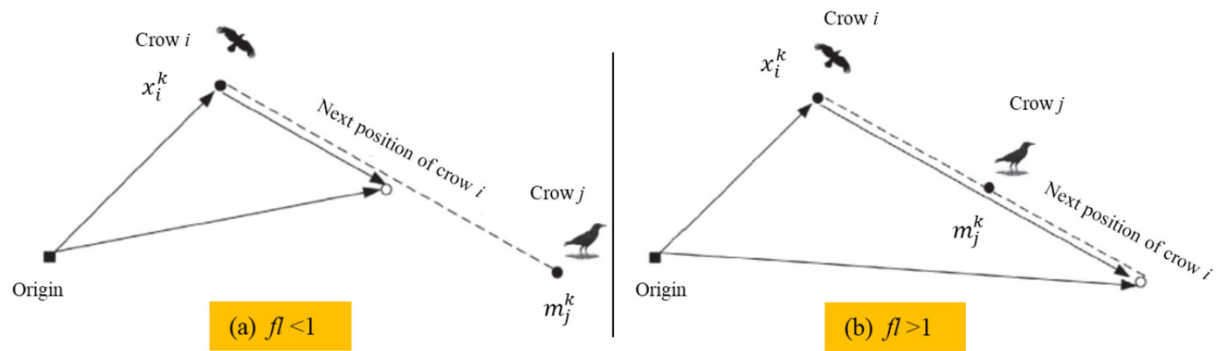
Fig. IV.6. Intelligent movements of crows in the search process for hidden food

We updates the crow position vector x_i^{iter} and its memory vector m_i^{iter} in each iteration based on the current and previous values of the fitness for each vector.

We explain the implementation steps of Crow Search Algorithm for global optimization problem in Table IV.2 [98].

IV.4.4.1. Conditions of convergence in CSA method

The convergence to global optimal solution in CSA algorithm is affected by its following parameters:

✓ Tuning parameters: The awareness probability (AP) *and* the flight length (fl).

✓ Initial parameters: Initial positions of crows x_i^0 in population at the initial iteration ($iter = 0$). The number of crows (N) in the flock, where $i = 1, 2,..., N$.

Table.IV.2. Implementation steps of Crow Search Algorithm in optimization problem

No	Procedure
1.	Initialize CSA: Crows flock size N. Initial positions x_i^0 of all crows $i = 1,2..,N$. Initial memory vectors of crows $m_i^0 = x_i^0$. Initial fitness $f_0(x_i^0)$. Tuning parameters: Awareness Probability AP and Flight length fl.
2.	Evaluate the initial fitness of each crow $f(x_i^0)$ to assess the initial positions x_i^0 to find the local best solutions x_{best}^0.
3.	While $iter < iter_{max}$
4.	For $i = 1:N$
5.	Suppose that crow i track the crow j.
6.	if $rand \geq AP$
7.	Mean that the crow j is unaware that crow i is track it, in this state crow i moves according to Eq. (IV-9) to generate the new position x_{inew}^{iter}.
8.	Else, the crow j is aware that crow i tracks it, so crow j take a new deceiving position x_{jnew}^{iter} is set as random point on the search space for the camouflage of its hidden food. Which results in a new position x_{inew}^{iter} of the tracker crow i.
9.	end if
10.	end for
11.	Updates crow position by the new best position (local best solutions x_{best}^{iter}) based on its fitness values $f(x_i^{iter})$, we accepts only the feasible solutions and rejects the others; the solutions is feasible if the current fitness value of the new position is better than the fitness value of the previous position, otherwise the solutions is non-feasible.
12.	The crow updates its memory m_i^{iter} by the new position x_{inew}^{iter}, if the fitness value $f(x_{inew}^{iter})$ of the new position of the crow is better than the fitness value of the memorized position $f(m_i^{iter})$ otherwise the memory vector keeps its previous values.
13.	Find the global best solution x_{gbest} that gives the global best fitness f_{gbest}.
14.	End While.

In this section, we carefully explain the effect of the tuning parameters on the convergence of the search process in the CSA method:

- The awareness probability AP provides a balance between diversification and

intensification in the search process of the CSA algorithm. If AP augmented then diversification in the search process is augmented and intensification is reduced.

▪ The flight length fl values are chosen between 0 and 1, the tuning parameter fl determines the step size of moving towards the interesting hiding place as shown in Eq. (IV-9) which represents the current optimal solution. In fact, it is the place of crow i which tracks crow j, where small fl values ($fl < 1$) orients the search process towards the local search (proximity of x_i^{iter}). However, greater values ($fl > 1$) steer the algorithm to the global search (far from x_i^{iter+1}) [105].

To ensure the convergence of the CSA, the following conditions must be met:

1- The flight length parameter fl must be greater than 1 ($fl > 1$), we selected in our work ($fl = 2$) because small fl values (very far from 1) lead the search process to a local search while large fl values ($fl > 1$) directs the search process to the global search. If fl values are between 0 and 1, this means that the new position of a crow will be between its current position and the position of the interesting hiding place (memorized location m_i^k), as shown in Fig.5. Conversely, if the value of fl is selected greater than 1, the crow can visit beyond the interesting hiding place (memorized place m_i^k).

2- The awareness probability AP parameter must be much less than 1 ($AP \ll 1$), we used in our work $AP = 0.1$. Because AP provides a balance between diversification and intensification in the search process, by increasing AP value, diversification increases and consequently, intensification decreases. On the other hand, if ($AP = 1$), CSA is converted to a random search method. The use of AP not only makes it possible for the crows to search those regions of the landscape that have not been visited but also allows them to move towards the best found solutions from different directions.

3- The values of the initial positions of each crow x_i^0 should not be chosen too far from the value of the global optimal solution.

IV.4.5. Crow Search Algorithm (CSA) based MPPT

To implement the CSA method in MPPT optimization problem, first the optimization problem must be formulated by defining the objective function and/or constraints, which are the information that drive the search process for an optimal solution, and list all the required variables involved in solving the problem. We consider that the extracted PV power P_{pv} as the maximized objective function (fitness), and the duty cycle D_i as the decision variable to be optimized, where the duty cycle D_i denotes the position x_i of crow i.

Figure.IV.7 shows a general schematic diagram of the utilized standalone PV system subjected to partial shading.
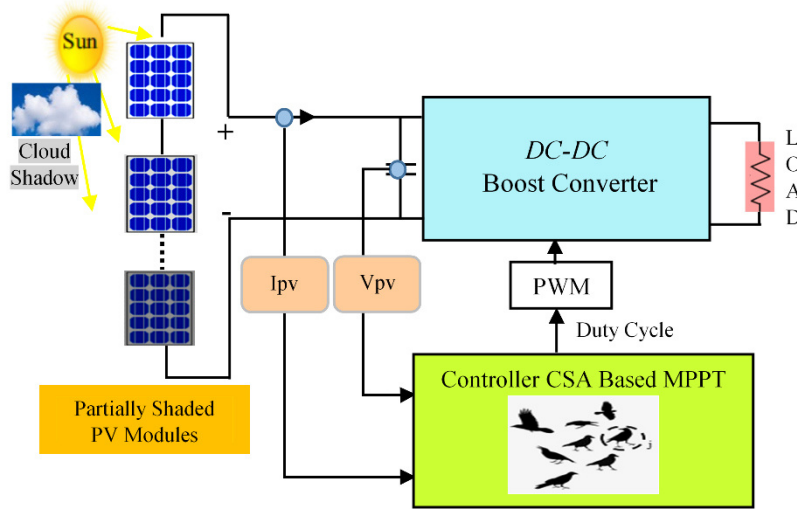
Fig. IV.7. General diagram of the partially shaded PV system with proposed CSA based MPPT controller

All the implementation steps of CSA for global optimization problem based MPPT are presented in Fig. IV.8.

Step 1: *Initialize duty cycle*, *memory of crows and tuning parameters of CSA.* Number of maximum iteration (k_{max}=25). Chosen number of crows in flock N=3, where i=1, 2 and 3. The Awareness probability AP=0.1. Flight length fl = 2. The limits on duty cycle D_{min} = 0.1 and D_{max} = 0.95. Initialize the memory vector of each crow $m_i^0 = D_i^0$. Initial values of duty cycle vector $D_i^0 = [D_1^0 \ D_2^0 \ D_3^0]^t$ representing the initial locations of crows and particles in CSA and PSO respectively, they differ for each of the three tested partial shading cases. For a fair comparison between the proposed CSA and PSO methods, we chose the same initial values for each method that are: D_i^0, N and $iter_{max}$, we selected the initial duty cycle values as follow:

Case 1: D_i^0 = [0.5 0.55 0.68]^t.

Case 2: D_i^0 = [0.35 0.5 0.65]^t.

Case 3: D_i^0 = [0.4 0.5 0.65]^t.

Step 2: *Evaluate the initial objective function P_i^0 to find* the *current optimal solution D_{best}^0 at initial iteration*

After calculating the PV power values $P_i^0 = [P_1^0 \ P_2^0 \ P_3^0]^t$ resulting from the initial duty cycle values D_i^0 for each crow (N =3), the initial PV power P_i^0 is evaluated to find the current optimal duty cycle D_{best}^0 that generates the maximum power P_{max}^0 (maximum fitness).

This is achieved by comparing the initial power values P_i^0 between each crow and the others in the population at initial iteration, where we take the greater power values corresponding to the optimal duty cycle values D_{best}^0 (local optimal solution).
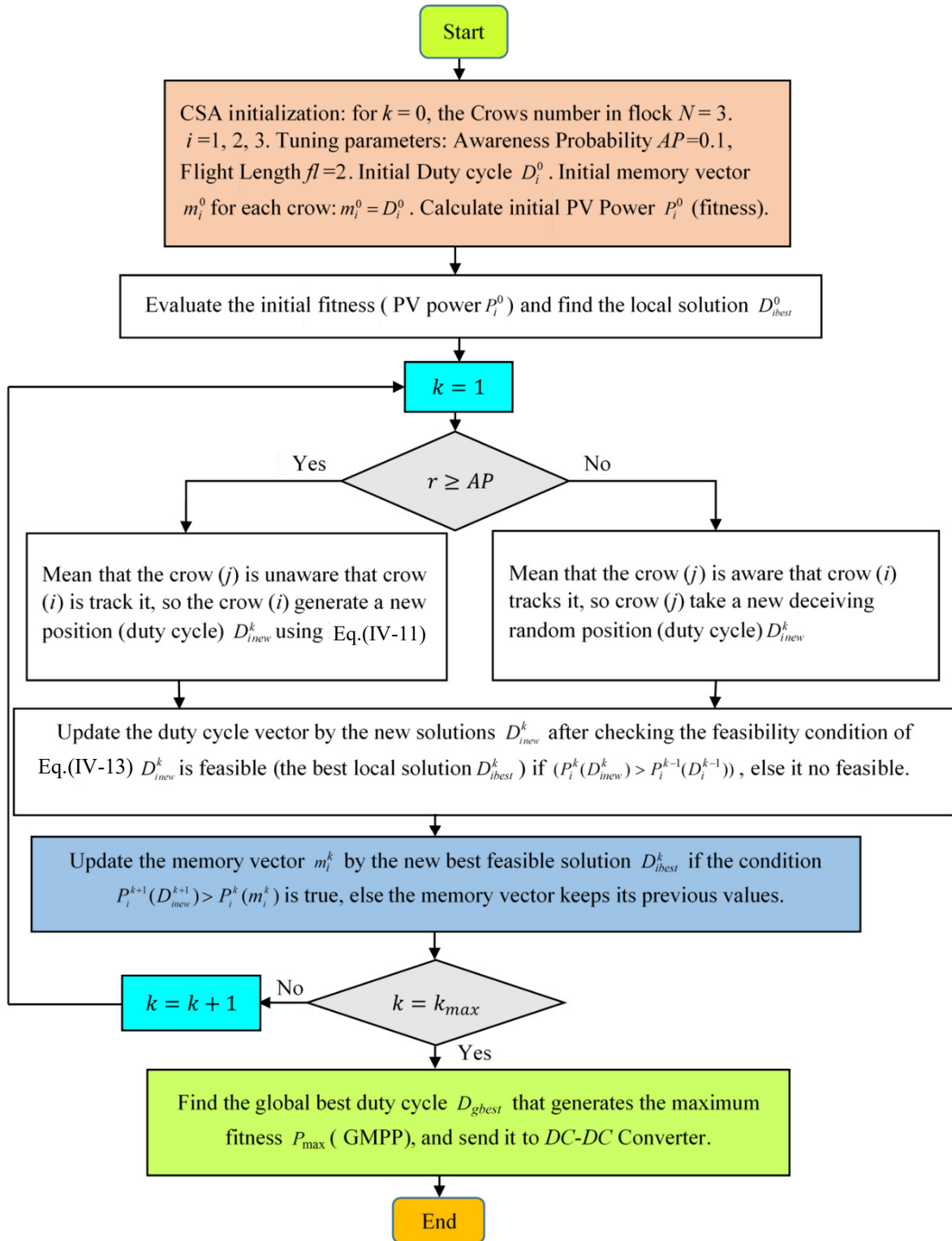
Fig. IV.8. Flowchart of the proposed CSA technique implemented for the global optimization problem based MPPT

Step 3: *Generate new solutions D_i^{k+1}.*

When each crow j in the flock begins to search for its hidden food, represented by the vector memory m_j^k, the steps of the optimization algorithm begin to be performed; at instant *iter = k*, crow j wants to retrieve its hidden food m_j^k from one of its memorized secret locations, which is considered as the best current duty cycle $D_{j\,best}^k$ (local optimal solution). At this moment, there are two possibilities: the first is that crow j does not realize that it is being tracked by crow i, and the second possibility is that crow j is aware of being followed by crow i to steal its food. The consciousness of the crow j is expressed by the parameter named the awareness probability *AP* in our MPPT application we selected *AP* = 0.1.

We summarize these two states with the mathematical expressions of Eq. (IV-12):

➢ **State 1:** if $r \geq AP$

This state means that when crow j searches for its hidden food in its memorized locations m_j^k but does not know it is being tracked by crow i. In this situation, crow i changes its place to approach the locations of the hidden food m_j^k of crow j to steal it. Based on this state, crow i takes new locations x_i^{k+1}, which represent the new duty cycle vector D_i^{k+1} in MPPT. This change of locations process corresponds to the generation of new duty cycles D_i^{k+1} that approaches the best local solution according to Eq. (IV-11):

$$D_i^{k+1} = D_i^k + r \times fl \times (m_j^k - D_i^k) \tag{IV-11}$$

Where D_i^{k+1} is the duty cycle vector of crow i in iteration $k+1$. m_j^k is the memory vector of crow j at iteration k. fl is the flight length parameter.

➢ **State 2:** if $r < AP$

In this state, for a new iteration *(iter = k+1),* crow j knows that the crow i is following it, so, in an attempt to protect its hidden food against the probability of theft from crow i, it uses a deception strategy that consists in randomly changing its current place to a new place x_j^{k+1}. This random change in the location of crow j results in a random change in the location x_i^{k+1} of crow i. for MPPT application. The random change in the location of each crow corresponds to random change in the duty cycle D_i^{k+1}.

Generally, the two previous states can be summarized by the following equation:

$$D_i^{k+1} = \begin{cases} D_i^k + r \times fl \times (m_j^k - D_i^k) & if \ r \geq AP \\ a \ random \ \ duty \ cycle & otherwise \end{cases} \quad \text{(IV-12)}$$

Step 4: *Evaluate the new fitness (PV power) P_i^{k+1} and update the new duty cycle D_i^{k+1}.*

To evaluate these new values of positions x_i^{k+1} of the crows that correspond to the new duty cycle D_i^{k+1} resulting from Eq. (IV-12) the new values of the fitness P_i^{k+1} are computed, from these new values, which are then accepted or rejected according to the following feasibility relation.

$$P_i^{k+1}(D_i^{k+1}) > P_i^k(D_i^k) \quad \text{(IV-13)}$$

We update the values of the locations of the crows that represent the new current solutions of the optimization problem (new duty cycles in MPPT). If these new locations meet the feasibility condition of Eq. (IV-9), we accept these new solutions and consider them feasible, else we reject them (in the reverse case) and consider them as not feasible, and the locations of the crows remain the same. Therefore, the duty cycles keep these values without updating.

Step 5: *Update the memory vector m_i^{k+1} of each crow in the flock.*

We update the memory vector of each crow in the flock by the feasible values of the positions that fulfill the condition of feasibility evaluated in step 4. For a new iteration (*iter = k+1*), we update the new memory vector m_i^{k+1} with the new values of the duty cycle D_i^{k+1} (correspond to the new positions x_i^{k+1}). If the new PV power (fitness) $P_i^{k+1}(D_i^{k+1})$ of the new duty cycle is greater than the previous PV power $P_i^k(m_i^k)$ of the memory vector m_i^k calculated at the instant (*iter = k)*, otherwise, the memory vector keeps its previous values. Eq. (IV-14) represents the process of updating the memory vector for all the crows in the flock.

$$m_i^{k+1} = \begin{cases} D_i^{k+1} & if \ \ P_i^{k+1}(D_i^{k+1}) > P_i^k(m_i^k) \\ m_i^k & otherwise \end{cases} \quad \text{(IV-14)}$$

Step 6: *Check termination criterion (iter = iter$_{max}$).*

We repeat steps 3–5 to calculate the new duty cycle D_i^{k+1} and evaluate them according to their power (fitness) values $P_i^{k+1}(D_i^{k+1})$ generated, and we continue to update the memory vector m_i^{k+1} of each crow by the best local duty cycle (feasible solutions) D_{ibest}^{k+1} at each iteration

according to the condition of Eq. (IV-14). We discard non-feasible solutions that generate power values lower than the previous ones and keep the feasible solutions that generate larger power values. This is repeated until we reach the termination condition *(iter = iter$_{max}$)*, and obtain the best global optimal duty cycle D_{gbest}. The latter represents the global optimal solution for the optimization problem based MPPT that generates the GMPP for all iterations when all duty cycles of crow *i* flock converge to D_{gbest}. Finally, send D_{gbest} to the boost converter to generate the global maximal power GMPP of PV system.

After the termination of all the previous steps of the optimization problem via CSA based MPPT, we obtain the final results, which are the global optimal duty cycles values D_{gbest} that represent the global optimal solutions of the studied global optimization problem using three proposed MPPT methods under different tested partial shading cases as follows:

For CSA based MPPT method:

Case 1: D_{gbest} = 0.6099, that generates the global maximum power point GMPP (fitness), $P_{max}(D_{gbest}) = 325.4\,W$.
Case 2: D_{gbest} = 0.5684 that generates the GMPP $P_{max}(D_{gbest}) = 280.6\,W$.
Case 3: D_{gbest} = 0.5851, that generates the GMPP, $P_{max}(D_{gbest}) = 143.1\,W$.

For PSO based MPPT method:

Case 1: D_{gbest} = 0.6086, that generates the global maximum power GMPP (fitness), $P_{max}(D_{gbest}) = 325.1\,W$.
Case 2: D_{gbest} = 0.552, that generates the GMPP, $P_{max}(D_{gbest}) = 275.7\,W$.
Case 3: D_{gbest} = 0.5836, that generates the, $P_{max}(D_{gbest}) = 142.4\,W$.

For P&O based MPPT method:

Case 1: D_{gbest} = 0.605, that generates the GMPP (fitness), $P_{max}(D_{gbest}) = 323.1\,W$.
Case 2: D_{gbest} = 0.690 that generates the maximum power GMPP $P_{max}(D_{gbest}) = 211.8\,W$.
Case 3: D_{gbest} = 0.695 that generates the maximum power GMPP $P_{max}(D_{gbest}) = 134\,W$.

IV.5. Lyapunov Stability Analysis:

The stability analysis is a necessary process in the control of systems. In this section Lyapunov function and Barbalat lemma are used to investigate the stability properties of the studied PV system. Salami *et al* [107] proposed a Lyapunov based nonlinear controller of the PV system for MPPT, using Lyapunov based single-loop as shown in Fig. IV.9. Considering PV power derivative as a feedback signal, which has fixed zero reference value in different operational conditions where the duty-cycle of the *DC-DC* boost converter is adjusted to ensure

maximum power conversion from the PV generator to the load. In this section, we determine the error variable z based on similar closed single loop of Fig. IV.9
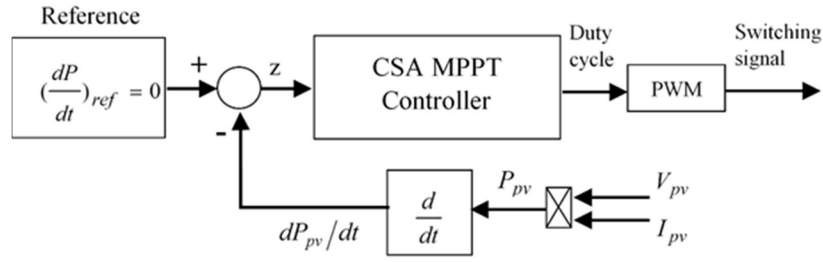
Fig. IV.9. Single loop control in PV system based CSA-MPPT controller

In order to analyze the stability of the proposed PV system using the Lyapunov theory. The main objective of this analysis is verifies the convergence of the error z to equilibrium point zero $(z = 0)$.

If the maximum power point (MPP) is reach by the MPPT controller, therefore the following condition is satisfied:

$$\frac{dP_{pv}}{dt} = 0 \tag{IV-15}$$

We define the error z between the time derivate of the reference power $(P_{pv})_{ref}$ and the time derivate of the obtained power P_{pv}

$$z = \left(\frac{dP_{pv}}{dt}\right)_{ref} - \frac{dP_{pv}}{dt} \tag{IV-16}$$

The target in the single loop control is the tracked maximum power point MPP is $(P_{pv})_{ref}$ that is constant, therefore the time derivate of this reference power is zero which gives as:

$$\left(\frac{dP_{pv}}{dt}\right)_{ref} = 0 \tag{IV-17}$$

By using Eq. (IV-17) in Eq. (IV-16) we get:

$$z = -\frac{dP_{pv}}{dt} \tag{IV-18}$$

The time derivate of the error z is gives as: $\dot{z} = \dfrac{d}{dt}\left(-\dfrac{dP_{pv}}{dt}\right)$

$$\dot{z} = -\frac{d}{dt}(\dot{P}_{pv}) \tag{IV-19}$$

According to Eq. (IV-18) we can write z as:

$$z = -\frac{dP_{pv}}{dt} = -\frac{d(V_{pv} \times I_{pv})}{dt} = -\frac{dV_{pv}}{dt}I_{pv} - \frac{dI_{pv}}{dt}V_{pv} \tag{IV-20}$$

We reformulate the error z as:

$$z = -(\dot{V}_{pv}I_{pv} + \dot{I}_{pv}V_{pv}) \tag{IV-21}$$

We set the variable state x_1 of the boost converter model in Eq. (IV-5) as: $x_1 = I_{pv}$

$$\dot{x}_1 = \dot{I}_{pv} \tag{IV-22}$$

By using x_1 in the Eq. (IV-21), the formula of the error z define as follow

$$z = -\dot{V}_{pv}x_1 - \dot{x}_1 V_{pv} \tag{IV-23}$$

The model of the boost converter of Eq. (IV-5) in the section 3.1 gives the following
equation:

$$\dot{x}_1 = \frac{V_{pv}}{L} - \frac{V_{out}}{L}(1 - D) \tag{IV-24}$$

By replacing the Eq. (IV-24) in Eq. (IV-23), we obtain:

$$z = -\frac{1}{L}V^2_{pv} + \frac{1 - D}{L}V_{pv}V_{out} - \dot{V}_{pv}x_1 \tag{IV-25}$$

After deriving the error z that defined in Eq. (IV-23), we obtain the following formula

$$\dot{z} = -\frac{2}{L}V_{pv}\dot{V}_{pv} - \frac{\dot{D}}{L}V_{pv}V_{out} + \frac{1 - D}{L}\dot{V}_{pv}V_{out} - \ddot{V}_{pv}x_1 - \dot{V}_{pv}\dot{x}_1 \tag{IV-26}$$

By replacing the Eq. (IV-24) in Eq. (IV-26), we get:

$$\dot{z} = -\frac{2}{L}V_{pv}\dot{V}_{pv} - \frac{\dot{D}}{L}V_{pv}V_{out} + \frac{1-D}{L}\dot{V}_{pv}V_{out} - \ddot{V}_{pv}x_1 - \frac{\dot{V}_{pv}}{L}\left(V_{pv} - (1-D)V_{out}\right) \quad \text{(IV-27)}$$

The simplification of Eq. (IV 27) gives the Eqs. (IV-28) and (IV-29):

$$\dot{z} = -\frac{2}{L}V_{pv}\dot{V}_{pv} - \frac{\dot{D}}{L}V_{pv}V_{out} + \frac{1-D}{L}\dot{V}_{pv}V_{out} - \ddot{V}_{pv}x_1 - \frac{1}{L}\dot{V}_{pv}V_{pv} + \frac{1}{L}\dot{V}_{pv}V_{out} - \frac{D}{L}\dot{V}_{pv}V_{out} \quad \text{(IV-28)}$$

We can write the final formula of the derivate error $\dot{z}$ as:

$$\dot{z} = -\frac{2}{L}V_{pv}\dot{V}_{pv} - \frac{\dot{D}}{L}V_{pv}V_{out} + \frac{2(1-D)}{L}\dot{V}_{pv}V_{out} - \ddot{V}_{pv}x_1 \quad \text{(IV-29)}$$

In order to assure the asymptotic stability, the Lyapunov function V must be positive definite and radially unbounded and its derivative with respect to time must be negative definite ($\dot{V} \leq 0$) [108].

We define the Lyapunov candidate function V as follow:

$$V = \frac{1}{2}z^2 \quad \text{(IV-30)}$$

The time derivative of the Lyapunov function gives as:

$$\dot{V} = z\dot{z} \quad \text{(IV-31)}$$

According the Eq. (IV-19) we can concluded that $\dot{z} = -cz$, where c is scalar positive parameter ($c > 0$), then derivative of the Lyapunov function $\dot{V}$ rewritten as:

$$\dot{V} = -cz^2 \quad \text{(IV-32)}$$

In the Eq. (IV-32) as the element ($z^2 \geq 0$) and c is a constant positive ($c > 0$), as a result than the derivative of the Lyapunov function will be a negative semi-definite function

$$\dot{V} \leq 0 \quad \text{(IV-33)}$$

According to Lyapunov theory, the Eq. (IV-33) describes the condition of the asymptomatic stability.

Based on the Eq. (IV-33) the asymptomatic stability condition of based Lyapunov is verified, as a result the asymptomatic stability of the PV system is guaranteed.

To ensure that the PV system operate in the maximum power MPP, it is necessary that the error z of Eq. (IV-18) converges to zero, in order to achieve this constraint, we uses the *Barbalat's lemma* which is proposed by Slotine and Li in the Ref [109], where its conditions are:

1- The Lyapunov function V must be a lower bounded.

2- $\dot{V}$ must be a negative semi-definite function ($\dot{V} \leq 0$).

3- $\dot{V}$ must be a uniformly continuous function (mean that $\ddot{V}$ be bounded).

The second derivative of the Lyapunov function $\ddot{V}$ formulated as follows:

$$\ddot{V} = -2cz\dot{z} \qquad (IV-34)$$

The Barbalat lemma conditions (1) and (2) are satisfied because the error z is bounded, and also according to $\dot{V} = -cz^2$ we previously proved that $\dot{V} \leq 0$ further, we know that the error z and parameters of the model are bounded, and according to the dynamics of the system error variable $\dot{z}$ that is shown in Eq. (IV-29), we can be infer that $\ddot{V}$ is bounded. As a result, the condition (3) is satisfied since $\dot{V}$ is uniformly continuous function.

Based on the previous mathematical proofs using Lyapunov function and *Barbalat lemma*, we can conclude that the adopted PV system exhibits an asymptotically stable behavior, and that the error z in the loop control will be zero ($z = 0$) during steady-state operation of the boost converter. This means that the condition of Eq. (IV-15) is satisfied and the PV system can operate in the MPP.

IV.6. Simulation results

To verify the effectiveness of the suggested CSA method in mitigating the adverse effects of partial shading on the performance of the MPPT controller in standalone PV system, simulation using MATLAB was performed under three different partial shading cases (as shown Fig. IV.10). This system comprises six modules connected in series (6S), a *DC-DC* boost converter and a resistive load (R).

As is known, the performances of MPPT methods are strongly related to their tuning parameters, which directly affect the quality of convergence to the GMPP. The values of all tuning parameters for each used MPPT methods are presented in Table IV.3 as follows:

▪ Two parameters of the proposed CSA method are Awareness probability (*AP*) and flight length (*fl*).

- Four parameters of PSO are limits of acceleration coefficients (c_1 and c_2), and limits of inertia weight w (w_{min} and w_{max}).

- Two parameters of P&O are the change in duty cycle (ΔD) and the initial duty cycle (D_0).

Table.IV.3. Tuning parameters of the simulated MPPT methods

P&O	PSO	CSA
$D = 0.75$	$w_{min} = 0.4$	$AP = 0.1$
$\Delta D = 0.005$	$w_{max} = 1$	$fl = 2$
	$c_1 = 1.4$	
	$c_2 = 1.6$	
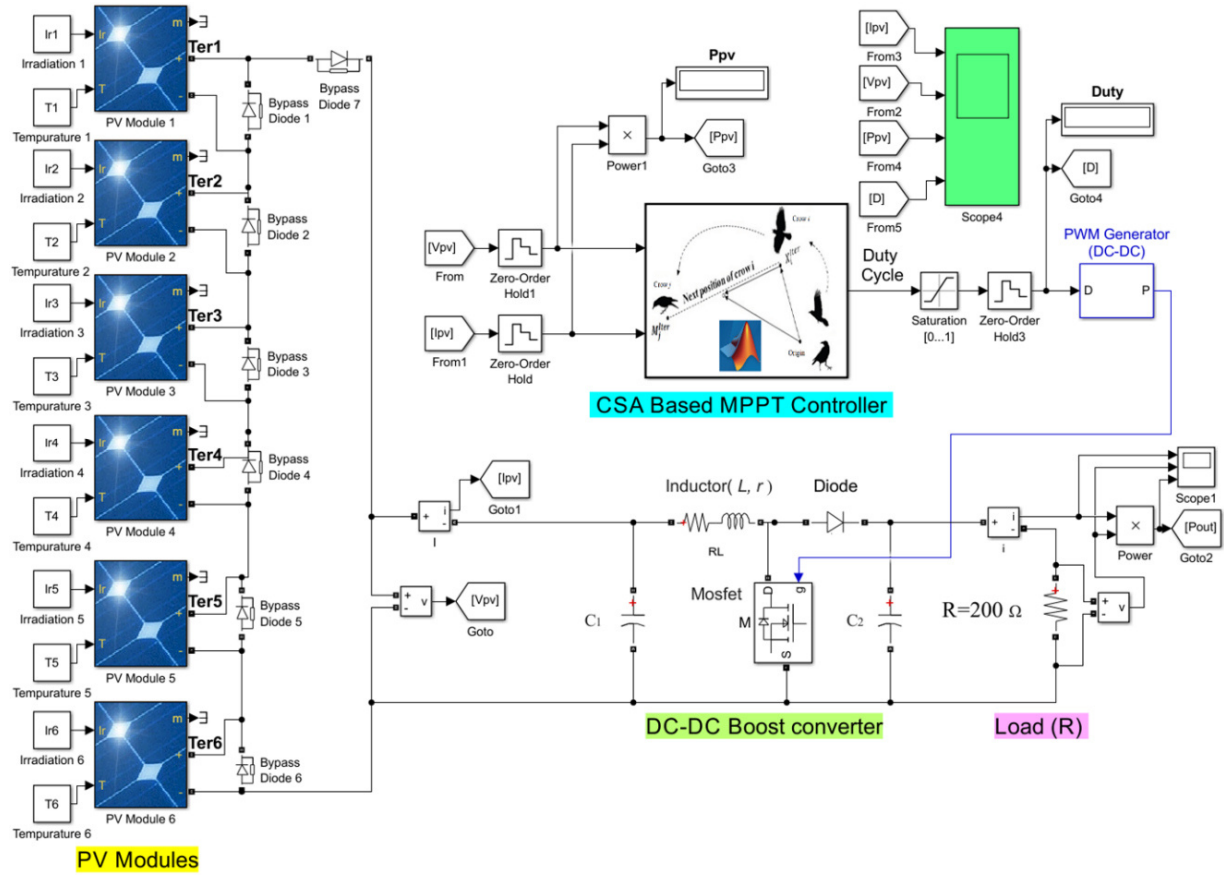
Fig. IV.10. Simulation model of the used PV system with CSA based MPPT controller

The specifications of the used boost converter are shown in Table IV.4.

Table.IV.4. Boost converter specifications

Parameter	Value
Frequency f_s	50kHz
Inductor (L, r)	$500\mu H, 0.23\Omega$
Capacitor C_1	$100\mu F$
Capacitor C_2	$100\mu F$
Load R_L	$200\ \Omega$
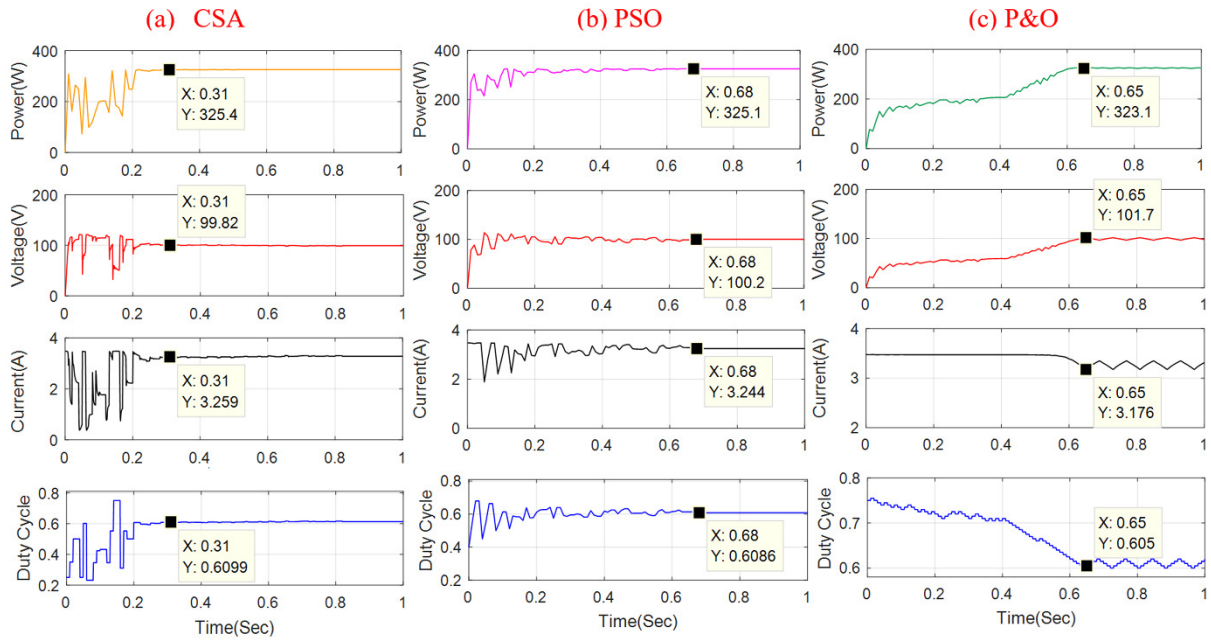
Fig.IV.11. Simulated system responses of CSA, PSO and P&O methods under case 1
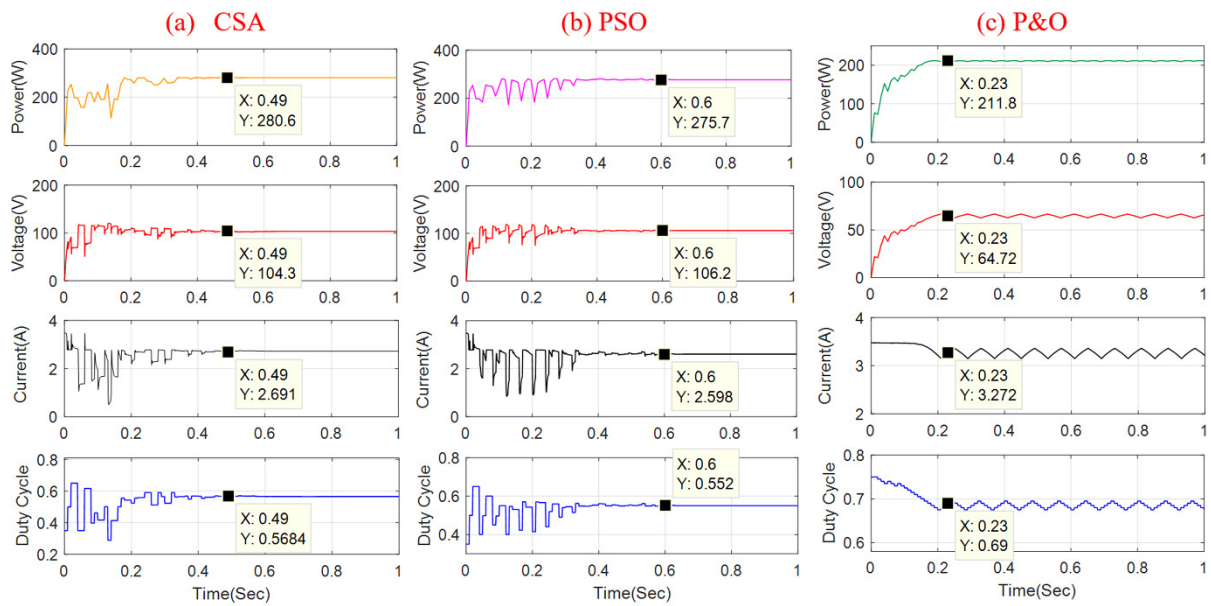
Fig.IV.12. Simulated system responses of CSA, PSO and P&O methods under case 2

Figures IV.11, 12 and 13 depict the response curves (power, voltage, current and duty cycle), resulting from the simulated standalone PV system shown in Fig. IV.10. using CSA, PSO and P&O methods under three various shading cases (zero, weak and severe shading).

Figure IV.14. illustrates the updating process of the extracted PV power in CSA and PSO methods for the total number of iterations $iter_{max} = 25$.

IV.6.1. Discussion and analysis

Based on the simulation results, an accurate quantitative comparison between CSA, PSO and P&O methods is illustrated in Table. IV.5, by considering the following performance criteria: efficiency, convergence time, extracted PV power and power loss.
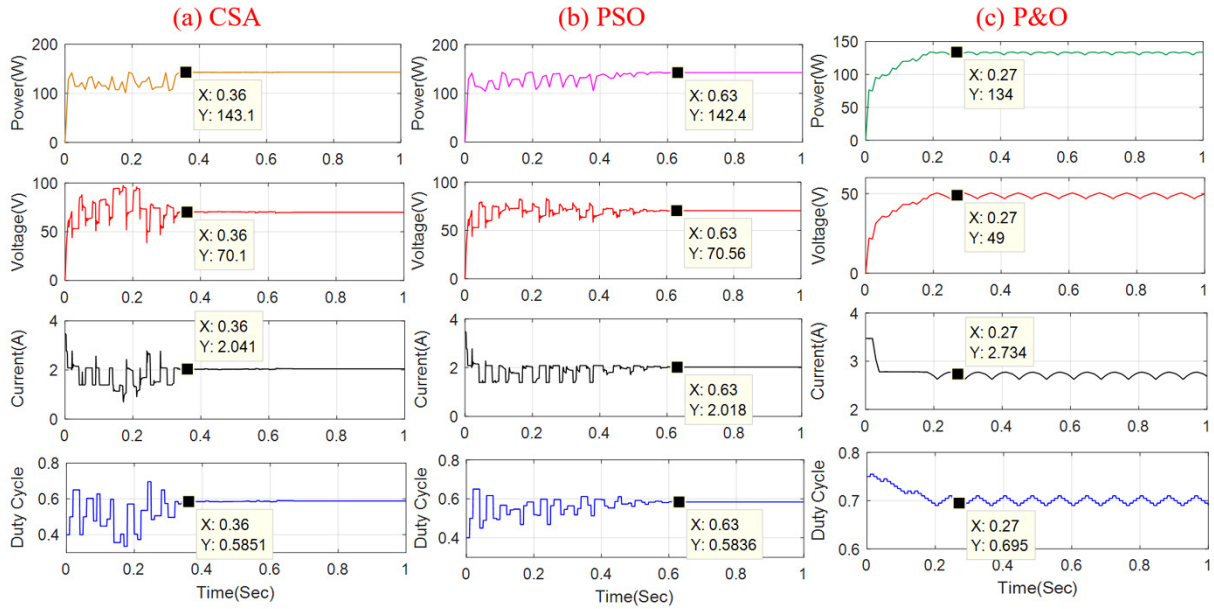
Fig. IV.13. Simulated system responses of CSA, PSO and P&O methods under case
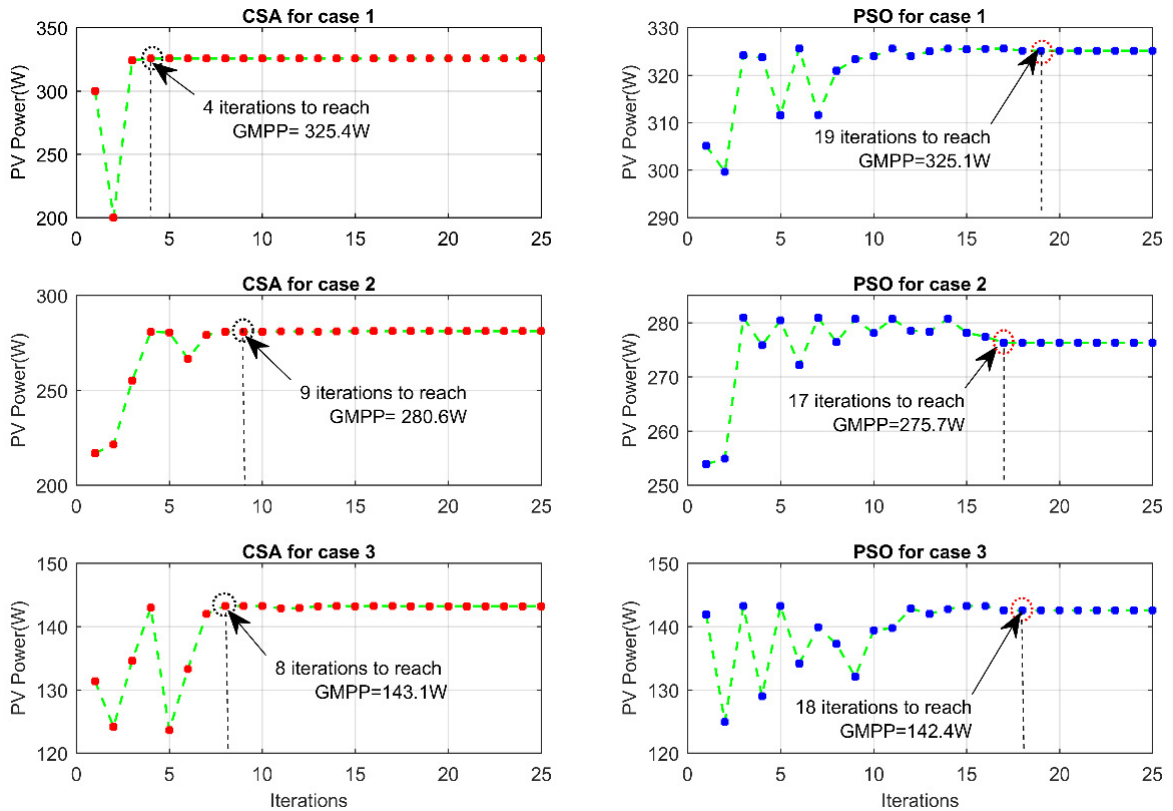
Fig. IV.14. The convergence process to GMPP versus iterations in CSA and PSO methods under three shading cases

A. Case **(1):** In this case, all PV modules are subjected to the same uniform irradiation (1000 W/m^2), where it generated only one GMPP peak at 325.5W on the P-V characteristic curve as shown in Fig. 3. CSA method in Fig IV.11, reached rapidly a GMPP at 325.4W after 0.31Sec, without any steady state oscillations, while PSO and P&O methods reached 325.1W and 323.1W respectively after 0.68 s and.0.65s with small steady state oscillations.

Table. IV.5. Performances comparison between CSA, PSO and P&O methods

Partial shading cases PSCs	Methods	Global MPP of P-V curve (W)	Extracted PV power (W) (fitness)	Power loss (W)	Power loss (%)	Efficiency (%)	Convergence time (Sec)	Optimal Duty cycle
Case (1)	CSA	325.5	325.40	0.1	0.031	99.97	0.31	0.609
	PSO		325.10	0.4	0.122	99.87	0.68	0.608
	P&O		323.10	2.4	0.737	99.26	0.65	0.605
Case (2)	CSA	281.2	280.60	0.6	0.213	99.64	0.49	0.568
	PSO		276.20	5	1.778	98.22	0.60	0.552
	P&O		211.80	69.4	24.679	75.32	0.23	0.690
Case (3)	CSA	143.2	143.10	0.1	0.069	99.93	0.36	0.585
	PSO		142.40	0.8	0.558	99.44	0.63	0.583
	P&O		134.00	9.2	6.424	93.57	0.27	0.695

B. Case **(2):** PV1, PV2, PV3, PV4 modules were exposed to the same solar irradiation of 1000W/m^2 whereas PV5 and PV6 modules received 800 W/m^2. This case yielded two peaks on the P-V curve (as shown in Fig. IV. 3) the first is a global peak at 281.2W and the second is a local peak LMPP=211.6W. Fig. IV.12, shows that the CSA method converged to GMPP of 280.6W after 0.49 s while PSO reached 276.2W after 0.6 s. One can see that CSA is faster than PSO. Furthermore, P&O was deceived by converging to a local peak LMPP of 211.8W.

C. Case **(3):** This case represents severe shading because it contains a great difference in received solar irradiation (1000, 1000, 800, 600, 400 and 200) W/m^2. As shown in the Fig.IV.3, this case produced one global peak GMPP=143.2W and four other local peaks LMPPs as follows: LMPP1=97.71W, LMPP2=134.1W, LMPP3=125W, LMPP4=77.66W. The CSA method achieved a GMPP=143.1W after a convergence time of 0.36s while PSO took longer (0.63s) to attain GMPP=142.4W (as shown Fig IV.13). On the other hand, P&O was deceived by the first local peak LMPP=134W and exhibited large oscillations around LMPP.

Based on the above numerical results, the average efficiency and power loss can be computed for all the partial shading cases for CSA, PSO and P&O methods as shown in Table. IV.6.

Table. IV.6. Average performance values for each used method in all combined PSCs

		Power loss Average (%)	Efficiency Average (%)	Convergence time average to reach GMPP (Sec)
MPPT Methods	CSA	0.104	99.85	0.338
	PSO	0.819	99.17	0.636
	P&O	10.613	89.38	Don't reach GMPP in PSCs

From Fig.IV.14, one can see that CSA needs only 4, 5 and 8 iterations to reach the GMPP in cases 1, 2 and 3 respectively whereas PSO requires 19, 17 and 18 iterations. Therefore, it is clear that CSA method converges to GMPP faster than the PSO method. Knowing that P&O cannot attain GMPP, it suffices to converge towards the one of the local peaks LMPPs.

For further clarification, Fig.IV.15, illustrates a quantitative comparison between CSA, PSO and P&O using the histogram column style based on the numerical data values of Table IV.6.
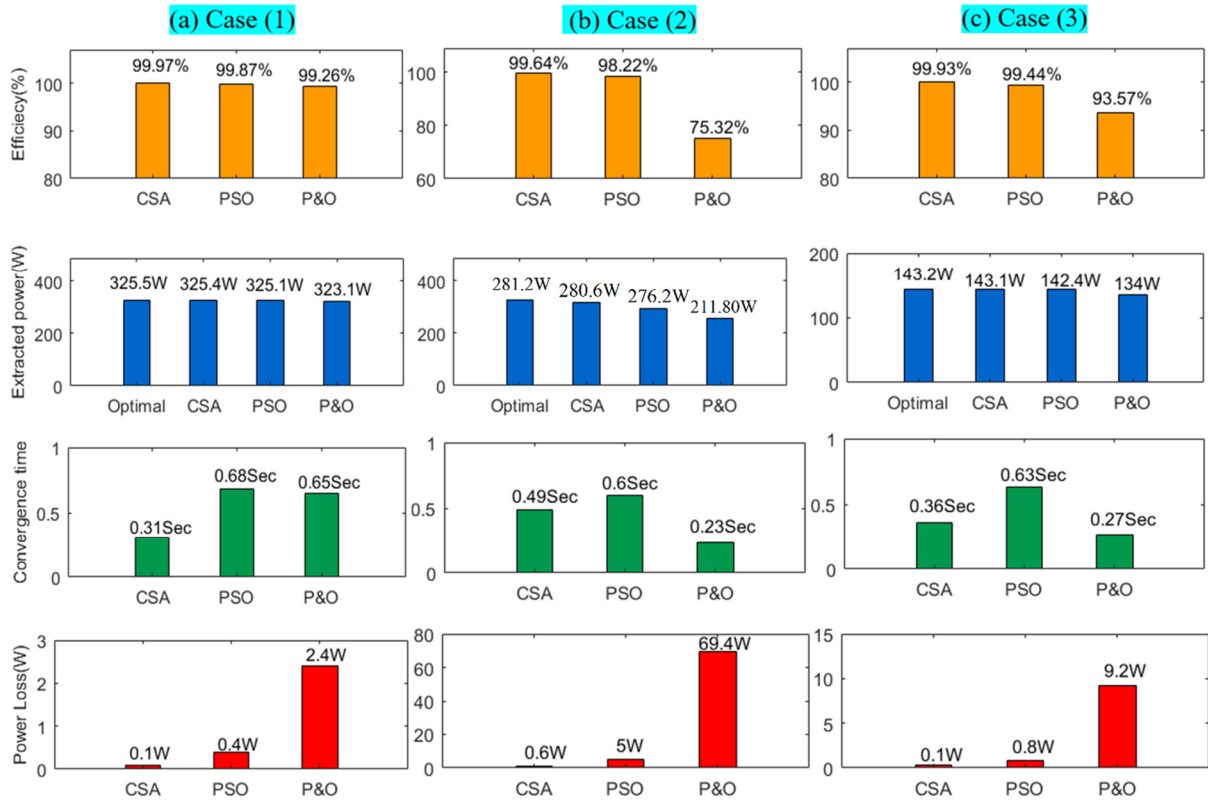
Fig.IV.15. Quantitative comparison between the performances of CSA, PSO and P&O methods for different PSCs

The previous data table confirm the evident superiority of CSA over PSO and P&O with respect to the considered performances criteria.

According on previous discussions and analysis, one can highlight the following points:

(1) CSA method converges to GMPP with a very high efficiency rate in all PSCs cases, where CSA increases the efficiency by an average of 1.43% and 24.41% in comparison to PSO and P&O respectively, for cases 2 and 3.

(2) The average efficiency of CSA, PSO and P&O is 99.85%, 99.17% and 89.38% respectively, for all tested shading cases.

(3) CSA reduces the convergence time by 54.41% compared to PSO in the case of zero shading (case 1), which corresponds to uniform irradiation, and reaches 42.86% and 18.33% in weak shading (case 2) and severe shading (case 3) respectively. Hence, CSA decreases the convergence time by an average of 38.53% compared to PSO.

(4) CSA always converges to GMPP in all partial shading cases whereas P&O is misled into one of the local peaks LMPPs.

(5) CSA increases the extracted PV power by an average of 2.6W compared to PSO and by 38.95W compared to P&O under PSC.

(6) The total power loss under all three cases for CSA is 0.8W, which represents 0.1%, and attains 6.2W for PSO (0.819%) and 81W for P&O (10.613%). Thus, CSA considerably reduces power loss compared to PSO and P&O.

(7) The CSA technique needs only two tuning parameters while PSO requires at least four.

IV.7. Qualitative comparison study

To confirm the superior performance of the CSA technique under PSC, a qualitative comparison with five MPPT methods, presented in Table.IV.7, was conducted, these methods include classical methods, Artificial Intelligence (AI) and metaheuristic methods namely P&O FLC, PSO, FPA and hybrid methods such as ELPSO-P&O.

Table. IV.7. Qualitative comparison of CSA performances with different MPPT methods

N	Criteria	P&O Elgendy et al.[33].	FLC Chen et al.[34].	PSO Miyatake et al.[17].	FPA Ram and Rajasekar[63]	ELPSO-P&O Ram et al.[36]	Proposed CSA
1	Convergence speed to GMPP in PSC	Low	Medium	Medium	Fast	Very Fast	Very Fast
2	Efficiency in PSC	Low	Low	High	Very High	Very High	Very High
3	Possibility of wrong convergence to local peak LMPP in PSC	High	High	Zero	Zero	Zero	Zero
4	Steady state oscillation in PSC	High	Medium	Zero	Zero	Zero	Zero
5	Number of tuning parameters	2	1	4	2	7	2
6	Algorithm complexity	Simple	Medium	Simple	Medium	Complex	Simple
7	Dependency on system	Yes	Yes	No	No	No	No
8	Difficulty in Hardware realization	Easy	Medium	Easy	Easy	Medium	Easy*

*The simplicity of the CSA algorithm with fewer tuning parameters (only two parameters) certainly implies an easy experimental implementation, which will be confirmed in a future work.

The evaluation considered the most critical criteria. This qualitative comparison study revealed the following points:

- P&O method generates higher oscillations around MPP in steady state because it uses fixed step size, however, no steady state oscillation is observed for the cited meta-heuristic methods,

- CSA is the fastest to converge to GMPP, even in cases of significant partial shading.

- CSA, FPA and ELPSO-P&O have very high efficiency, which greatly decreases power loss.

- The CSA and FPA methods use the fewest tuning parameters (only two parameters), but the structure of the CSA algorithm is simpler than that of FPA.

- The performances of the CSA, PSO, FPA and ELPSO-P&O methods are independent of the PV system characteristics whereas the performances of the FLC and P&O are strongly dependent on those characteristics.

- Despite the good performance of the ELPSO-P&O hybrid method, its algorithm is more complex than that of CSA, FPA and PSO, which require up to seven tuning parameters.

IV.8. Optimality proof for the CSA based MPPT method

The CSA is a nature-inspired stochastic optimization method. The results of this work confirm that CSA method is simple, fast and efficient compared to other methods for the MPPT optimization problem. This section provides a mathematical proof to show that the CSA method guarantees to find the best global optimal solution for the optimization based MPPT, which gives the global maximum power point GMPP. To evaluate the performance of the proposed MPPT methods, we used the statistical analysis based on a set of metrics to examine the sensitivity of each methods for varying cases of partial shading. These metrics are Relative Error (RE), Mean Absolute Error (MAE) and Standard Deviation (STD) presented in the following equations:

The Relative Error (RE):

$$RE = \frac{\sum_{i=1}^{K}(P_{mi} - P_{pv})}{P_{pv}} * 100\% \qquad \text{(IV-35)}$$

The Mean Absolute Error (MAE):

$$MAE = \frac{\sum_{i=1}^{K}\left|P_{mi} - P_{pv}\right|}{K} \qquad \text{(IV-36)}$$

The Standard Deviation (STD):

$$STD = \sqrt{\frac{\sum_{i=1}^{K}(P_{pv} - \overline{P}_{mi})^2}{K}} \qquad \text{(IV-37)}$$

Where P_{mi} represents the extracted output power for each proposed methods (measured power). P_{pv} is the ideal tracked PV power, $\overline{P}_{mi}$ is the mean of the extracted output power P_{mi}. K is the total number of samples [2].

The last case of partial shading (case 3) is the most critical case compared to cases 1 and 2, as shown in Table IV.1, because it contains a severe shading. For this reason, we calculate the statistical indicators RE, MAE and STD in this critical case.

The statistical data for the CSA, PSO and P&O methods are given in Table IV.8.

Table. IV.8. Comparison of statistical results of the used MPPT methods in the critical case 3 of PSC

Methods	Relative Error RE	Mean Absolute Error MAE	Standard Deviation STD
CSA	0.4958	2.8578	2.8398
PSO	0.5476	3.1457	3.1366
P&O	5.7193	32.7601	43.3721

From this table, it is observed that CSA has the lowest RE, MAE and STD than others. The index STD confirms the stability of CSA compared with PSO and P&O. These statistical results confirm the superiority of CSA method compared to the others in terms of the ability to find the best global optimal solution, and avoid falling in the optimal local solutions despite the critical case of partial shading (case 3). The performance of CSA is interpreted by the smallness of all types of measured errors between the obtained power values by CSA method and the ideal power value, as confirmed by the statistical indexes.

Through the previous discussion and comparative study, we can say that the proposed CSA technique is an advantageous technique for effective and rapid control of GMPP in changing weather conditions (uniform irradiation and partial shading cases) compared to the above mentioned conventional and soft computing MPPT methods. Hence, the merits of the CSA technique can be summarized in the following points:

(1) Fast convergence to GMPP in case of uniform irradiation in all partial shading cases.

(2) Very high efficiency despite significant partial shading.

(3) CSA has a simple structure with only two tuning parameters, which reduces computation time and facilitates implementation.

(4) CSA always converges to the GMPP, and can clearly distinguish between LMPP and GMPP optimal solutions peaks under all PSCs.

(5) CSA considerably minimize power losses, despite the adverse effects of PSC.

(6) No steady state oscillations around GMPP.

IV.9. Conclusion

This chapter presents a meta-heuristic optimization technique called Crow Search Algorithm (CSA), to mitigate the negative effects of partial shading on the tracking of the global maximum power point GMPP of a standalone photovoltaic system. Simulation results demonstrated the high ability of the CSA technique for successfully track GMPP under three tested partial shading cases (PSCs): zero, weak and severe shading. Despite these changing climatic situations, the proposed CSA technique operated very effectively and better than PSO and P&O techniques. The CSA based MPPT controller extracts maximum power from the PV generator with an average efficiency of 99.85%, for the three tested cases whereas 99.17% and 89.38%, were recorded for PSO and P&O techniques, respectively. Furthermore, CSA technique greatly reduces the total power loss in the combined partial shading cases to 0.1% against 0.82% and 10.61% for PSO and P&O respectively. Moreover, CSA decreases the convergence time by an average of 38.53% compared to PSO whereas P&O fails even to reach the GMPP in weak and severe shading cases, and it deceives by a wrong convergence to a local peak. Thus, the classic P&O method is ineffective in tracking GMPP under PSCs. On the contrary, the results revealed that the CSA method significantly outperformed the PSO and P&O methods under all PSCs in terms of algorithm simplicity with fewer adjustment parameters, which reduces computation time and facilitates implementation. Furthermore, it offers high efficiency in extracting maximum power, rapid convergence towards the global power peak GMPP, and clear-cut distinction between the latter and local power peaks (LMPPs), with no steady state oscillations. Moreover, we checked the stability of the proposed PV system using Lyapunov function and Barbalat lemma. Finally, a qualitative evaluation based on statistical analysis confirmed the superior performances of the CSA technique.

General Conclusion

We interested in this thesis by the control and the optimization of the extracted photovoltaic (PV) power in an autonomous system subjected to critical changing weather conditions, the control is based on metaheuristic optimization techniques. We aim via this thesis to propose an efficient and simple metaheuristic technique to control the global maximum power point (GMPP), where we focused in this thesis on attenuating the negative effects of partial shading, on extracting PV power from a partially shaded PV system. After performing an review study for the maximum power point tracking (MPPT) methods, we found that this field is experiencing great progress with a wide range of techniques being suggested, ranging from simple but ineffective methods to more effective but complex ones. Therefore, it is very important to propose a strategy that is both simple and effective in controlling the global maximum power point (GMPP) for a photovoltaic (PV) system under changing weather conditions. In this context, and to achieve this objective, the major contribution of this thesis work was to design and implement an metaheuristic technique called Crow search algorithm on MPPT application that combine the simplicity of algorithm and the high efficiency under all critical cases.

Firstly, we presented in the first chapter, a state of the art of different exists MPPTs methods in literature. Based on this review study we found that the MPPTs methods classified into three groups, conventional, soft computing, and hybrid methods. First, comprises the conventional methods such as perturb and observe (P&O), incremental conductance (INC). The second group is based on soft computing approaches. These methods include fuzzy logic control (FLC), artificial neural network (ANN) and metaheuristic methods like: Particle Swarm Optimization (PSO), Cuckoo Search (CS), Bat Algorithm (BA), Grey Wolf Optimization (GWO), Firefly Algorithm (FA), Flower Pollination Algorithm (FPA). The last group comprises of hybrid methods like: P&O-PSO, GWO-FLC, ANFIS-GA, DE-PSO, PSO-GSA. In addition, an overview on the factors influencing the efficiency of the photovoltaic system has been presented, we have explained in this chapter the basic principles with performance analysis of the most used classical and modern MPPT techniques.

Subsequently in the second chapter, we studied the partial shading problem and its influences in the extracted PV power performance from PV generators. By using Matlab/Simulink software, we simulated in this part the models of PV cells and some PV array configurations

under uniform irradiation case and partial shading conditions, the simulation results illustrated the electrical characteristics Power-Voltage (P-V) and Current-Voltage (I-V) of each proposed model. Based on these results, we conclude that the shadow decreased significantly the output PV power of PV cells of PV module. Thus extracted PV power decreases in all PV array configurations, moreover we confirmed that TCT configuration has the highest output power during all tested scenarios of partial shading comparing to all other examined PV configurations, whereas the S configuration has the lowest output power.

Then in third chapter, we evaluated the performances of some MPPT techniques operates in standalone PV system. The PV system is simulated for each time of test by three MPPT controllers based on two metaheuristic methods are Particle Swarm Optimization (PSO), and Cuckoo Search (CS) and one traditional method is Perturb and Observe (P&O). For this reason, we simulated in MATLAB/Simulink a standalone PV system comprises a PV generator configured in 3S2P, a DC-DC boost converter, a MPPT controller and a resistive load. This proposed PV system subjected to four different cases represent changing weather conditions of irradiation and temperature. The results of simulation showed that the two metaheuristic techniques trackers have high efficiency and stability (zero steady state oscillation) in extracting the GMPP in all the tested cases, with a clear superiority of CS than PSO and PO in term of more efficiency, fastness of convergence, and reducing power loss in all different tested cases. On the other hand the traditional P&O-MPPT method, operate effectively in the standard test conditions case (STC) but become incompetent to track the GMPP in critical weather cases like the case of partial shading PSC, finally we concluded that CS is better than PSO and P&O in all different tested cases.

To improve the tracking performance of MPPT controller under critical climatic situations, like partial shading cases. We proposed in the fourth chapter a new contribution to control the maximum power of PV system for different critical operating conditions. This new contribution is the implementation of a simple and efficient meta-heuristic technique, called Crow Search Algorithm (CSA) for MPPT application, CSA technique is a nature-inspired optimization method based on the intelligent skills of the crow in the search process of hidden food places. CSA technique combines efficiency and simplicity that require only two tuning parameters. It can extract the maximum power in a standalone photovoltaic system, attenuating the negative effects of partial shading on the tracking process of GMPP. In this chapter, we carried out an accurate quantitative and qualitative comparison between CSA, and others classic and metahueristics MPPT methods to evaluate the performance of proposed CSA method.

Simulation results using MATLAB/Simulink software, given the average efficiency of each simulated methods, which are CSA, PSO and P&O for three PSC cases, where CSA can extracts the maximum PV power with an average efficiency of 99.85%, for the three tested cases whereas 99.17% and 89.38%, were recorded for PSO and P&O techniques, respectively. In addition, CSA decreases the convergence time by an average of 38.53% compared to PSO and P&O. These results confirm the superior performance of CSA compared to PSO and P&O techniques in term of easy implementation, high efficiency and low power loss, decrease the convergence time.

Perspectives and Future work

This paper represents the first application of the metaheuristic technique Crow Search Algorithm (CSA) for MPPT application. Motivated by the excellent and encouraging simulation results of this thesis and following the famous saying "*Every answer breeds new questions*" and this thesis is no exception. In the following, recommendations for future research are given in two essential points. Firstly, we suggest to implement an improved CSA based MPPT technique, to attenuate the disadvantages of proposed CSA technique. Secondly, we propose the experimental validation of the obtained results with the proposed CSA-MPPT technique, in order to extend this work from simulation study to practical application, and this is what we are currently trying to achieve. It is envisaged that this work will attract considerable interest of renewable energies community, both researchers and practitioners.

References

1. Ram J-P, Rajasekar N (2017) A new robust, mutated and fast tracking LPSO method for solar PV maximum power point tracking under partial shaded conditions. Applied energy 201: 45-59.

2. Mirza A-F, Ling Q, Javed M-Y, Mansoor M (2019) Novel MPPT techniques for photovoltaic systems under uniform irradiance and Partial shading. Solar Energy 184:628-648.

3. Motahhir S. (2018). Contribution to the optimization of energy withdrawn from a PV panel using an Embedded System: thesis doctorat. Université Sidi Mohamed Ben Abdellah morocco.

4. Park M-S, Chun Y-H, Lee Y-S (2019). Estimation of Renewable Energy Volatility and Required Adjustable Speed Pumped Storage Power Generator Capacity Considering Frequency Stability in Korean Power System. Journal of Electrical Engineering & Technology 14(3):1109-1115.

5. Ahmed J, Salam Z (2015). A critical evaluation on maximum power point tracking methods for partial shading in PV systems. Renewable and Sustainable Energy Reviews 47:933-953.

6. Venkateswari R, Sreejith S. (2019), Factors influencing the efficiency of photovoltaic system. Renewable and Sustainable Energy Reviews. 101:376-94.

7. Sundareswaran K, Vigneshkumar V, Sankar P, Simon SP, Nayak P-S-R, Palani S. (2015) Development of an improved P&O algorithm assisted through a colony of foraging ants for MPPT in PV system. IEEE Transactions on Industrial Informatics.;12(1):187-200.

8. Eltamaly A-M, Farh HM and Othman M-F (2018). A novel evaluation index for the photovoltaic maximum power point tracker techniques. Solar Energy 174:940-956.

9. Ahmed J, Salam Z. (2015). A critical evaluation on maximum power point tracking methods for partial shading in PV systems. Renewable and Sustainable Energy Reviews, 47:933-953.

10. Ram JP, Rajasekar N. (2016). A novel flower pollination based global maximum power point method for solar maximum power point tracking. IEEE Transactions on Power Electronics 32(11):8486-8499.

11. Salah CB, Ouali M. (2011). Comparison of fuzzy logic and neural network in maximum power point tracker for PV systems. Electric Power Systems Research 81(1):43-50.

12. Karatepe E, Hiyama T. (2009). Artificial neural network-polar coordinated fuzzy controller based maximum power point tracking control under partially shaded conditions. IET Renewable Power Generation 3(2): 239-253.

13. Ismail M-M, Bendary A-F. (2020). Smart battery controller using ANFIS for three phase grid connected PV array system. Mathematics and Computers in Simulation 167:104-118

14. Shaik RB, Kannappan EV. (2020). Application of Adaptive Neuro-Fuzzy Inference Rule-based Controller in Hybrid Electric Vehicles. Journal of Electrical Engineering & Technology. https://doi.org/10.1007/s42835-020-00459-w.

15. Adly M, Besheer A. (2013). A meta-heuristics search algorithm as a solution for energy transfer maximization in stand-alone photovoltaic systems. International Journal of Electrical Power & Energy Systems 51:243-254.

16. Wang Z, Luo Q, Zhou Y. (2020). Hybrid metaheuristic algorithm using butterfly and flower pollination base on mutualism mechanism for global optimization problems. Engineering with Computers. https://doi.org/10.1007/s00366-020-01025-8.

17. Miyatake M, Veerachary M, Toriumi F, Fujii N, Ko H (2011). Maximum power point tracking of multiple photovoltaic arrays: A PSO approach. IEEE Transactions on Aerospace and Electronic Systems 47(1):367-380.

18. Ishaque K, Salam Z (2012). A deterministic particle swarm optimization maximum power point tracker for photovoltaic system under partial shading condition. IEEE transactions on industrial electronics 60(8):3195-3206.

19. Chowdhury SR, Saha H (2010). Maximum power point tracking of partially shaded solar photovoltaic arrays. Solar energy materials and solar cells 94(9):1441-1447.

20. Kaced K, Larbes C, Ramzan N, Bounabi M, elabadine D-Z. (2017) Bat algorithm based maximum power point tracking for photovoltaic system under partial shading conditions. Solar Energy 158:490-503.

21. Ahmed J, Salam Z. (2014). A Maximum Power Point Tracking (MPPT) for PV system using Cuckoo Search with partial shading capability. Applied energy 119:118-130.

22. Sundareswaran K, Sankar P, Nayak P-S-R, Simon SP, Palani S. (2014). Enhanced energy output from a PV system under partial shaded conditions through artificial bee colony. IEEE Transactions on Sustainable Energy 6(1):198-209.

23. Mohanty S, Subudhi B, Ray P-K (2015) A new MPPT design using grey wolf optimization technique for photovoltaic system under partial shading conditions. IEEE Transactions on Sustainable Energy 7(1):181-188.

24. Duman S, Yorukeren N, Altas IH. (2018). A novel MPPT algorithm based on optimized artificial neural network by using FPSOGSA for standalone photovoltaic energy systems. Neural Computing and Applications 29(1):257-278.

25. Li L-L, Lin G-Q, Tseng M-L, Tan K, Lim MK (2018). A maximum power point tracking method for PV system with improved gravitational search algorithm. Applied Soft Computing 65:333-348.

26. Wu Z, Yu D (2018). Application of improved bat algorithm for solar PV maximum power point tracking under partially shaded condition. Applied Soft Computing 62:101-109.

27. Abdalla O, Rezk H, Ahmed EM. (2019). Wind driven optimization algorithm based global MPPT for PV system under non-uniform solar irradiance. Solar Energy 180:429-444.

28. Lian K, Jhang J, Tian I. (2014). A maximum power point tracking method based on perturb-and-observe combined with particle swarm optimization. IEEE journal of photovoltaics 4(2):626-633.

29. Seyedmahmoudian M, Rahmani R, Mekhilef S, Maung Than Oo A, Stojcevski A, Soon TK (2015). Simulation and hardware implementation of new maximum power point tracking technique for partially shaded PV system using hybrid DEPSO method. IEEE Trans Sustain Energy 6:850–62. http://dx.doi.org/10.1109/TSTE.2015.2413359.

30. Tan A, Tang Z, Sun X, Zhong J, Liao H, Fang H (2020). Genetic Algorithm-Based Analysis of the Effects of an Additional Damping Controller for a Doubly Fed Induction Generator. Journal of Electrical Engineering & Technology. https://doi.org/10.1007/s42835-020-00440-7.

31. Sundareswaran K, Vigneshkumar V, Palani S. (2015). Development of a hybrid genetic algorithm/perturb and observe algorithm for maximum power point tracking in photovoltaic systems under non-uniform insolation. IET Renewable Power Generation 9(7):757-765.

32. Mohamed M-A, Diab A-A-Z, Rezk H. (2019). Partial shading mitigation of PV systems via different meta-heuristic techniques. Renewable energy 130:1159-1175.

33. Elgendy M-A, Zahawi B, Atkinson D-J (2014). Operating characteristics of the P&O algorithm at high perturbation frequencies for standalone PV systems. IEEE transactions on energy conversion 30(1):189-198.

34. Chen Y-T, Jhang Y-C, Liang R-H. (2016). A fuzzy-logic based auto-scaling variable step-size MPPT method for PV systems. Solar Energy 126, 53-63.

35. Eltamaly A-M, Farh HM (2019) Dynamic global maximum power point tracking of the PV systems under variant partial shading using hybrid GWO-FLC. Solar Energy 177:306-316.

36. Ram J-P, Pillai DS, Rajasekar N, Strachan S-M (2019). Detection and identification of global maximum power point operation in solar PV applications using a hybrid ELPSO-P&O tracking technique. IEEE Journal of Emerging and Selected Topics in Power Electronics. doi 10.1109/JESTPE.2019.29 00999.

37. Shi J-Y, Ling L-T, Xue F, Qin Z-J, Li Y-J, Lai Z-X, Yang T (2017). Combining incremental conductance and firefly algorithm for tracking the global MPP of PV arrays. Journal of Renewable and Sustainable Energy 9(2):023501.

38. Fathy A, Rezk H. (2016). A novel methodology for simulating maximum power point trackers using mine blast optimization and teaching learning based optimization algorithms for partially shaded photovoltaic system. Journal of Renewable and Sustainable Energy 8(2):023503.

39. Ahmed J, Salam Z. (2018). An enhanced adaptive P&O MPPT for fast and efficient tracking under varying environmental conditions. IEEE Transactions on Sustainable Energy 9(3):1487-1496.

40. Seyedmahmoudian M, Horan B, Rahmani R, Oo A-M-T, Stojcevski A. (2016). Efficient photovoltaic system maximum power point tracking using a new technique. Energies 9(3):147.

41. Sundareswaran K, Peddapati S, Palani S. (2014). MPPT of PV systems under partial shaded conditions through a colony of flashing fireflies. IEEE transactions on energy conversion 29(2):463-472.

42. Yang B, Zhong L, Zhang X, Shu H, Yu T, Li H, Jiang L, Sun L (2019). Novel bio-inspired memetic salp swarm algorithm and application to MPPT for PV systems considering partial shading condition. Journal of cleaner production 215: 1203-1222. https://doi.org/10.1016/j.jclepro.2019.01.150.

43. Yang B, Yu T, Zhang X, Li H, Shu H, Sang Y, Jiang L. (2019). Dynamic leader based collective intelligence for maximum power point tracking of PV systems affected by partial shading condition. Energy conversion and management 179:286-303.

44. Dileep G, Singh S. (2017). Selection of non-isolated DC-DC converters for solar photovoltaic system. Renewable and Sustainable Energy Reviews. 76:1230-47.

45. Li G, Jin Y, Akram M, Chen X, Ji J. (2018), Application of bio-inspired algorithms in maximum power point tracking for PV systems under partial shading conditions–A review. Renewable and Sustainable Energy Reviews; 81:840-73.

46. Pandey A, Dasgupta N, Mukerjee A-K. (2008). High-performance algorithms for drift avoidance and fast tracking in solar MPPT system. IEEE Transactions on Energy conversion. 23(2):681-9

47. Abdelsalam A-K, Massoud A-M, Ahmed S, Enjeti P-N. (2011). High performance adaptive perturb and observe MPPT technique for photovoltaic-based microgrids. IEEE Transactions on power electronics. 26(4):1010-21.

48. Ram J-P, Babu T-S, Rajasekar N. (2017). A comprehensive review on solar PV maximum power point tracking techniques. Renewable and Sustainable Energy Reviews. 67:826-47.

49. Balamurugan M, Sahoo S-K, Sukchai S. (2017). Application of soft computing methods for grid connected PV system: a technological and status review. Renewable and Sustainable Energy Reviews. 75:1493-508.

50. Eltamaly A-M. (2018). Performance of MPPT techniques of photovoltaic systems under normal and partial shading conditions. chapter of book, In Advances in renewable energies and power technologies (pp. 115-161). Elsevier.

51. Al-Diab A, Sourkounis C. (2010). Variable step size P&O MPPT algorithm for PV systems. 12th International Conference on Optimization of Electrical and Electronic Equipment 2010 May 20 (pp. 1097-1102). IEEE.

52. Amrouche B, Belhamel M, Guessoum A. (2007). Artificial intelligence based P&O MPPT method for photovoltaic systems. Revue des Energies Renouvelables ICRESD-07 Tlemcen. Sep 5:11-6.

53. Houam Y, Saidi L, Adouane M, Si Tayeb A. (2015). Fuzzy Logic Control for Photovoltaic Power System Using DC-DC Buck Converter, The First International Conference On Solar Energy INCOSOL'15, University of Bordj_bouariridj Algeria

54. Dileep G, Singh S. (2017). Application of soft computing techniques for maximum power point tracking of SPV system. Solar Energy. 141:182-202.

55. Jordehi AR. (2016) Maximum power point tracking in photovoltaic (PV) systems: A review of different approaches. Renewable and Sustainable Energy Reviews. 65:1127-38.

56. Shaiek Y, Smida MB, Sakly A, Mimouni MF. (2013). Comparison between conventional methods and GA approach for maximum power point tracking of shaded solar PV generators. Sol Energy 90:107-22.

57. Hashim N, Salam Z, Ayob S-M. (2014). Maximum power point tracking for stand-alone photovoltaic system using evolutionary programming. In: Proceedings of the IEEE 8th international power engineering and optimization conference (PEOCO). http://dx.doi.org/10.1109/PEOCO.2014.6814390.

58. Salam Z, Ahmed J, Merugu B-S. (2013).The application of soft computing methods for MPPT of PV system: A technological and status review. Applied Energy. 107:135-48.

59. Rezk H, Mazen A-O, Gomaa MR, Tolba M-A, Fathy A, Abdelkareem M-A, et al. (2019). A novel statistical performance evaluation of most modern optimization-based global MPPT techniques for partially shaded PV system. Renewable and Sustainable Energy Reviews.115:109372.

60. Taheri H, Salam Z, Ishaque K, Syafaruddin G. (2010). A novel maximum power point tracking control of photovoltaic system under partial and rapidly fluctuating shadow conditions using differential evolution. IEEE Symp Ind Electron Appl:82–7.

61. Rezk H, Fathy A, Abdelaziz A-Y. (2017). A comparison of different global MPPT techniques based on meta-heuristic algorithms for photovoltaic system subjected to partial shading conditions. Renewable and Sustainable Energy Reviews 74:377-386.

62. Yang X-S, Karamanoglu M, He X. (2014). Flower pollination algorithm: a novel approach for multiobjective optimization. Eng Optim; 46:1222−37.

63. Ram J-P, Rajasekar N. (2017). A new global maximum power point tracking technique for solar photovoltaic (PV) system under partial shading conditions (PSC). Energy. Jan 1-118:512-25.

64. Eltamaly A-M, Abdelaziz A-Y. (2019). Modern Maximum Power Point Tracking Techniques for Photovoltaic Energy Systems: Book. Springer.

65. Mohanty S, Subudhi B, Ray P-K. (2016). A grey wolf-assisted perturb & observe MPPT algorithm for a PV system. IEEE Transactions on Energy conversion. 32(1):340-7.

66. Olivares-Rodríguez C, Castillo-Calzadilla T, Kamara-Esteban O. (2018). Bio-inspired approximation to MPPT under real irradiation conditions. International Symposium on Intelligent and Distributed Computing. Springer.

67. Yang, X-S. (2010). A new metaheuristic bat-inspired algorithm. In: Nature Inspired Cooperative Strategies for Optimization (NICSO 2010). Springer, pp. 65–74.

68. Da Rocha M.V, Sampaio LP, da Silva SAO. (2020). Comparative analysis of MPPT algorithms based on Bat algorithm for PV systems under partial shading condition. Sustainable Energy Technologies and Assessments. 40:100761.

69. Rezk H, Fathy A. (2017). Simulation of global MPPT based on teaching–learning-based optimization technique for partially shaded PV system. Electrical engineering. 99(3):847-59.

70. Saremi S. Mirjalili S. (2017). Lewis A. Grasshopper optimisation algorithm: theory and application. Advances in Engineering Software.105:30-47.

71. Mansoor M, Mirza A-F, Ling Q, Javed M-Y. (2020). Novel Grass Hopper optimization based MPPT of PV systems for complex partial shading conditions. Solar Energy.198:499-518.

72. Aygül K, Cikan M, Demirdelen T, Tumay M. (2019). Butterfly optimization algorithm based maximum power point tracking of photovoltaic systems under partial shading condition. Energy Sources, Part A: Recovery, Utilization, and Environmental Effects Taylor & Francis: 1-19.

73. Fathy A. (2020). Butterfly optimization algorithm based methodology for enhancing the shaded photovoltaic array extracted power via reconfiguration process. Energy Conversion and Management. 220:113115.

74. Sundareswaran K, Vignesh kumar V, Palani S. (2015). Application of a combined particle swarm optimization and perturb and observe method for MPPT in PV systems under partial shading conditions. Renew Energy;75:308–17
http:// dx.doi.org/10.1016/j.renene.2014.09.044.

75. Pilakkat D, Kanthalakshmi S. (2019). An improved P&O algorithm integrated with artificial bee colony for photovoltaic systems under partial shading conditions. Solar Energy, 178: 37-47.

76. Yang B, Zhu T, Wang J, Shu H, Yu T, Zhang X, (2020). Comprehensive overview of maximum power point tracking algorithms of PV systems under partial shading condition. Journal of Cleaner Production.121983.

77. Patel H, Agarwal V. (2008). MATLAB-based modelling to study the effects of partial shading on PV array characteristics. IEEE Transactions on Energy conversion. 23(1):302-10.

78. Acanski M. (2019). PV Module Integrated Converter for Distributed MPPT PV Systems. Doctoral Thesis, Delft University of Technology, Belgrade, Serbia.

79. Moballegh S, Jiang J. (2013). Modelling, prediction, and experimental validations of power peaks of PV arrays under partial shading conditions. IEEE transactions on sustainable energy. 5(1):293-300.

80. Kim K-A, Krein P-T. (2015). Reexamination of photovoltaic hot spotting to show inadequacy of the bypass diode, IEEE Journal of Photovoltaics, vol. 5, pp. 1435-1441.

81. Dhimish M, Holmes V, Mehrdadi B, Dales M, Mather P. (2018). PV output power enhancement using two mitigation techniques for hot spots and partially shaded solar cells. Electric Power Systems Research, vol. 158, pp. 15-25.

82. Daliento S. Mele L. Bobeico E. Lancellotti L, Morvillo P. (2007). Analytical modelling and minority current measurements for the determination of the emitter surface recombination velocity in silicon solar cells. Solar energy materials and solar cells, vol. 91, pp. 707-713.

83. Coppola M, Daliento S, Guerriero P, Lauria D, Napoli E. (2012). On the design and the control of coupled-inductors, boost dc-ac converter for an individual PV panel. International Symposium on Power Electronics Power Electronics, Electrical Drives, Automation and Motion, pp. 1154-1159.

84. Daliento S, Di Napoli F, Guerriero P, d'Alessandro V. (2016). A modified bypass circuit for improved hot spot reliability of solar panels subject to partial shading. Solar Energy, vol. 134, pp. 211-218.

85. Dhimish M, Holmes V, Mather P, Sibley M. (2018). Novel hot spot mitigation technique to enhance photovoltaic solar panels output power performance Solar Energy Materials and Solar Cells 179 (2018) 72-79.

86. Silvestre S, Boronat A, and Chouder A. (2009). Study of bypass diodes configuration on PV modules. Applied Energy, vol. 86, pp. 1632-1640.

87. Guerriero P, Di Napoli F, d'Alessandro V, Daliento S. (2015). Accurate maximum power tracking in photovoltaic systems affected by partial shading. International Journal of Photoenergy. 1 Jan 2015.

88. d'Alessandro V, Di Napoli F, Guerriero P, Daliento S. (2015). An automated high-granularity tool for a fast evaluation of the yield of PV plants accounting for shading effects. Renewable Energy. 1Nov 2015. 83:294-304.

89. Mohammadnejad S, Khalafi A, Ahmadi SM. (2016). Mathematical analysis of total-cross-tied photovoltaic array under partial shading condition and its comparison with other configurations. Solar energy. 133:501-11.

90. Pendem S-R, Mikkili S. (2018). Modelling and performance assessment of PV array topologies under partial shading conditions to mitigate the mismatching power losses. Solar Energy. 2018; 160: 303-21.

91. Ishaque K, Salam Z, Taheri H, (2011). Modeling and simulation of photovoltaic (PV) system during partial shading based on a two-diode model. Simul. Model. Pract. Theory 19 (7), 1613–1626.

92. Jazayeri M, Uysal S, Jazayeri K. (2014). A comparative study on different photovoltaic array topologies under partial shading conditions. In: 2014 IEEE PES T&D Conf. Expo. pp. 1–5.

93. Ramaprabha R, Mathur B. (2012). A comprehensive review and analysis of solar photovoltaic array configurations under partial shaded conditions. Int. J. Photoenergy 2012, 1–16.

94. Houam Y, Terki A, Bouarroudj N. (2021). An Efficient Metaheuristic Technique to Control the Maximum Power Point of a Partially Shaded Photovoltaic System Using Crow Search Algorithm (CSA). Journal of Electrical Engineering & Technology.16(1): 381-402.

95. Fathi A.O.A. (2015) Maximum power point tracking techniques for photovoltaic water pumping system. Doctoral thesis, University of Bath.

96. Mao M, Zhou L, Yang Z, Zhang Q, Zheng C, Xie B, et al. (2019). A hybrid intelligent GMPPT algorithm for partial shading PV system. Control Engineering Practice. 83: 108-15.

97. Diab A.A.Z, Rezk .H. (2017). Global MPPT based on flower pollination and differential evolution algorithms to mitigate partial shading in building integrated PV system, Solar Energy. 157:171–186.

98. Askarzadeh A. (2016). A novel metaheuristic method for solving constrained engineering optimization problems: crow search algorithm. Computers & Structures 169: 1-12.

99. Hinojosa S, Oliva D, Cuevas E, Pajares G, Avalos O, Gálvez J. (2018). Improving multi-criterion optimization with chaos: a novel Multi-Objective Chaotic Crow Search Algorithm. Neural Computing and Applications 29(8):319-335.

100. Sutherland shire community energy (2020). https://sunnyshire.org.au/how-i-justified-getting-solar-on-a-partially-shaded-roof/. Accessed 05 March 2020.

101. Kchaou A, Naamane A, Koubaa Y and M'sirdi N. (2017). Second order sliding mode-based MPPT control for photovoltaic applications. Solar Energy 155:758-769.

102. Abdel-Salam M, El-Mohandes MT, El-Ghazaly M. (2020). An Efficient Tracking of MPP in PV Systems Using a Newly-Formulated P&O-MPPT Method under Varying Irradiation Levels. Journal of Electrical Engineering & Technology, 15(1):501-513.

103. Liu Y-H, Huang S-C, Huang J-W, Liang W-C. (2012). A particle swarm optimization-based maximum power point tracking algorithm for PV systems operating under partially shaded conditions. IEEE transactions on energy conversion 27(4):1027-1035.

104. Dileep G, Singh S. (2017). An improved particle swarm optimization based maximum power point tracking algorithm for PV system operating under partial shading conditions. Solar Energy 158:1006-1015.

105. Jain M, Rani A, Singh V. (2017). An improved Crow Search Algorithm for high-dimensional problems. Journal of Intelligent & Fuzzy Systems 33(6):3597-3614.

106. Askarzadeh A. (2016). Capacitor placement in distribution systems for power loss reduction and voltage improvement: a new methodology. IET Generation, Transmission & Distribution 10(14):3631-3638.

107. Salami, M (2018) Practical implementation of the lyapunov based nonlinear controller in DC-DC boost converter for MPPT of the PV Systems. Solar Energy 173:246-255.

108. Armghan H, Ahmad I, Armghan A, Khan and Arsalan M (2018) Backstepping based non-linear control for maximum power point tracking in photovoltaic system. Solar Energy 159:134-141.

109. Slotine, J.-J.E. and Li, W. (1991) Applied nonlinear control, Prentice hall Englewood Cliffs, NJ.